NASA CR-135050

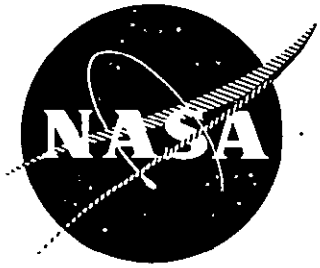

COATINGS FOR DIRECTIONAL EUTECTICS

NAS 3-17815

FINAL REPORT

J.R. Rairden

and

M.R. Jackson

Metallurgy Laboratory
Corporate Research and Development
General Electric Company
Schenectady, New York 12301

July 25, 1976

Prepared for:

National Aeronautics and Space Administration
Lewis Research Center
Cleveland, Ohio 44135

REPRODUCED BY
NATIONAL TECHNICAL
INFORMATION SERVICE
U.S. DEPARTMENT OF COMMERCE
SPRINGFIELD, VA. 22161

Project Manager: John Merutka

PRICES SUBJECT TO CHANGE

(NASA-CR-135050) COATINGS FOR DIRECTIONAL EUTECTICS Final Report (General Electric Co.) 82 p HC $5.00 CSCL 11D

N76-29370

G3/24 Unclas 48391

ORIGINAL PAGE IS
OF POOR QUALITY

1 Report No NASA CR-135050	2. Government Accession No.	3. Recipient's Catalog No.
4 Title and Subtitle Coatings for Directional Eutectics		5 Report Date July 1976 6 Performing Organization Code
7. Author(s) J.R. Rairden and M.R. Jackson		8 Performing Organization Report No SRD-76-076
9. Performing Organization Name and Address General Electric Company Corporate Research and Development Schenectady, New York 12301		10 Work Unit No 11. Contract or Grant No. NAS 3-17815
12 Sponsoring Agency Name and Address National Aeronautics and Space Administration Washington, D.C. 20546		13. Type of Report and Period Covered Contractor Report 14 Sponsoring Agency Code
15. Supplementary Notes Project Manager, John P. Merutka NASA Lewis Research Center, Cleveland, Ohio		

16. Abstract

Significant advances have been made in the development of an environmentally stable coating for a very high strength, directionally solidified eutectic alloy (TaC fiber strengthened γ/γ') designated NiTaC-13 (Ni-3.3Co-4.4Cr-3.1W-5.4Al-5.6V-6.2Re-8.1Ta-0.5Hf). Three duplex (two-layer) coatings survived 3000 hours on a cyclic oxidation test (1100°C to 90°C). These coatings were fabricated by first depositing a layer of NiCrAl(Y) by vacuum evaporation from an electron beam heated source, followed by depositing an aluminizing overlayer. The coating compositions were:

Ni-20Cr-5Al-1Y+Al
Ni-20Cr-5Al-1Y+Al
Ni-20Cr-10Al-1Y+Al

The alloy after exposure with these coatings was denuded of carbide fibers at the substrate/coating interface.

It was demonstrated that TaC fiber denudation can be greatly retarded by applying a carbon-bearing coating. The coating was applied by thermal spraying followed by aluminization. Specimens coated with NiCrAlCY+Al survived over 2000 hours in the cyclic oxidation test with essentially no TaC denudation.

The mechanical behavior under load for NiTaC samples coated with the following two compositions were evaluated:

Ni-20Cr-5Al+Al and Ni-20Cr-5Al-0.1C-0.1Y+Al

Coating ductility was studied for coated and heat-treated bars, and stress rupture life at 871°C and 1100°C was determined for coated and cycled bars.

17. Key Words (Suggested by Author(s)) Coatings Superalloys Eutectic - NiTaC-13	18. Distribution Statement Unclassified-Unlimited		
19. Security Classif. (of this report) Unclassified	20 Security Classif. (of this page) Unclassified	21. No. of Pages	22. Price*

* For sale by the National Technical Information Service, Springfield, Virginia 22161

FOREWORD

This report describes results of work sponsored by the National Aeronautics and Space Administration from June 28, 1974, to June 28, 1975, under Contract NAS 3-17815, Mr. John Merutka, Project Manager, and was prepared by Corporate Research and Development, General Electric Company, Schenectady, New York.

Also included in this report is additional work sponsored by the General Electric Company in areas that are of interest to the current effort but not within the scope of this contract. Specifically, results of (a) 750°C and 1150°C cyclic exposure of pins, and (b) cyclic exposure of coated rupture bars in static air furnace exposures, and subsequent stress rupture testing and metallography.

TABLE OF CONTENTS

PRECEDING PAGE BLANK NOT FILMED

LIST OF ILLUSTRATIONS

LIST OF ILLUSTRATIONS (cont'd)

LIST OF ILLUSTRATIONS (cont'd)

LIST OF ILLUSTRATIONS (cont'd)

LIST OF TABLES

UNIT CONVERSION TABLE

S.I. units are used throughout the report. Tables and figures (where possible) have S.I. units with standard American units in parentheses. In the text, only S.I. units are shown. The conversions for commonly encountered values are listed below. The principal measurements were taken with instruments calibrated in American units, except for weight, which was measured directly in milligrams.

Linear measure	0.00254 cm	0.001 inch
	0.075 cm	0.030 inch
	0.254 cm	0.1 inch
	0.635 cm	0.250 inch
Temperature	871°C	1600°F
	1100°C	2012°F
Stress	434.4 MN/m^2	63.0 ksi
	103.4 MN/m^2	15.0 ksi

SUMMARY

This program was undertaken to develop an environmentally stable coating for a very high strength, directionally solidified eutectic alloy designated NiTaC-13 (Ni-3.3Co-4.4Cr-3.1W-5.4Al-5.6V-6.2Re-8.1Ta-0.54C). The program consists of the following tasks:

Task I - Coating Development Study
Task II - Testing of Coatings
Task III - Reports of Work

In Task I, coatings were deposited onto pin substrates, and screening tests were performed on several base protection systems:

- Ni-20Cr-10Al-1Y
- Ni-20Cr-5Al plus aluminide
- Co-30Cr-5Al-1Y

The most promising coatings were three duplex (two-layer) coatings which survived 3000 hours on a cyclic oxidation test (1100° to 90°C). These coatings were fabricated by first depositing a layer of NiCrAl(Y) by vacuum evaporation from an electron beam heated source followed by depositing an aluminizing overlayer using a pack cementation process. The coating compositions were variations of those designated NASCOAT 70 by NASA:

Ni-20Cr-5Al+Al
Ni-20Cr-5Al-1Y+Al
Ni-20Cr-10Al-1Y+Al

With these coatings, the substrate after cyclic exposure, showed denuded carbide fibers.

It was demonstrated that TaC fiber denudation can be greatly retarded by applying a carbon-bearing coating. The composition Ni-20Cr-5Al-0.1C-0.1Y was applied by thermal spraying using a wire source followed by aluminization to achieve the best oxidation resistance. Specimens coated with NiCrAlCY+Al survived more than 2000 hours on the cyclic oxidation test with essentially no TaC denudation.

In Task II, two coatings from Task I were selected for further study:

Ni-20Cr-5Al+Al
Ni-20Cr-5Al-0.1C-0.1Y+Al

These coatings were given detailed evaluation as follows:

(a) Bend ductility tests,

(b) Stress-rupture tests at 871°C and 1100°C after cyclic burner rig exposure at 1100°C,

(c) Metallurgical analyses.

Both coatings provided for stress rupture lives far in excess of lives for uncoated, cycled NiTaC-13. Lives were superior to those for bars coated with Ni-35Cr+Al, and nearly equivalent to those for bars coated with Ni-20Cr-15Al-1Y, reported in an earlier study (ref. 6).

In room-temperature bend ductility tests, cracks in the Ni-20Cr-5Al+Al occur at 0.5% to 0.6% strain; however, no crack propagation into the substrate was observed.

INTRODUCTION

Directionally solidified eutectic alloys are being considered as possible jet engine turbine blade materials (ref. 1). Because their highly aligned microstructures are formed during solidification, they offer potential structural stability and property retention to a greater fraction of their solidification temperatures than do other materials. To maintain surface integrity at service temperatures approaching 1100°C, protective coatings are required.

To ease the transition from present conventional alloys to aligned eutectics, it is desirable from a design standpoint to develop eutectics which have characteristics similar to, but improved over, these alloys. One of the most advanced eutectic alloys designed by the General Electric Company Aircraft Engine Business Group (AEBG) to approach this goal is NiTaC-13. The melt composition from which this eutectic alloy is grown is Ni-3.3Co-4.4Cr-3.1W-5.4Al-5.6V-6.2Re-8.1Ta-0.54C, in weight percent (ref. 2). Transverse and longitudinal views of the aligned microstructure are shown in figure 1. The brightest phase is the monocarbide fiber formed at solidification, (Ta, V)C. The fibers are approximately 1 μm in cross section and are 2 to 4 volume percent of the microstructure. The darkest phase is γ', the face-centered-cubic ordered structure based on Ni_3Al. This phase precipitates from the austenitic γ matrix during the cool-down following solidification. It is present, as basically cubic particles, about 1 μm on a side. Relative to the surrounding f.c.c. γ network, the γ' phase is enriched in Al, and Ta, and is poor in Re, Cr, V, and W.

For alloys similar in composition to NiTaC-13, the f.c.c. fiber and γ have a common growth axis, $\langle 100 \rangle$, and $\{110\}_{TaC} \parallel \{110\}_{\gamma} \parallel \gamma$-TaC interface (refs. 3 and 4). From longitudinal and transverse sections, it can be found that the cube faces of the γ' precipitate are $\{100\}$ planes and are parallel to the same plane in the γ matrix.

Unlike conventional superalloys containing 15 to 20 wt% Cr, NiTaC-13 contains only 4.4 wt% Cr. As might be expected, the alloy exhibits poor oxidation resistance (ref. 5). A coating with a high concentration of Cr and/or Al should provide oxidation protection. In a previous study (ref. 6), seven coating compositions deposited by electron beam evaporation were evaluated for NiTaC-13. These coatings included three NiCrAlY compositions (30-5-1,

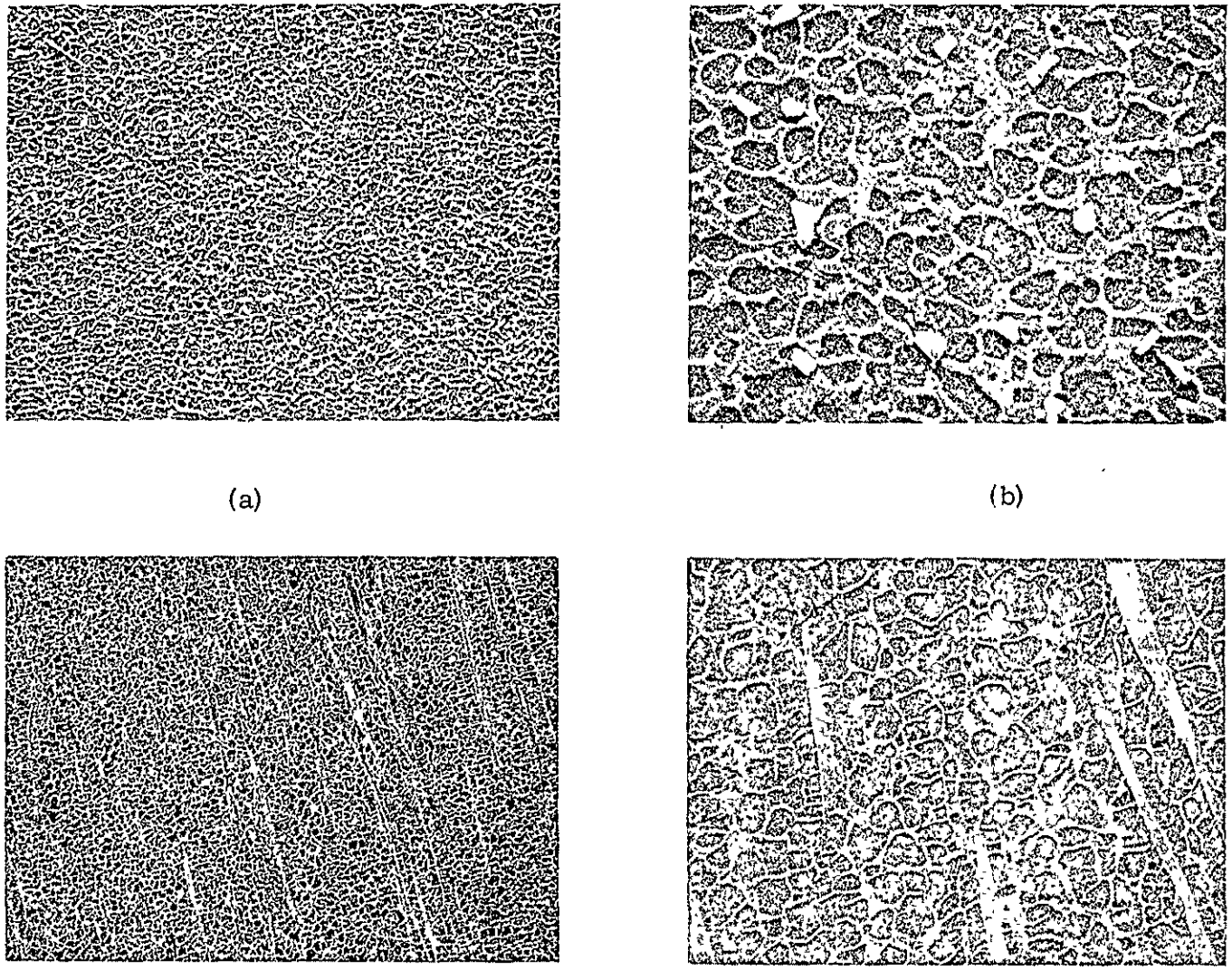

Figure 1. Scanning electron micrographs of as-directionally solidified NiTaC-13: (a) transverse, 620X, (b) transverse, 2580X, (c) longitudinal, 620X, (d) longitudinal, 2580X.

25-10-1, and 20-15-1), two FeCrAlY compositions (30-5-1 and 25-10-1), one CoCrAlY composition (25-10-1), and one duplex coating, Ni-35Cr+Al. Based on cyclic oxidation tests and stress rupture tests, it was determined that the Ni-Cr-Al-Y coating compositions were preferred, and these compositions were potentially very useful.

This present study was undertaken to further study and develop coatings for NiTaC-13. It consisted of the following tasks:

Task I - Coating Development Study
Task II - Testing of Coatings
Task III - Reports of Work

In Task I, coatings were deposited onto pin substrates, and screening tests were performed on the following base protection systems:

Ni-20Cr-10Al-1Y
Ni-20Cr-5Al plus aluminide
Co-30Cr-5Al-1Y

The low aluminum Ni-base alloy plus aluminide coatings are compositional variations of NASA Lewis Research Center developed and patented protective layers that have been designated NASCOAT 70 (refs. 7 through 10). The duplex aluminizing of vacuum-deposited coatings has been patented by the General Electric Company (refs. 11 and 12). The Ni-20Cr-10Al-1Y system was modified by: (a) the addition of carbon, (b) employing a platinum layer as a possible diffusion barrier between the substrate and the NiCrAlY coating, and (c) shot-peening the coating. The first two modifications are aimed at avoiding fiber denudation. During the previous study (ref. 6), it was found that near the coating-substrate interface, TaC fibers disappeared during high-temperature oxidation. In an attempt to identify the cause of carbide denudation, a NiTaC-13 pin coated with 75 μm of a NiCrAlY composition was machined to remove ~37 μm of the coating thickness over regions ~0.3 cm long. After 1000 hours of oxidation exposure at 1100°C, the pins were examined along the midplane of longitudinal sections. Regions with 75-μm-thick coatings showed approximately twice the fiber denudation as the regions with 37 μm of coating. The conclusion was that the coating acts as sink for carbon. Two possible methods of avoiding fiber loss were investigated. These were including carbon in the coating and using a platinum layer to suppress diffusion of carbon into the coating.

The shot-peening process was used to densify the coating and, perhaps, to induce recrystallization of the coating. Yttrium was added to the Ni-base coating systems to evaluate the possible decrease in the tendency for Al_2O_3 film spallation from the coatings.

The Co-30Cr-5Al-1Y system was modified by use of a ductile Ni interlayer and by post-aluminizing treatments. Earlier work (ref. 6) indicated a tendency for delamination at the coating-substrate interface.

Duplicate specimens of coated pins were subjected to thermal cyclic testing. Metallographic evaluations were made on all tested specimens.

For Task II, the most promising coating modifications developed in Task I were given detailed evaluations as follows:

a. Room-temperature bend ductility tests,

b. Stress-rupture tests after cyclic burner rig exposure,

c. Metallurgical analyses.

In addition to the tasks described above, some supplemental testing is reported here which was performed in General Electric-supported studies which complements the work in the tasks.

MATERIALS AND TEST SPECIMENS

Ingots of the source alloys were prepared by induction-melting high-purity metals in a low-pressure, nonoxidizing environment, and then casting the alloys in an argon atmosphere.

The specimens used for this study were electrodischarge machined from directionally solidified NiTaC-13 ingots that were melted with an r-f heated (radio frequency) graphite susceptor system and solidified at 0.635 cm/hr. The pin samples were 4.4 cm long and 0.25 cm in diameter while test bars were 0.25 cm in diameter by 0.95-cm-long gauge sections. The TaC fiber direction was along the axis of the specimens.

In previous studies of the oxidation behavior of coated NiTaC-13, it was found that uncoated or thinly coated ends led to rapid weight losses (ref. 6). The losses were caused by oxidation of the ends and subsequent interfacial oxidation at the coating-substrate interface. To avoid this behavior, each pin was "end-capped" by depositing a weld bead of Ni20Cr at one end and welding on an~1-cm-long, 0.24-cm-diameter Ni20Cr wire to the other. The wire extension was fitted into holders during coating procedures. In this way, the NiTaC-13 was given a uniform coating exposure, while the parts of the pins that were more lightly coated as a result of line-of-sight limitations were Ni20Cr. Localized coating perforation caused by the thin deposition in these regions is therefore less likely to result in rapid oxidation, and should produce more representative weight-change data.

For the coatings deposited by vacuum evaporation using electron beam heating, a section was cut from the source ingot and placed in the water-cooled crucible. Prior to deposition, the specimens were centerless ground and lightly abraded with alumina powder. One or more specimens were mounted approximately 10 cm from the source in a specially designed motor-driven rotating device which turns them at approximately 10 rpm during deposition. The specimen temperature was controlled by use of a resistance-heated refractory metal foil mounted behind the pins. The pin temperature was measured using a Pt/Pt-Rh thermocouple placed in a stainless steel

tube (approximately the same mass as the specimens) which was mounted in close proximity to the specimens. The specimens were coated with a layer 75 to 100 μm thick, using a deposition temperature of 950° to 1000°C and a deposition rate of 4 to 5 μm/min.

The metal-sprayed specimens were coated using a flame-spray gun (wire feed) and a thermo spray gun (powder feed). A motor-driven rotating device turned a substrate pin at 200 rpm during deposition. The gun-to-substrate distances used were about 15 cm for the wire-source spraying and about 7 cm for the powder-source spraying.

The Pt layers were deposited by r-f sputtering. Several pin specimens held in fixed positions were placed 3.5 cm from the cathode and were sputter-deposited for 74 minutes, using a power of 500 watts. The system was cooled, opened, and the pins were rotated 120°. Then, the previously described sputter process was repeated. Again, the pins were rotated 120° and the sputter process was repeated. By this technique, a reasonably uniform Pt layer approximately 5 μm thick was deposited on the pin specimens.

Duplex coated samples were pack-aluminized in a 1% Al pack at 1060°C for 3 hours. The furnace atmosphere was dry argon. Sufficient Al-Al_2O_3 mixed powder was included in the pack to produce approximately 6 mg/cm^2 of Al during the pack cementation.

COATING EXPERIMENTS

Electron Beam Coatings

The following source ingots were used for E.B. depositions:

Ni-20Cr-10Al-1Y
Ni-20Cr-5Al
Ni-20Cr-5Al-1Y
Co-30Cr-5Al-1Y

Previous experience has shown that a nearly steady-state vapor composition is reached using NiCrAlY-type sources under the conditions of these experiments after the equivalent of one deposition run. Hence, the coatings in this study were deposited after the source ingot had been so conditioned.

At least three pins were coated with each of the above compositions. Representative samples were cut from one of the specimens for metallographic examination in the as-deposited and as-heat-treated (3 hours at 1160°C in argon) conditions. The other two or more pins were subjected to the cyclic oxidation test.

Figure 2(a) shows the Ni-20Cr-10Al-1Y coating in the as-deposited condition. The coating is practically flaw-free and is well bonded to the substrate.

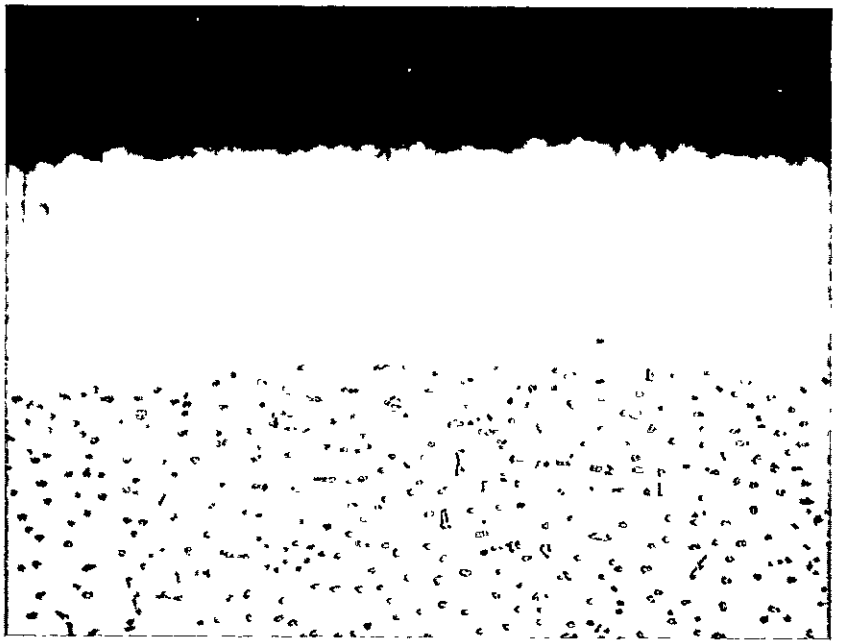

(a)

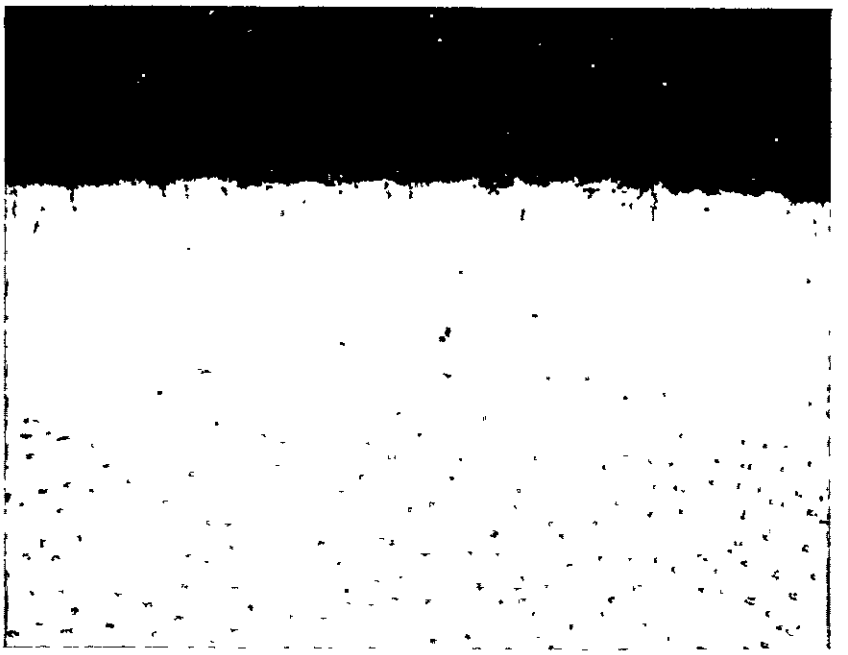

(b)

Figure 2. Ni-20Cr-10Al-1Y coating E. B. deposited onto NiTaC-13: (a) as-deposited, (b) heat treated 3 hours at 1160°C in Ar. 500X

After heat treatment, the coating is further densified, as is shown in figure 2(b). It can be noted that there is a region of carbide denudation after heat treatment and that a nearly continuous layer of a second-phase precipitate, probably a high-chromium phase, is present near the coating substrate interface.

The as-deposited Ni-20Cr-5Al coating is shown in figure 3(a). It can be seen that there are some radial flaws in this coating. These flaws were not healed by heat treatment, as can be seen in figure 3(b).

In contrast, there are very few flaws in the as-deposited Ni-20Cr-5Al-1Y coating shown in figure 4(a). This coating after heat treatment is shown in figure 4(b). It can be seen that the coating is very flaw-free and that the precipitate layer observed near the Ni-20Cr-10Al-1Y/substrate interface is almost nonexistent. There is evidence of oxidation at the surface of the heat-treated Ni-20Cr-5Al-1Y coating; perhaps the furnace atmosphere was not thoroughly dry.

The as-deposited Co-30Cr-5Al-1Y coating is quite flaw-free, as can be seen in figure 5(a). After heat treatment, the coating is further densified and there is little or no evidence of substrate decarburization as is shown in figure 5(b).

Pin specimens were coated with a 12-μm-thick layer of Ni, followed by a 75-μm-thick layer of Co-30Cr-5Al-1Y. Metallographic samples were prepared in the as-deposited, as-heat-treated, and as-aluminized conditions. These are shown in figure 6. The Ni layer forms an excellent bond between the substrate and the coating; however, some evidence of carbide denuding, apparently caused by the Ni layer, can be seen. Three of these specimens were aluminized and placed on the cyclic oxidation test; one of them was heat treated and placed on the cyclic oxidation test.

Three E.B. deposited Ni-20Cr-10Al-1Y coated pin specimens were shot-peened, heat treated, and placed on the cyclic oxidation test. Samples of this coating were examined metallographically before and after the shot-peening; the shot-peening had densified the coating, as can be seen in figure 7.

Metal Spray Coatings

An ingot containing Ni-20Cr-10Al-0.3Y-0.3C was melted and cast. Several attempts were made to fabricate this composition into wire to be used for applying carbon bearing coatings by metal spraying. However, the excessive brittleness of this alloy precluded that approach. An attempt was made to reduce the ingot to powder so that it could be applied by plasma arc spraying. Unfortunately, it was too tough to be ball-milled effectively.

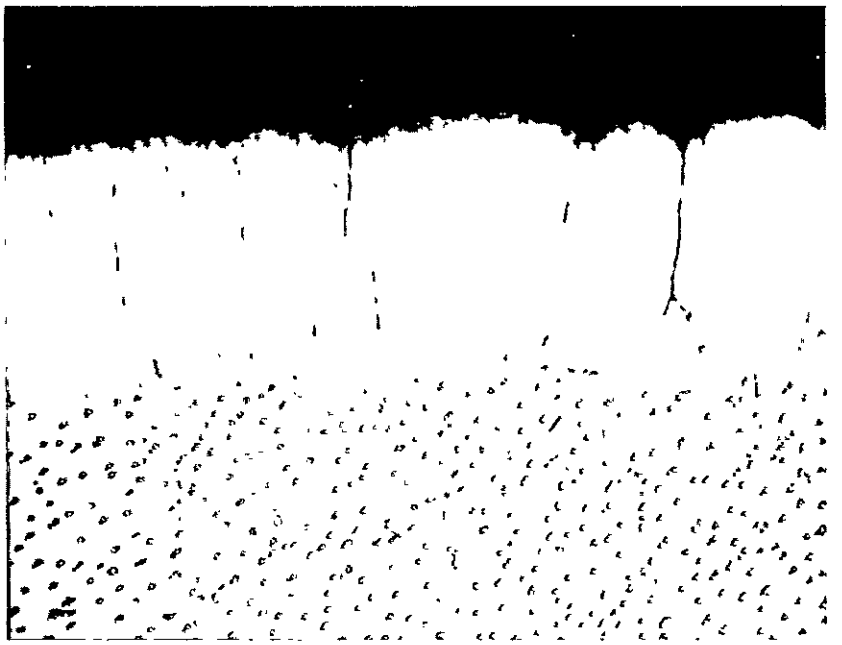

(a)

(b)

Figure 3. Ni-20Cr-5Al coating E.B. deposited onto NiTaC-13: (a) as-deposited, (b) heat treated 3 hours at 1160°C in Ar. 500X

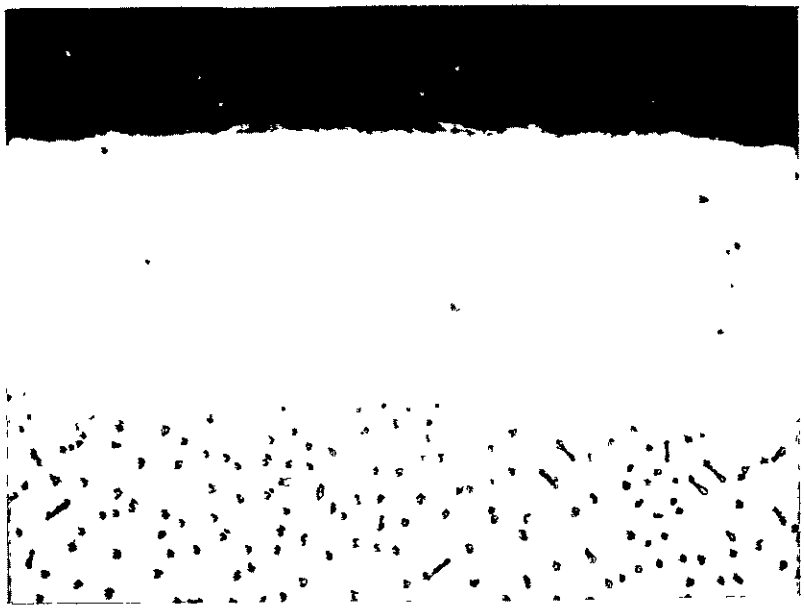

(a)

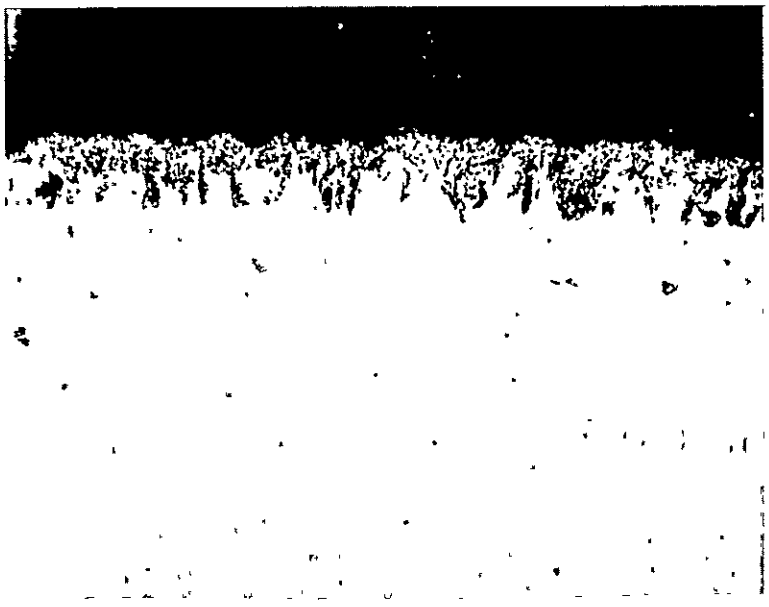

(b)

Figure 4. Ni-20Cr-5Al-1Y coating E.B. deposited onto NiTaC-13: (a) as-deposited, (b) heat treated 3 hours at 1160°C in Ar. 500X

(a)

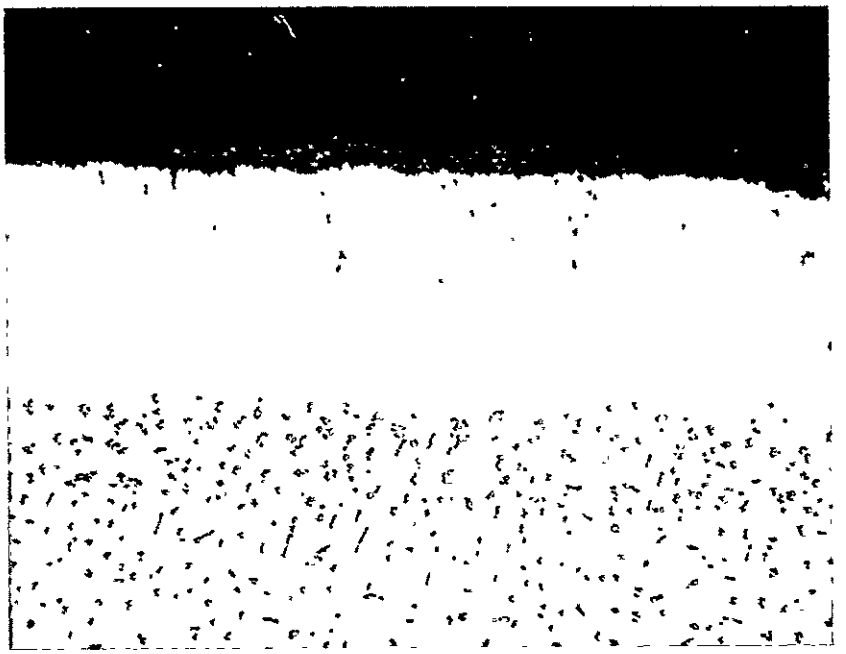

(b)

Figure 5. Co-30Cr-5Al-1Y coating E.B. deposited onto NiTaC-13: (a) as-deposited, (b) heat treated 3 hours at 1160°C in Ar. 500X

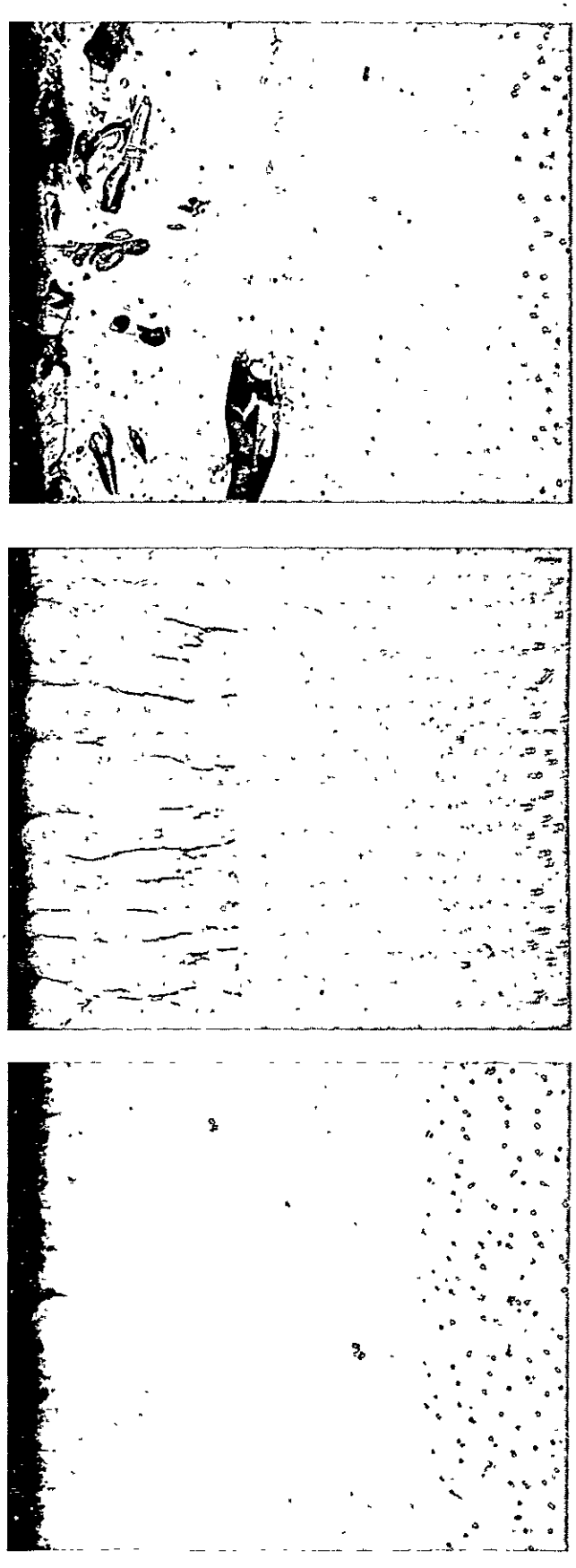

(a) (b) (c)

Figure 6. E.B. deposited Ni + Co-30Cr-5Al-1Y on NiTaC-13: (a) as-deposited, (b) after heat treatment, (c) after aluminization. 500X

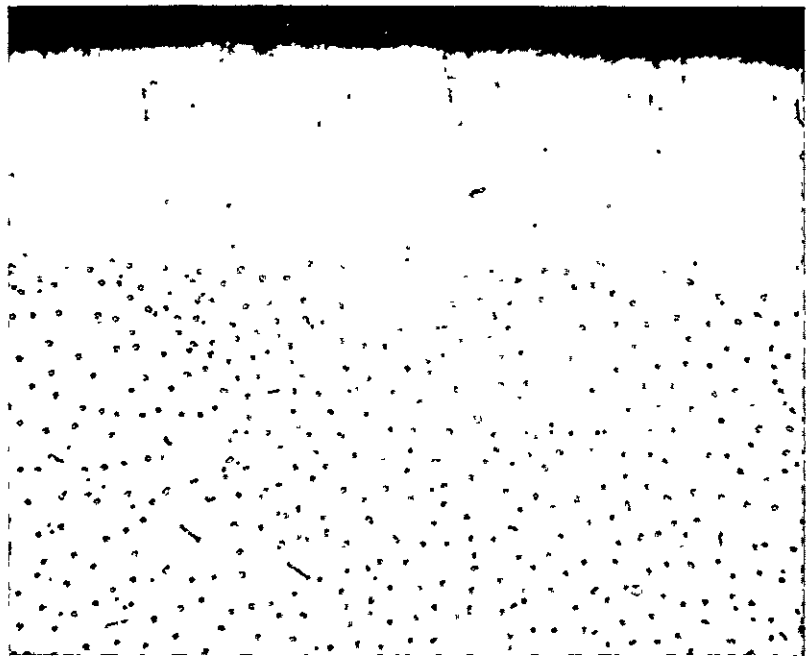

(a)

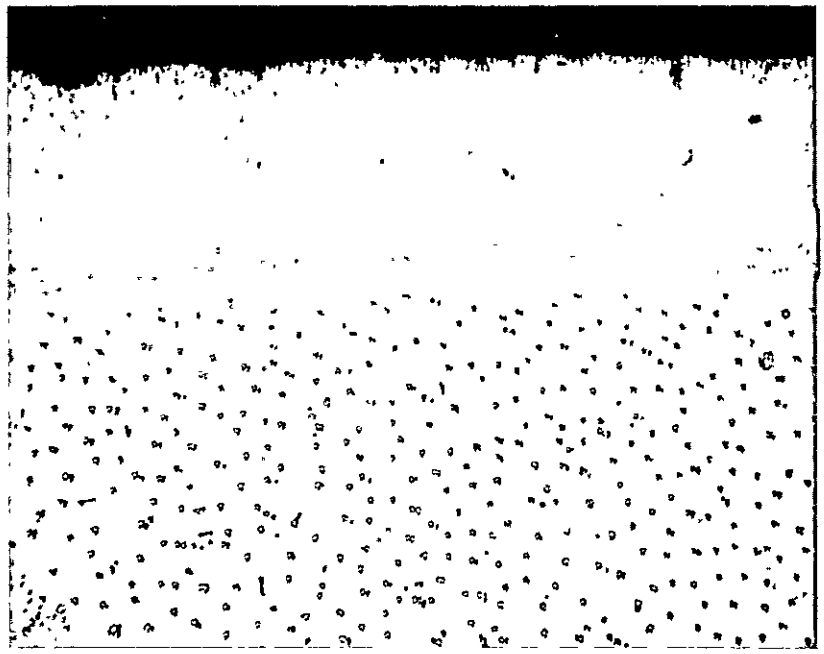

(b)

Figure 7. E.B. deposited Ni-20Cr-10Al-1Y on NiTaC-13: (a) as-deposited and shot peened, (b) after shot peening and heat treatment. 500X

An ingot containing Ni-20Cr-5Al-0.1Y-0.1C was prepared and this was successfully swaged to 0.32-cm-diameter wire suitable for metal spraying. Pin specimens were coated with layers about 50 to 100 μm thick using gun flame to preheat the surface. The coating as deposited is quite nonuniform in thickness and is porous as is shown in figure 8(a). Heat treatment did not densify the coating much, as can be seen in figure 8(b). However, it should be noted that there is very little substrate decarburization which indicates that this concept of carburizing the coating is a valid approach. However, the preheating did result in the formation of a thin oxide layer at the substrate-coating interface. It was considered possible that the denudation resistance might be a result of this oxide layer, rather than the carbon-bearing coating. Therefore, new specimens were prepared without the substrate preheat step. Micrographs of one of these specimens are shown in figure 9 in the as-deposited and as-heat treated conditions. In many regions of this sample, the bond between the coating and substrate was intimate. As before, the tendency toward carbide denudation is essentially eliminated.

A powder metal spray coating containing Ni-20Cr-10Al-0.1C was deposited onto pin specimens. This source material was prepared by mixing together powders of (CrC-Ni-Cr)+Al+Ni+Cr. These specimens were heat treated and placed on the thermal cycle test. Micrographs of samples of this coating are shown in figure 10, where it can be seen that the coating is quite porous and that carbide denudation has occurred. The carbon-bearing powder forms only a small fraction of the total powder volume. It is concluded that this coating approach will not prevent decarburization unless carbon can be more generally distributed throughout each powder particle, rather than being present in a small fraction of the powder particles.

Diffusion Barrier Coatings

A pin specimen was partially coated with variable thickness platinum layers by r-f sputter deposition. The pin was held in a fixed position and partially masked during sputtering so that the deposit covered about 270° of the circumference of the pin. Because of the angle-of-incidence effect, the Pt layer was 12-μm-thick maximum and tapered to less than 1 μm. A segment of this specimen was overcoated with a layer of E.B. deposited Ni-20Cr-10Al-1Y; then heat treated for 3 hours at 1160° C in argon.

Figure 11 shows metallographic cross sections of this coating system at three points: (a) no Pt; (b) medium thickness ($\sim$5 μm) Pt; and (c) thick ($\sim$12 μm) Pt. It appeared that the Pt layer was effective in reducing interaction between the NiTaC-13 and the Ni-20Cr-10Al-1Y. Note that there is an indication of porosity in the thick Pt region [figure 11(c)]. We concluded that a Pt layer 5 to 7 μm thick should be applied uniformly to additional samples.

(a)

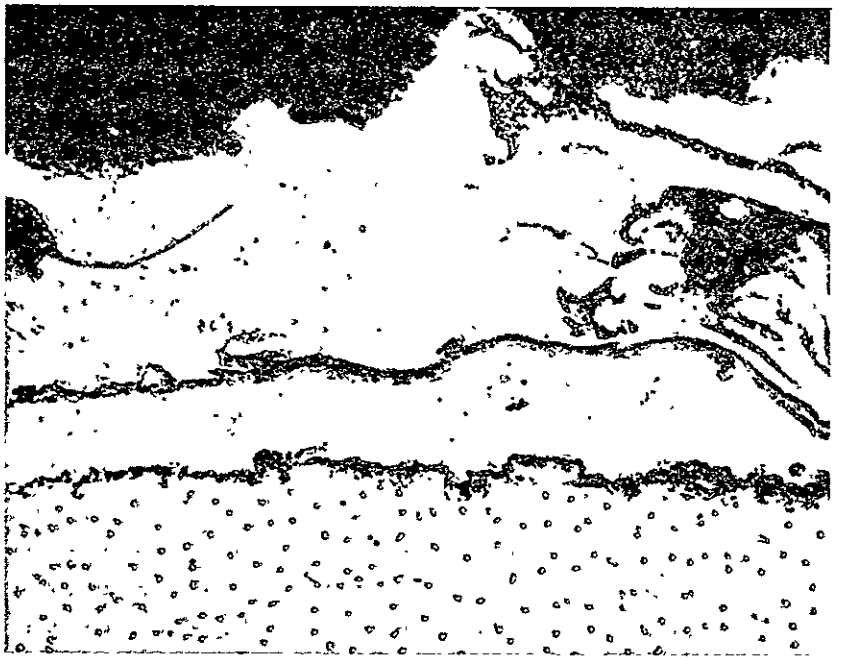

(b)

Figure 8. Ni-20Cr-5Al-0.1Y-0.1C coating metal spray deposited onto NiTaC-13: (a) as-deposited, (b) heat treated 3 hours at 1160°C in Ar. 500X

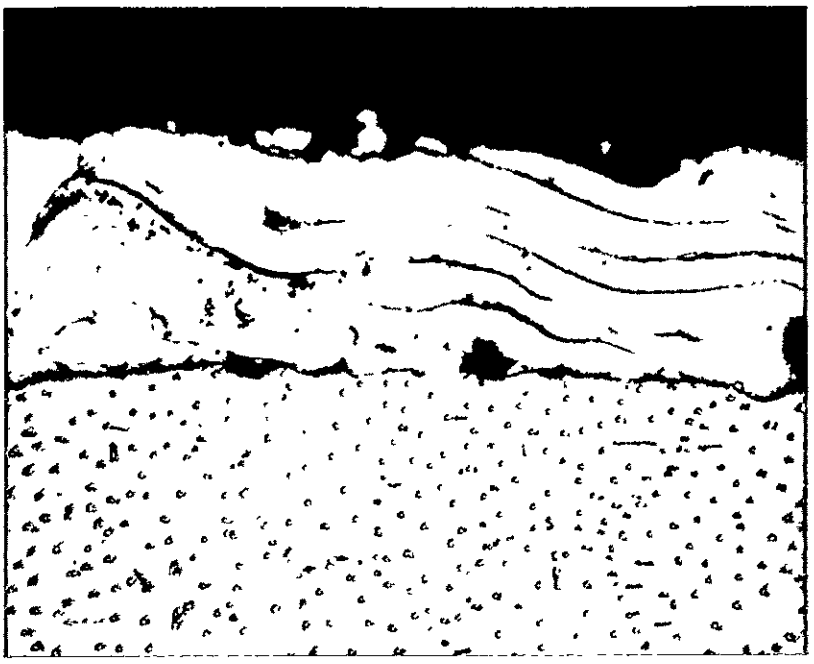

(a)

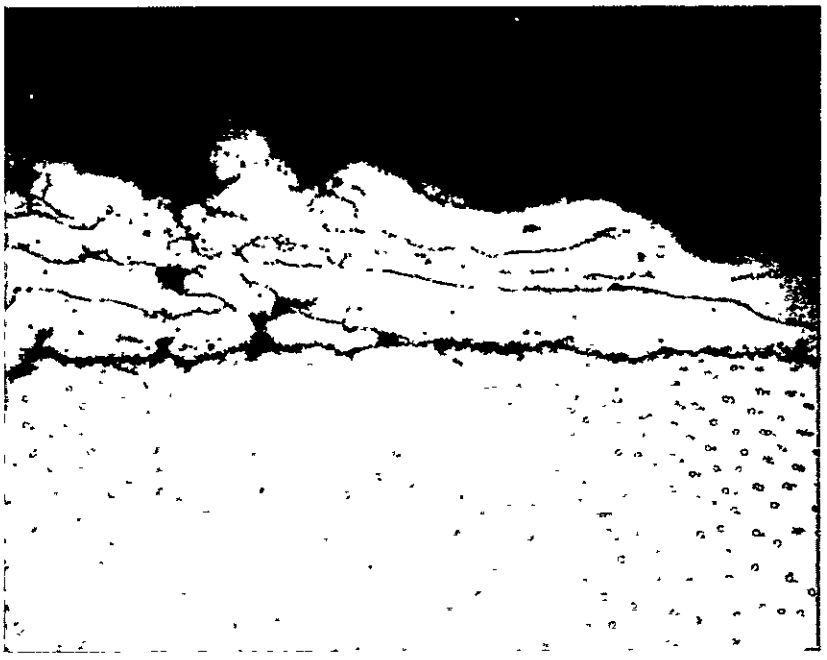

(b)

Figure 9. Ni-20Cr-5Al-0.1Y-0.1C spray deposited on NiTaC-13 without preheating the substrate: (a) as-deposited, (b) after heat treatment. 500X

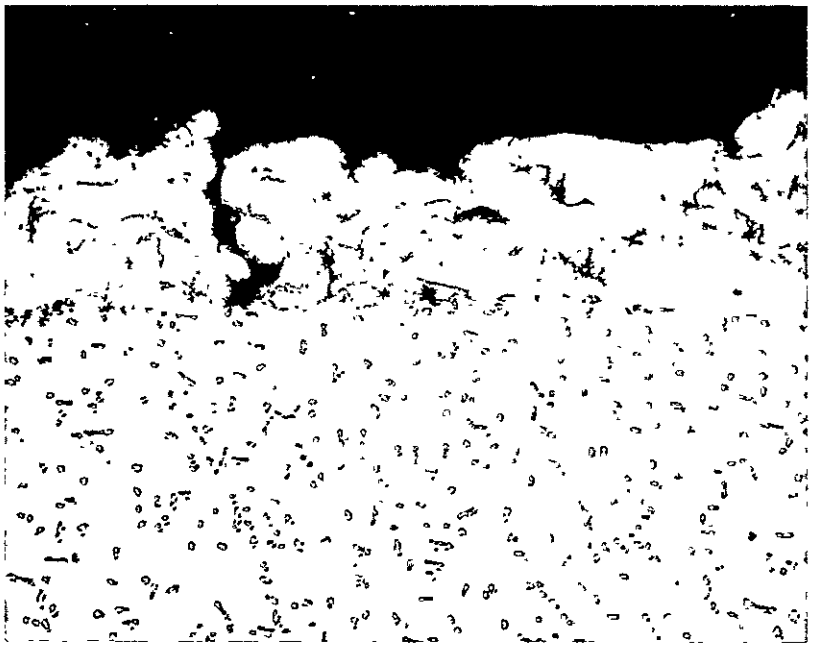

(a)

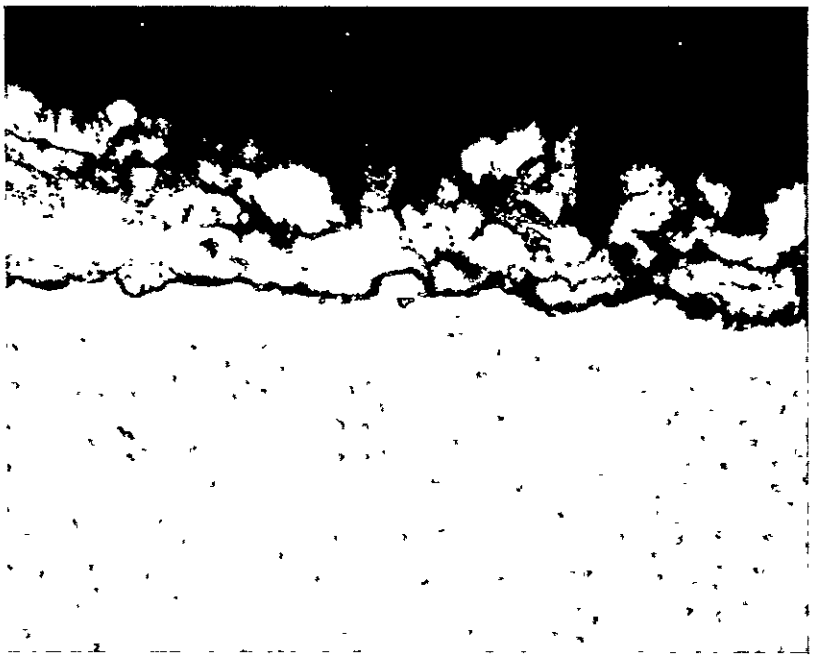

(b)

Figure 10. Mixed powders spray coating containing Ni-20Cr-10Al-0.1C on NiTaC-13: (a) as-deposited, (b) after heat treatment. 500X

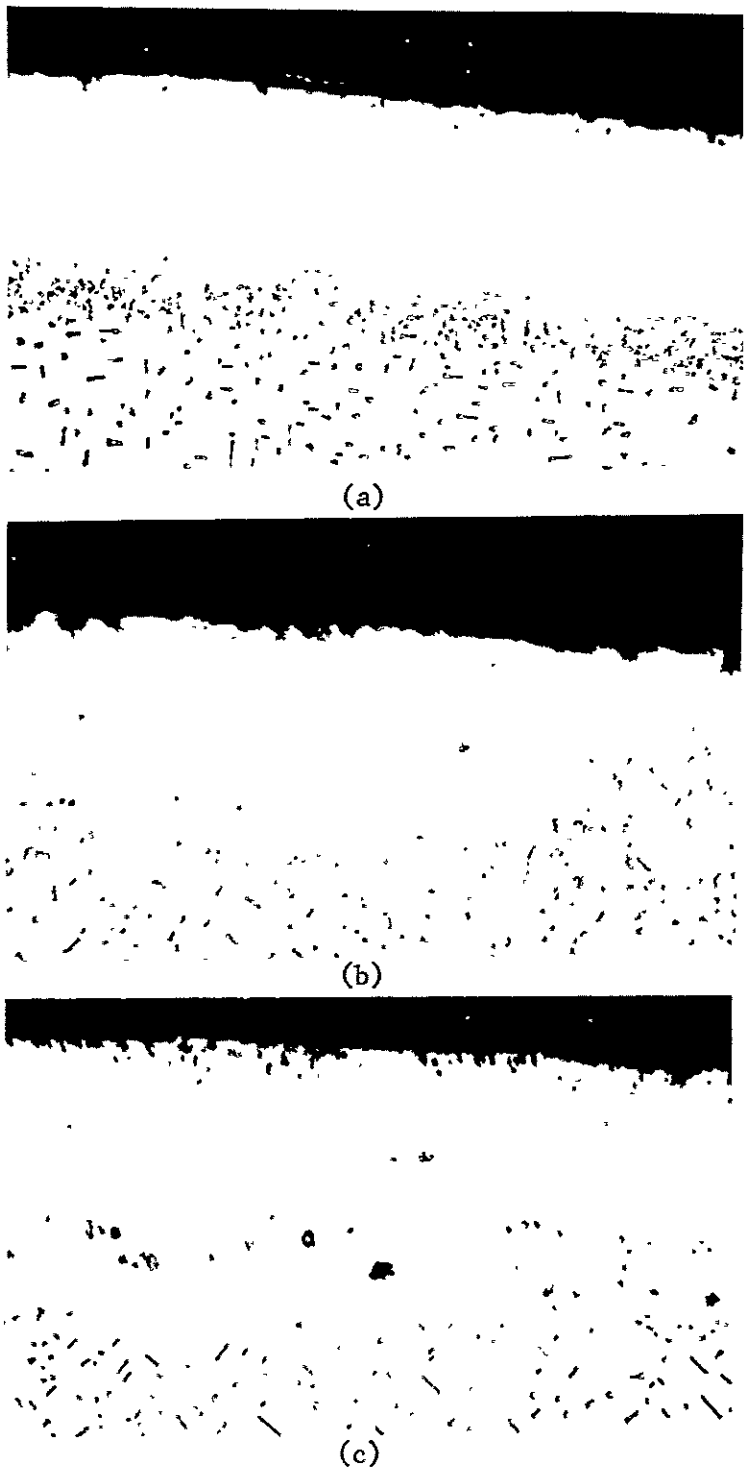

Figure 11. NiTaC-13 partially coated with a variable thickness layer of Pt; then coated with an E.B. deposited layer of Ni-20Cr-10Al-1Y; then heat treated for 3 hours at 1160°C in Ar: (a) no Pt; (b) medium thickness (5 μm) Pt; (c) thick (12 μm) Pt. 500X

Pin specimens were coated with a 5-μm-thick layer of Pt by sputtering; then they were overcoated with a 75-μm-thick layer of Ni-20Cr-10Al-1Y. Sections were cut from one of these specimens for metallographic examination.

As deposited, the Pt coating was adherent and quite uniform, but the NiCrAlY overcoat layer had many spike-type flaws as is shown in figure 12(a).

Samples of these pins were heat treated for either 3 hours at 1160° C in argon or 1 hour at 1230° C in argon. These are shown in figures 12(b) and (c). The 1230° C heat treatment closed the flaws better than the 1160° C heat treatment. However, there was a tendency for the coating to separate from the substrate in the Pt region after 1230° C heat treatment. Therefore, the 1160° C heat treatment was used for the pins placed on the cyclic oxidation test.

There is a carbide-denuded region adjacent to the Pt layer after heat treatment. A carbide-free region (including originally 5 μm of Pt) below the NiCrAlY layer is 22 μm thick after NiCrAlY deposition, and 38 to 44 μm thick after 3 hours at 1160° C or 1 hour at 1230° C. Apparently, the 1000° C NiCrAlY deposition causes substantial Pt-substrate interaction and carbide denudation. This indicates that the concept of Pt as a diffusion barrier is not valid; however, the samples were placed on the cyclic oxidation test.

Duplex Coating by Pack-Aluminization

Some of the E.B. coatings and the metal spray coatings were pack-aluminized to increase the aluminum concentration in the outer region. The aluminization was done in a 1% Al-99%Al_2O_3 pack that was activated by reacting the Al powder with HF prior to mixing it with the Al_2O_3. The processing conditions were 3 hours at 1060° C in an argon atmosphere. This aluminizing technique has previously been used to apply ~6 mg/cm^2 Al to superalloy substrates.

This duplex treatment densifies coatings such as is shown in figure 13(a) for the Ni-20Cr-5Al. There is a region of a predominantly white phase (probably high Cr) about 25 to 50 μm from the surface of Ni-20Cr-5Al. A similar region is found in the duplexed Ni-20Cr-5Al-1Y coating as can be seen in figure 13(b).

Of particular interest is the densification of the sprayed NiCrAlYC coating as is shown in figure 13(c). The white precipitate phase is not seen in this coating; however, there is an interaction region about 38 μm thick in the substrate. Carbide fibers remain intact.

Figure 13(d) is the duplexed Co-30Cr-5Al-1Y coating. Very little white phase precipitate is observed in this coating.

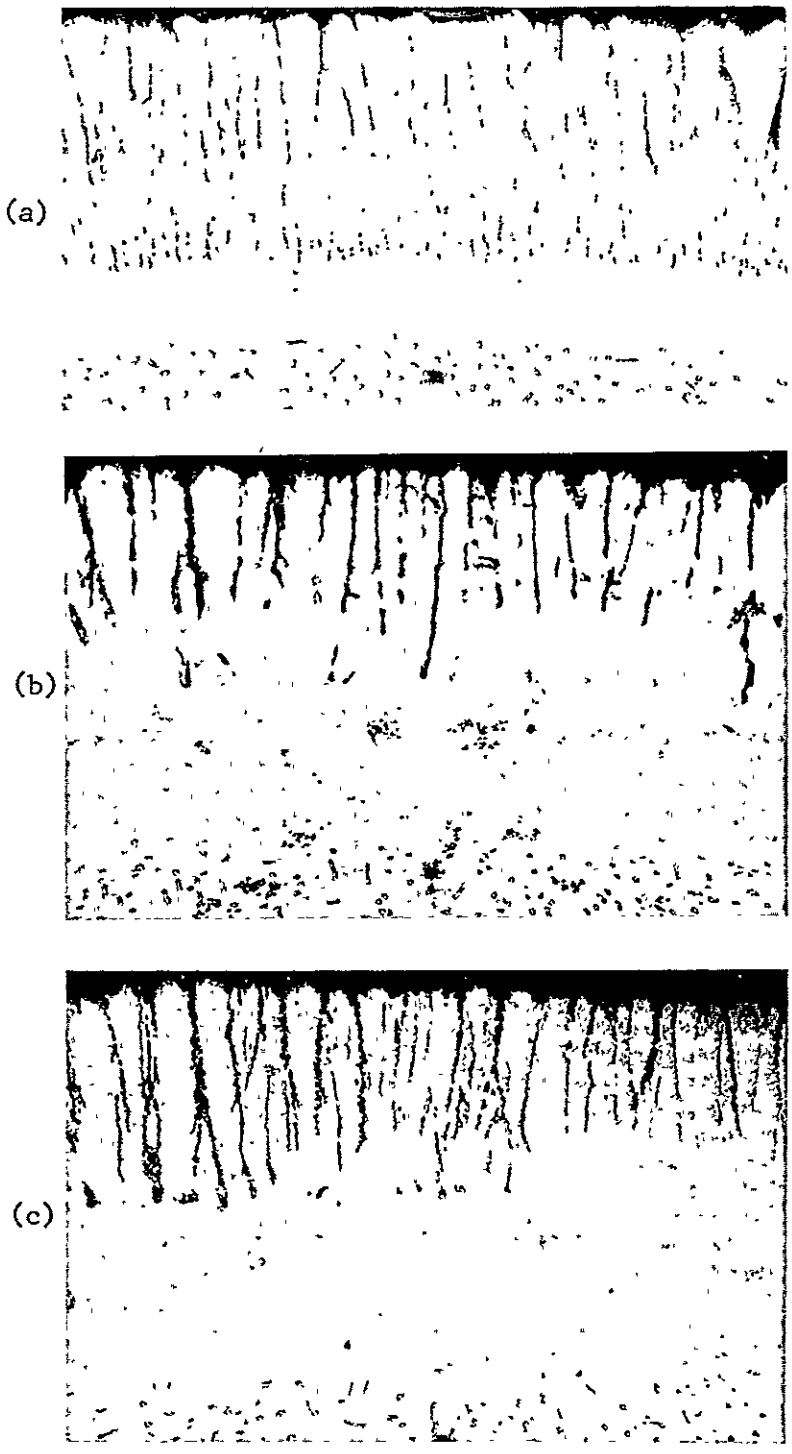

Figure 12. Sputtered Pt + E.B. deposited Ni-20Cr-10Al-1Y on NiTaC-13: (a) as-deposited, (b) after heat treatment: 3 hours at 1160°C; (c) after heat treatment; 1 hour at 1230°C. 500X (trans.)

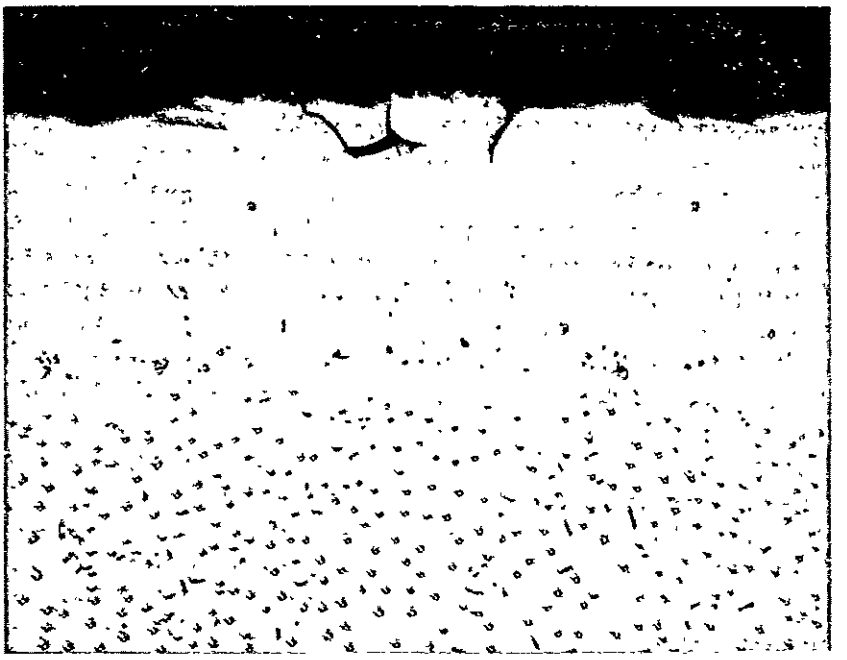

(a)

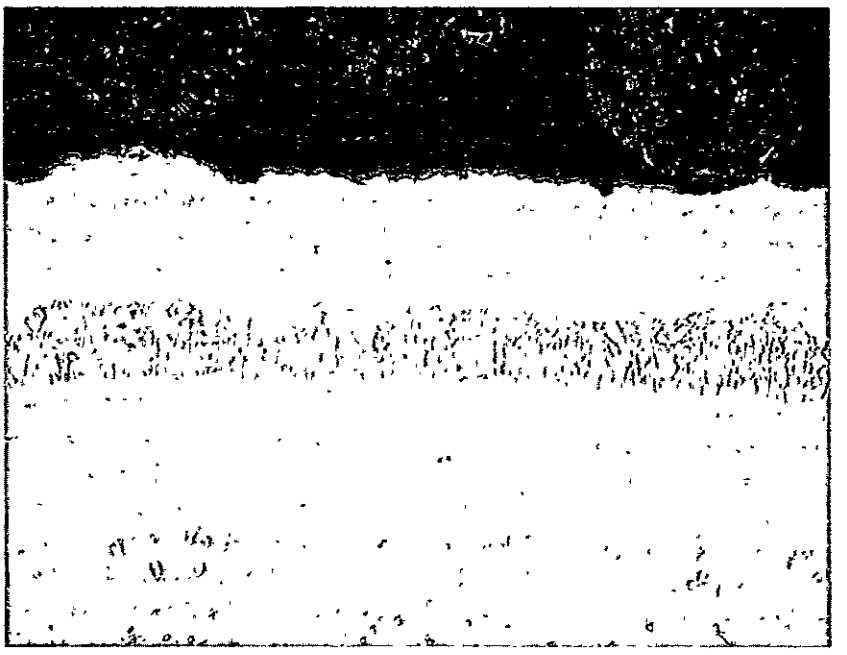

(b)

Figure 13. Duplex treated (aluminized) coatings on NiTaC-13: (a) E.B. deposited Ni-20Cr-5Al, (b) E.B. deposited Ni-20Cr-5Al-1Y. 500X

(c)

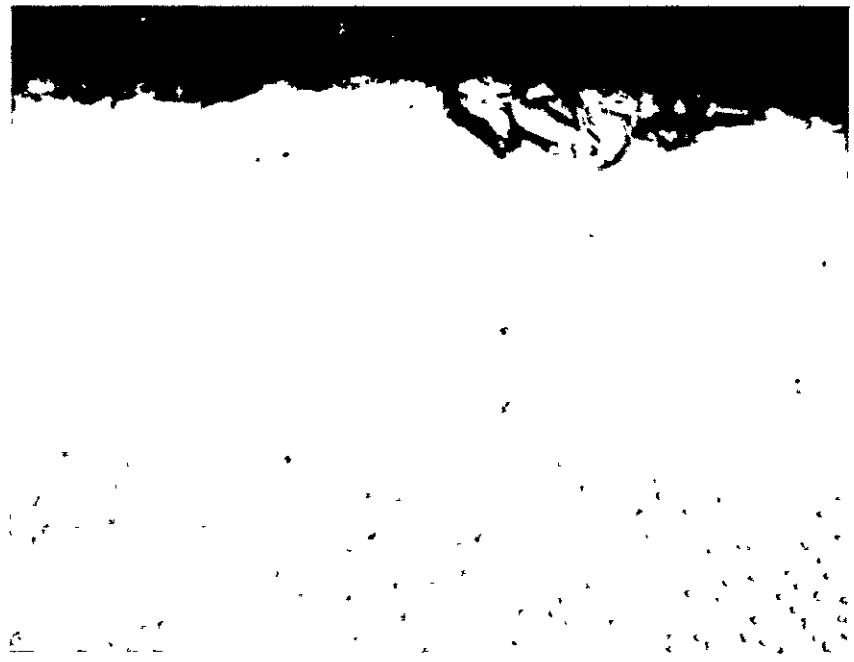

(d)

Figure 13. (Cont'd) Duplex treated (aluminized) coatings on NiTaC-13. (c) metal spray deposited Ni-20Cr-5Al-0.1Y-0.1C, (d) E.B. deposited Co-30Cr-5Al-1Y. 500X

CYCLIC OXIDATION TESTS

1100°C Maximum Temperature Cycling

A specimen holder for the cyclic furnace oxidation test was fabricated from X-750 with a capacity for up to 100 pins. One-hour cycle times were used. During each one-hour cycle, the specimens were in the 1100°C static air furnace for 50 minutes and then were removed for 10 minutes and forced-air-cooled to 93°C. Two or more specimens with the following coatings were tested:

E.B. Ni-20Cr-5Al-1Y
E.B. Ni-20Cr-5Al-1Y+aluminize
E.B. Ni-20Cr-5Al
E.B. Ni-20Cr-5Al+aluminize
E.B. Ni-20Cr-10Al-1Y
E.B. Ni-20Cr-10Al-1Y+aluminize
E.B. Co-30Cr-5Al-1Y
E.B. Co-30Cr-5Al-1Y+aluminize
Sprayed Ni-20Cr-5Al-0.1Y-0.1C
Sprayed Ni-20Cr-5Al-0.1Y-0.1C+aluminize

These specimens were removed from test at approximately 50- to 60-hour intervals for weight change measurements.

A difficulty was encountered with several of the oxidation test samples in that they tended to "stick" in the specimen holder. This was particularly true of the metal spray-coated samples. In forcibly removing these samples for weight change measurements, there was a tendency to damage the coating. Accelerated oxidation occurred in the damaged areas.

A new specimen holder was fabricated from X-750 and pack-aluminized prior to use. This holder was very resistant to oxidation and the problem of specimen sticking was largely overcome.

Table I is a summary of the cyclic oxidation test results of all of the specimens from this program. Specimens of the following six coating compositions survived at least 2000 hours of testing:

E.B. Ni-20Cr-5Al+aluminize (Specimens 4 and 5)
E.B. Ni-20Cr-5Al-1Y+aluminize (Specimens 15 and 16)
E.B. Ni-20Cr-10Al-1Y; heat treated (Specimen 19)
E.B. Ni-20Cr-10Al-1Y+aluminize (Specimens 21 and 22)
E.B. Co-30Cr-5Al-1Y+aluminize (Specimen 27)
Spray Ni-20Cr-5Al-0.1C-0.1Y+aluminize (Specimens 11 and 38)

Specimens coated with the three following compositions were available for further cyclic oxidation testing:

E.B. Ni-20Cr-5Al+aluminize (Specimen 5)
E.B. Ni-20Cr-5Al-1Y+aluminize (Specimen 16)
E.B. Ni-20Cr-10Al-1Y+aluminize (Specimen 22)

These specimens survived 3000 hours of testing.

The weight change measurements beyond 1500 to 2000 hours were not meaningful because of accelerated oxidation effects that occurred on all samples at or near the NiTaC-13/NiCr end-cap interface. Therefore, for the 2000-hour and 3000-hour specimens, the primary evaluation technique was metallographic examination. It appears that the E.B. coatings without duplex aluminizing are generally subject to early failure, probably because of accelerated oxidation through coating flaws. Duplex aluminizing apparently greatly improves coating life by sealing the flaws and by increasing the aluminum concentration in the outer region of the coating.

Cross sections of the three 3000-hour E.B. coatings (without carbon) are shown in figure 14. All show retention of 50 to 100 μm of coating. Of these coatings, it was decided that the Ni-20Cr-5Al+Al would be evaluated on Task II because the TaC fibers were retained better than for any of the other E.B. coatings. The reasons for this are unclear; however, this observation has been made on the 1000-, 2000-, and 3000-hour samples. Even so, the carbide denudation after 2000 hours was 250 to 500 μm deep into the substrate, and the remaining fibers were severely affected.

The second coating selected for Task II evaluation was spray-deposited Ni-20Cr-5Al-0.1Y-0.1C+Al. This coating was designed to minimize fiber denudation in the substrate by saturating the coating with carbon. It was found in two specimens tested in cyclic oxidation for 2000 hours that this approach is sound. Despite coating-substrate interactions, TaC fibers remained out to the original interface. Cross sections of these two specimens are shown in figure 15. Both show retention of 100 to 125 μm of coating. One of the specimens was oxidized by preheat treatment prior to spray coating; the other was coated without preheating. It can be seen that the TaC fibers were retained right up to the original substrate-coating interface.

The E.B. Ni-20Cr-10Al-1Y coating was highly oxidation-resistant; however, without the duplex aluminizing, it showed spike oxidation as can be seen in figure 16. This spike oxidation is believed to have occurred along flaws in the as-deposited coating.

Except for the Ni-20Cr-10Al-1Y coating, the nonaluminized coatings showed quite poor oxidation resistance. These failed coatings included:

E.B. Ni-20Cr-5Al
E.B. Ni-20Cr-5Al-1Y
E.B. Ni-20Cr-10Al-1Y (shot-peened)
Spray Ni-20Cr-5Al-0.1C-0.1Y

ORIGINAL PAGE IS
OF POOR QUALITY

TABLE I. - CYCLIC OXIDATION OF COATED NiTaC-13

[Conditions: 1 cycle per hour; 50 min at 1100° C, 10 min cooling to 93° C]

Specimen No.	Coating Composition	Heat treat[a] or Alum.[b]	% Weight Change				Remarks
			Maximum Increase		Last Reading		
			Hour	Δwt (mg/cm²)	Hour	Δwt (mg/cm²)	
1	E.B.Ni-20Cr-5Al	H.T.	465	+0.72	886	-94.9	(x) Specimen stuck in holder; completely damaged.
2	" "	"	563	+1.09	886	-51.8	(x) Coating breakthrough
3	E.B.Ni-20Cr-5Al	Alum	414	+0.73	1002	+ 0.25	(y)
4	" "	"	465	+0.86	2002	-19.5	(x)
5	" "	"	414	+1.02	3023	-108	(x)
6	Spray Ni-20Cr-5Al-0.1C-0.1Y	H.T.	Cont.	Wt. loss	Cont.	wt. loss	(x) Coating breakthrough
7	" "	"	"	" "	"	" "	(x) " "
8	" "	"	"	" "	"	" "	(x) " "
9	Spray Ni-20Cr-5Al-0.1C-0.1Y	Alum	326	+2.69	1002	+0.74	(y)
10	" "	"	30	+0.74	1510	-132	(x) End cap broke off in holder
11	" "	"	30	+0.86	2002	-17.8	(y)
12	E.B.Ni-20Cr-5Al-1Y*	H.T.	63	+0.80	497	-118	(x) Stuck in holder at 563 hours; removed from test.
13	" "	H.T.	326	+1.18	870	- 95	(x)
14	E.B. Ni-20Cr-5Al-1Y	Alum	414	+1.26	1002	-6.92	(y)
15	" "	"	414	+1.64	2002	-64	(x) End cap off
16	" "	"	414	+1.49	3023	-283	(x) Both end caps off
17	E.B.Ni-20Cr-10Al-1Y	H.T.	414	+2.78	659	-132	(y)
18	" "	"	1454	+6.36	1002	-68	(y)
19	" "	"	63	+0.91	2002	-232	(y) Both end caps off
20	EBNi-20Cr-10Al-1Y	Alum	414	+1.24	1002	-3.73	(x)
21	" "	"	414	+0.92	2002	-60	(y) End cap off
22	" "	"	326	+1.17	3023	-236	(y) End caps off.

TABLE I. - CYCLIC OXIDATION OF COATED NiTaC-13 (Cont'd)

[Conditions: 1 cycle per hour; 50 min at 1100° C, 10 min cooling to 93° C]

Specimen No.	Coating Composition	Heat treat[a] or Alum.[b]	% Weight Change				Remarks
			Maximum Increase		Last Reading		
			Hour	Δwt (mg/cm²)	hour	Δwt (mg/cm²)	
23	E.B.Co-30Cr-5Al-1Y	H.T.	119	+0.44	659	-152	(y) Stuck in holder
24	" "	"	119	+0.12		-113	(y)
25	E.B.Co-30Cr-5Al-1Y	Alum.	414	+1.12	768	-3.03	(x) Stuck in holder. Removed from test at 1002 hrs.
26	" "	"	414	+1.33	1306	-64	(y) Severe end oxidation.
27	" "	"	727	+2.19	2002	-131	(y) Severe end oxidation
28	Sputter Pt + E.B.Ni-20Cr-10Al-1Y	H.T.	94	+5.97	259	-51	(z)
29	" " "	"	94	+0.95	94	+0.95	(z)
30	" " "	"	94		94	+5.26	(z)
31	Spray-mixed powder Ni-20Cr-10Al-0.1C	H.T.	Not Measured		Not Measured		(z) Removed from test at 94 hr. Bad spalling; no weight measurement
32	" "	"	Continuous weight loss		259	-62	(z)
33	" "	"	Continuous weight loss		142	-39	(z)
34	Spray Ni-20Cr-5Al-0.1C-0.1Y (No pre-heat)	H.T.	No weight gain		94	-0.71	Specimen stuck in holder; coating flaking. Removed from test.
35.	" "	"	No weight gain		142	-13.3	Specimen stuck in holder; coating flaking. Removed from test.
36.	" "	"	94	+0.84	142	-2.77	Specimen stuck in holder. Coating flaking. Removed fm. test.

ORIGINAL PAGE IS
OF POOR QUALITY

TABLE I.- CYCLIC OXIDATION OF COATED NiTaC-13 (Cont'd)

[Conditions: 1 cycle per hour; 50 min at 1100°C, 10 min cooling to 93°C]

Coating Composition	Heat treat (a) or Alum. (b)	% Weight Change				Remarks
		Maximum Increase		Last Reading		
		Hour	Δwt (mg/cm²)	hour	Δwt (mg/cm²)	
37 Spray Ni-20Cr-5Al-0.1C-0.1Y (No pre-heat)	Alum	259	+5.26	1000	-5.01	(y)
38 " " "	"	304	+3.41	2020	-443	(x) End cap off
39 E.B.Ni-20Cr-10Al-1Y (shot peened)	H.T.	556	+2.67	1548	-258	(y) End cap off
40 " " "	"	120	+2.59	282	-8.18	(z) Removed from test.
41 " " "	"	282	+1.69	1000	-116	(y)
42 " " "	"	131	+2.69	943	-263	(y) End cap off
43 E.B.Ni+E.B.Co-30Cr-5Al-1Y	H.T.	304	+0.53	830	-23.7	(y) General oxidation. Ends oxidizing.
44 E.B.Ni+E.B.Co-30Cr-5Al-1Y	Alum.	344	+3.92	1719	-119	(y) End cap off
45 " " "	"	578	+3.62	1719	-288	(y) End cap off
46 " " "	"	344	+2.44	1000	-41	(y)

(a) = Heat treatment: 3 hr. at 1160°C in argon.
(b) = Aluminization: 3 hr. at 1060°C in argon.

(x) = Severe oxidation near end caps.
(y) = Moderate oxidation near end caps
(z) = Coating splitting.

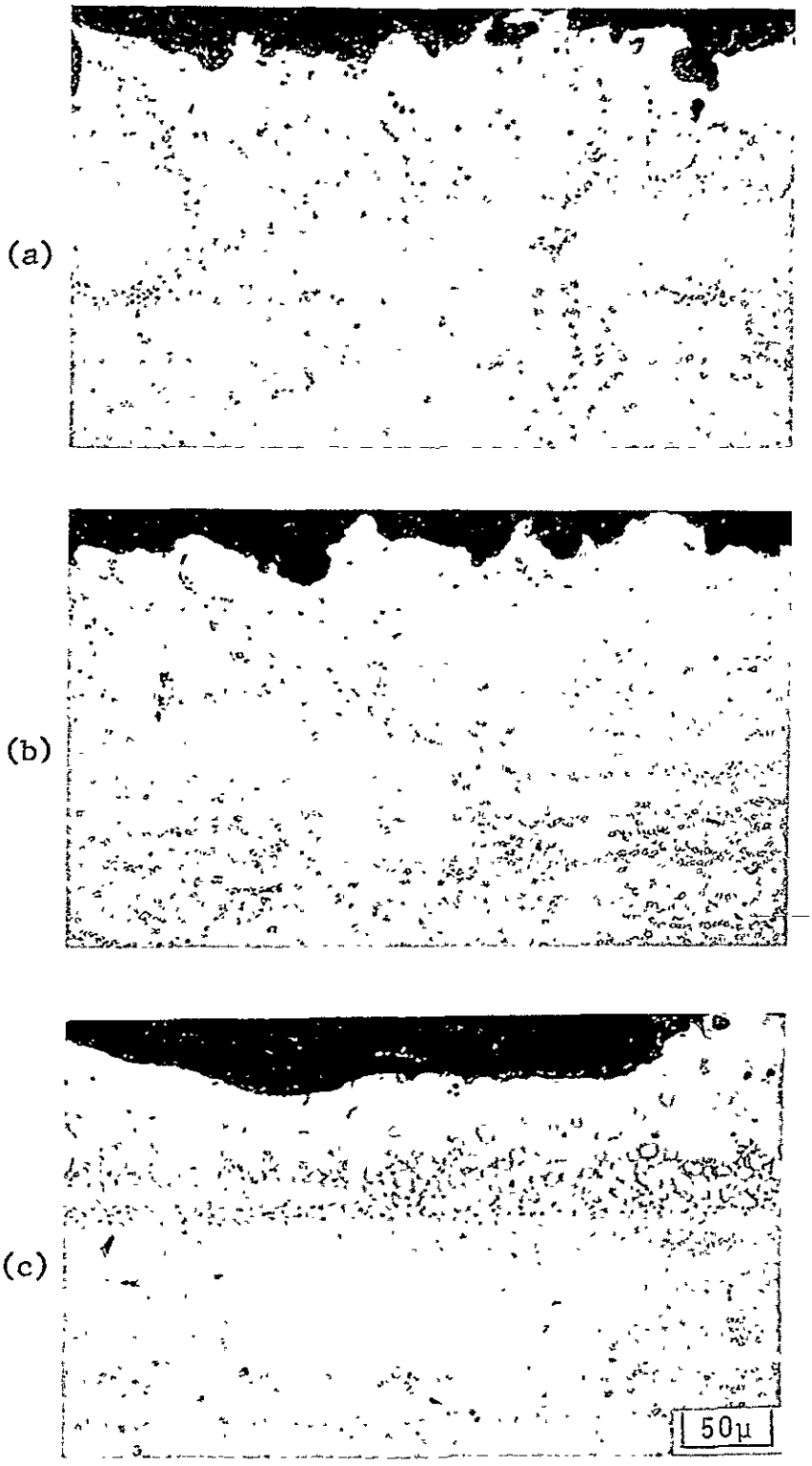

Figure 14. E.B. coatings on NiTaC-13 after 3023 hours of cyclic oxidation to 1100° C: (a) Ni-20Cr-5Al+Al, (b) Ni-20Cr-5Al-1Y+Al, (c) Ni-20Cr-10Al-1Y+Al.

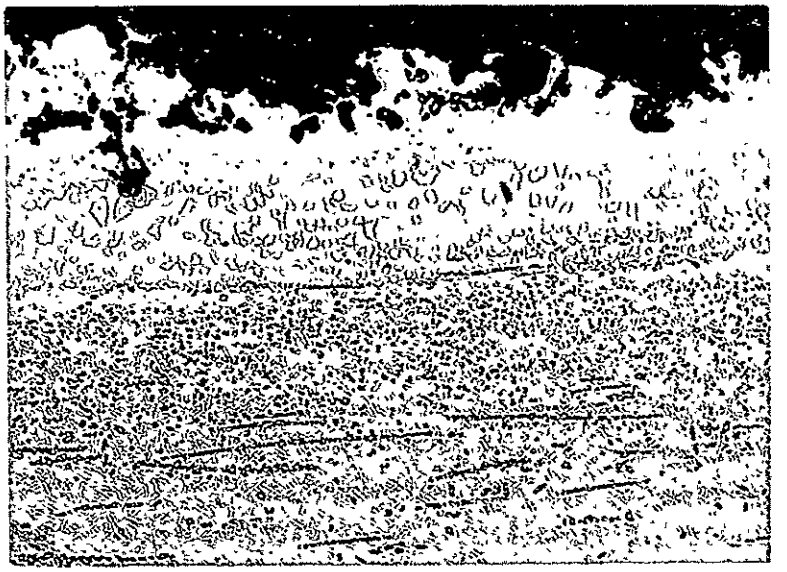

(a)

(b)

Figure 15. Spray Ni-20Cr-5Al-0.1Y-0.1C+aluminize on NiTaC-13 after 2000 hours of cyclic oxidation (1100°-93°C): (a) substrate oxidized prior to spray coating, (b) substrate not oxidized prior to spray coating.

Figure 16. E.B. Ni-20Cr-10Al-1Y on NiTaC-13 after 2000 hours cyclic oxidation (1100° -93° C).

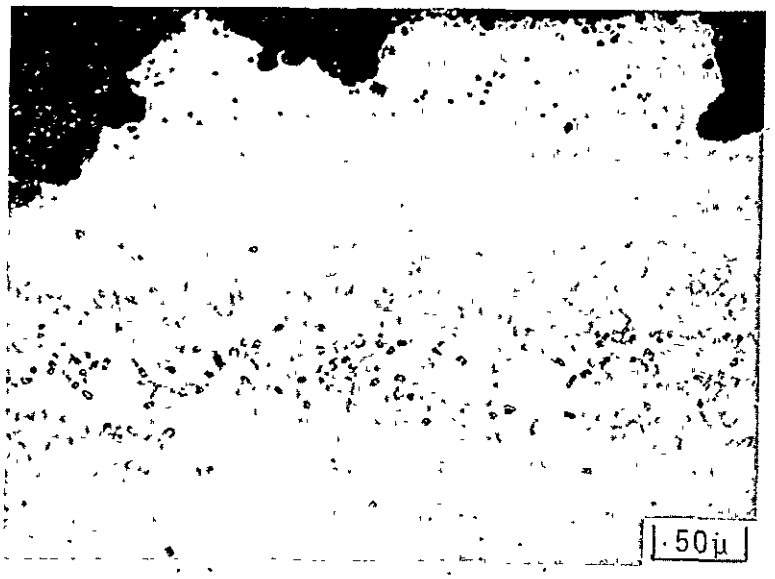

Figure 17. E.B. Co-30Cr-5Al-1Y+aluminize on NiTaC-13 after 2000 hours cyclic oxidation (1100° -93° C).

The E.B. Co-30Cr-5Al-1Y+aluminize coating after 2000 hours of cyclic oxidation is shown in figure 17. There was no tendency for this coating to delaminate at the coating-substrate interface. The same coating without pack-aluminizing has exhibited failure by delamination (ref. 6), and that result was confirmed in this study.

The Pt+Ni-20Cr-10Al-1Y coated samples (Specimens 28 to 30) all failed and were removed from test. The coating "split" off the substrate in what appears to be the Pt region. Possibly a brittle PtAl-type phase forms which fails during thermal cycling.

The powder spray deposited Ni-20Cr-10Al-0.1C coatings also failed early during testing. The coating was severely oxidized at particle boundaries. Because the carbon was initially present in relatively few of the particles (1.5 wt%), the coating did not retard substrate denudation of TaC fibers.

1150° C Maximum Temperature Cycling

In a parallel General Electric-supported effort, samples were subjected to one-hour cycling in a static air furnace between 93° C and 1150° C. The temperature of 1150° C was chosen to determine if the full temperature advantage anticipated for directional eutectic alloys may be realized (ref. 13). Because weight change had not been measured for uncoated γ/γ' NiTaC-13 for cycling to 1150° C, this alloy was included with coated samples. Another eutectic type system under consideration for jet engine turbine blade application γ/γ'-δ (Ni, 2.5Al, 19.0Cb, 6Cr), was cast and also cycled for comparison.

The cyclic oxidation response of γ/γ' NiTaC-13 and γ/γ'-δ are compared in figure 18. The advantage held by γ/γ'-δ 1100° C cyclic oxidation no longer exists for 1150° C cyclic oxidation. Weight change data for the two alloys at 1150° C are indistinguishable.

The appearance of pins after 100 hours of cyclic oxidation is illustrated in figure 19. All pins were initially 0.25 cm in diameter, with coatings increasing the diameters to 0.27 cm. Substantial cross section has been lost on the uncoated NiTaC-13 and γ/γ'-δ pins. Most of the coated pins exhibit well-protected midsections, but the ends show signs of cracking and interaction with the cyclic oxidation holder. The coatings shown include E.B. Ni-20Cr-5Al, Ni-20Cr-5Al-1Y, Ni-20Cr-5Al-0.1C-0.1Y (wire-sprayed), and Ni-20Cr-10Al-1Y. All coatings shown were pack-aluminized as well. The spray coating was thicker than is optimum, and subsequent aluminizing did not completely bond and densify the spray coating. Localized oxidation can be seen on the spray coated pins.

In terms of weight change measurements for the coated pins cyclically oxidized at 1150° C, data for the four coatings are very similar. Figure 20 compares weight change for one of each of these coatings through 100 hours

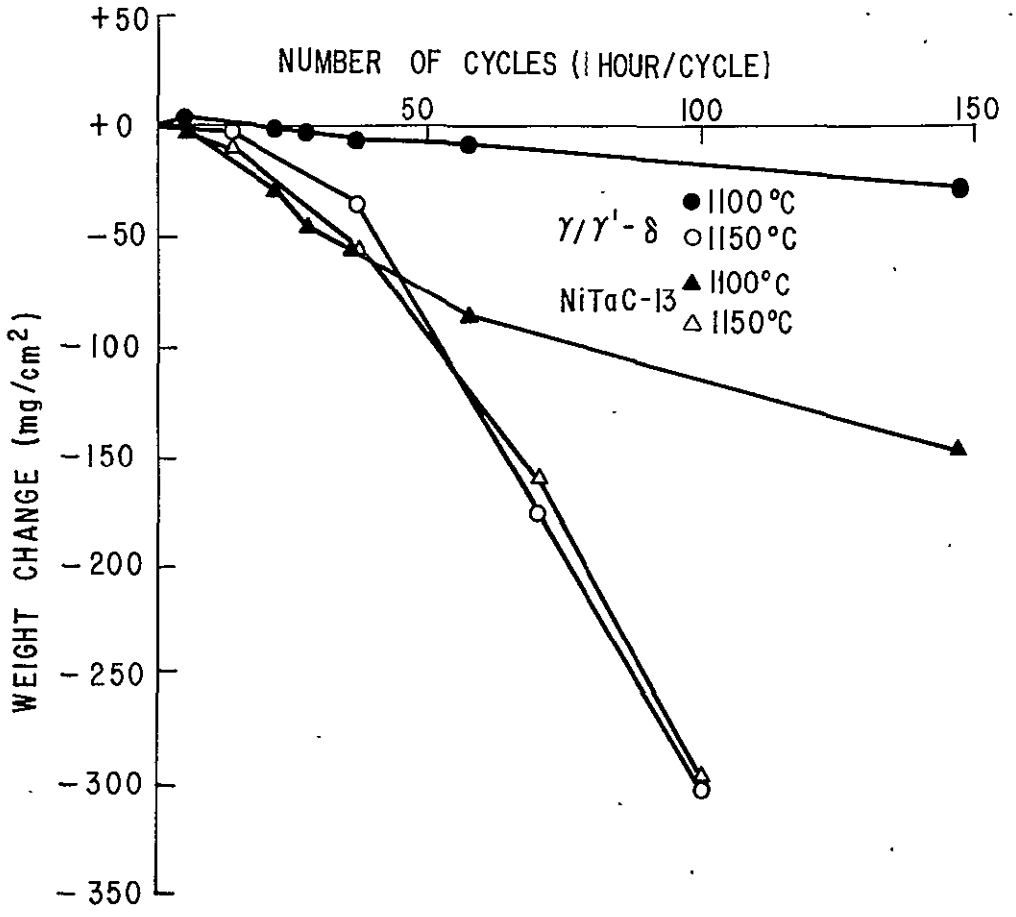

Figure 18. Weight Change as a function of number of 1-hour cyclic oxidation exposures to 1100° or 1150° C for NiTaC-13 and γ/γ'-δ pins.

of cycling. The end-cap attack must be considered in analyzing the data in figure 20. Except for data for the spray coated pins exhibiting localized oxidation, data probably reflect changes occurring at the end caps, with the midsections being much more resistant to oxidation and spallation.

Microstructures through longitudinal sections of coated NiTaC-13 are shown in figure 21. As noted for 1100° C cyclic oxidation, no denudation of TaC fibers is seen for 1150° C cyclic oxidation of NiTaC-13 coated with the Ni-20Cr-5Al-0.1C-0.1Y+Al coating. The denudation in the E.B. Ni-20Cr-5Al+Al was very slight in the 100-hour test. Both of the other E.B. coatings shown in figure 21 caused fiber denudation. The yttrium in the coatings seems to have a dominant part in denudation. The presence of Y alone is not sufficient, since the carbon-containing spray coating also includes 0.1Y in its wire composition. Nor is the absence of Y sufficient to avoid denudation, since fiber loss was noted previously for aluminized Ni35Cr coatings (ref. 6).

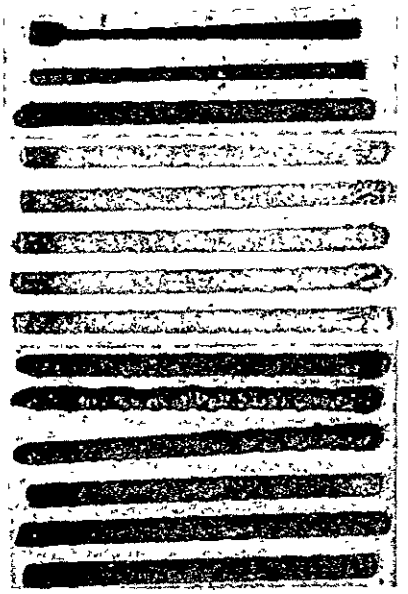

Figure 19. Macrophotographs of pins cycled 100 hours to 1150° C. From the top: bare NiTaC-13, bare $\gamma/\gamma'-\delta$, and pins of NiTaC-13 coated with Ni-20Cr-5Al+5Al (3 pins), Ni-20Cr-5Al-1Y+Al (3 pins), Ni-20Cr-5Al-0.1Y-0.1C+Al (3 pins), Ni-20Cr-10Al-1Y+Al (3 pins). 1.3X

750° C Maximum Temperature Cycling

In a parallel General Electric-supported effort, samples of uncoated γ/γ NiTaC-13 $\gamma/\gamma'-\delta$ type eutectics with Hastelloy-X were subjected to one-hour cycling in a static air furnace between 93° C and 750° C. The temperature of 750° C was chosen to simulate the maximum temperature likely to be reached in the root (or dovetail) section of jet engine turbine blades.

Weight change data for the three alloys are shown in figure 22. The total weight changes for both eutectics after 3100 hours of cycling are small. The weight gains correspond to ~3 μm of Al_2O_3 formation for NiTaC-13, and ~15 μm of Al_2O_3 formation for $\gamma/\gamma'-\delta$, if oxidation is uniform. For NiTaC-13, the surface of the sample retains a metallic sheen with a slight green cast to it. The $\gamma/\gamma'-\delta$ is no longer metallic in surface appearance, but is covered with a yellow-green layer of oxide. Microstructures of transverse sections of the two alloys are shown in figure 23. Apparently, NiTaC-13 type alloys will not require a coating for turbine blade roots. The preferential oxidation in $\gamma/\gamma'-\delta$, observed here and under another NASA program

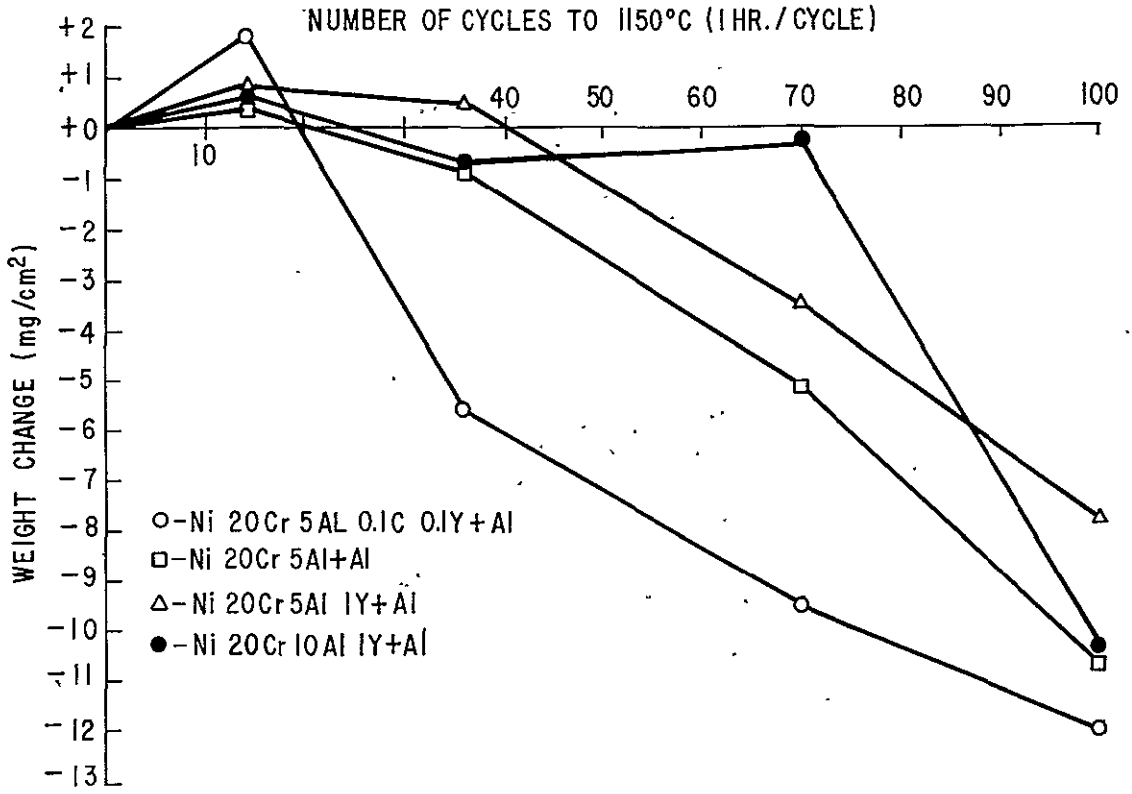

Figure 20. Weight change as a function of number of 1-hour cyclic oxidation exposures to 1150° C for coated NiTaC-13 pins.

(ref. 17), may require coatings for root sections of turbine blades. This probability has been noted previously (ref. 13).

CYCLIC EXPOSURE OF COATED RUPTURE BARS

Burner Rig Cyclic Exposure

For the first part of Task II, stress rupture test bars of NiTaC-13 were coated with the two preferred coatings: EBNi-20Cr-5Al+Al and wire sprayed Ni-20Cr-5Al-0.1C-0.1Y+Al. These bars were then cycle exposed in a burner rig as described in ref. 6. The burner rig used in this study is shown in figure 24 (ref. 14). Jet engine fuel (JP-5) was combusted in the front section of the furnace, and the hot gases impinged at a low velocity (Mach 0.05) on the bars supported on a rotating sample holder located at the rear of the furnace. The combusted fuel heated the bars to 1100° C. The rear section of the furnace is split and hinged to rotate away so that it exposes the sample holder. Samples were removed about once an hour and placed in a cooling rack until they cooled to below 93° C. The samples were then returned to the burner rig. This process was repeated 6 to 8 times during normal working hours, and the samples remained at 1100° C for 16 hours overnight.

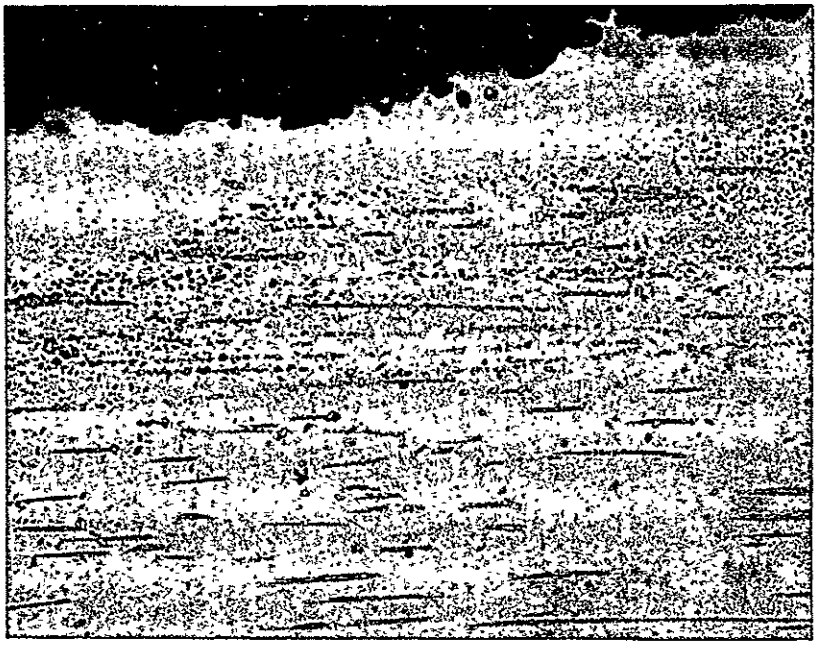

(a)

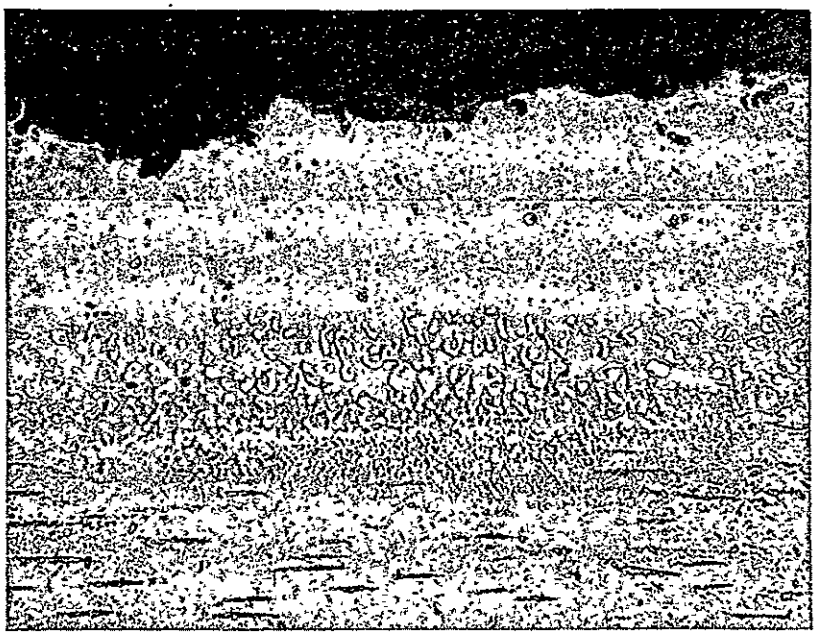

(b)

Figure 21. Longitudinal sections through coated NiTaC-13 pins cyclically oxidized 100 hours to 1150° C: (a) Ni-20Cr-5Al-0.1Y-0.1C+Al, (b) Ni-20Cr-5Al+Al. 500X

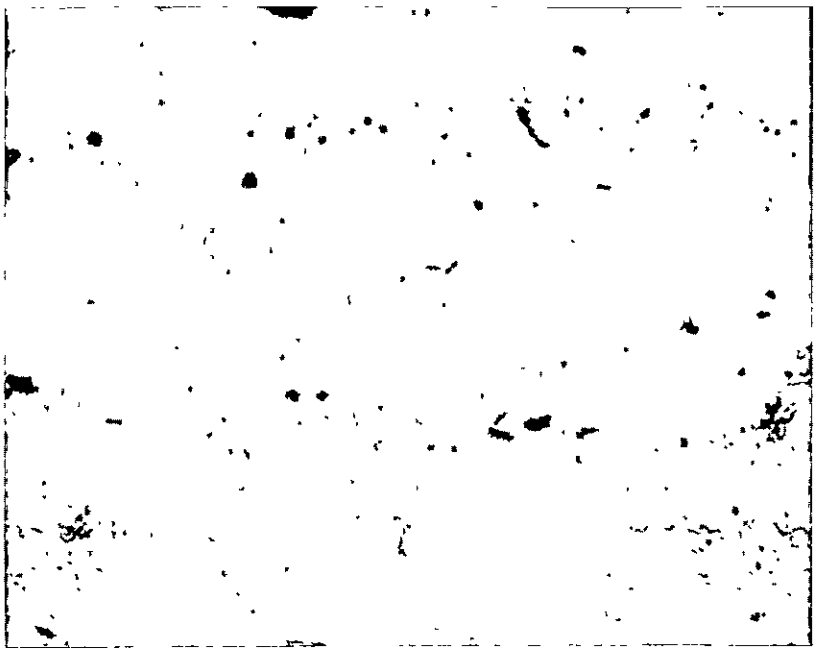

(c)

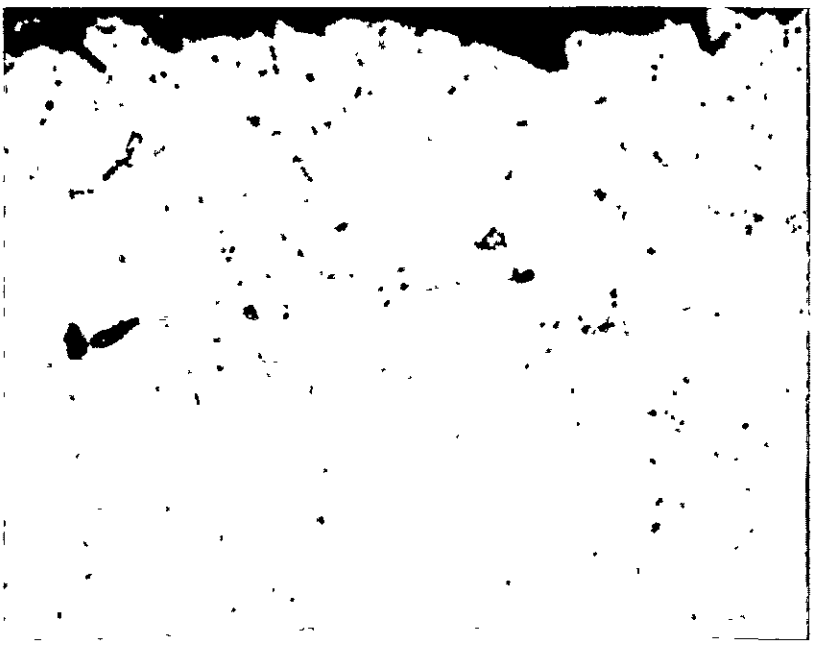

(d)

Figure 21. (Cont'd) Longitudinal sections through coated NiTaC-13 pins cyclically oxidized 100 hours to 1150°C: (c) Ni-20Cr-5Al-1Y+Al, (d) Ni-20Cr-10Al-1Y+Al. 500X

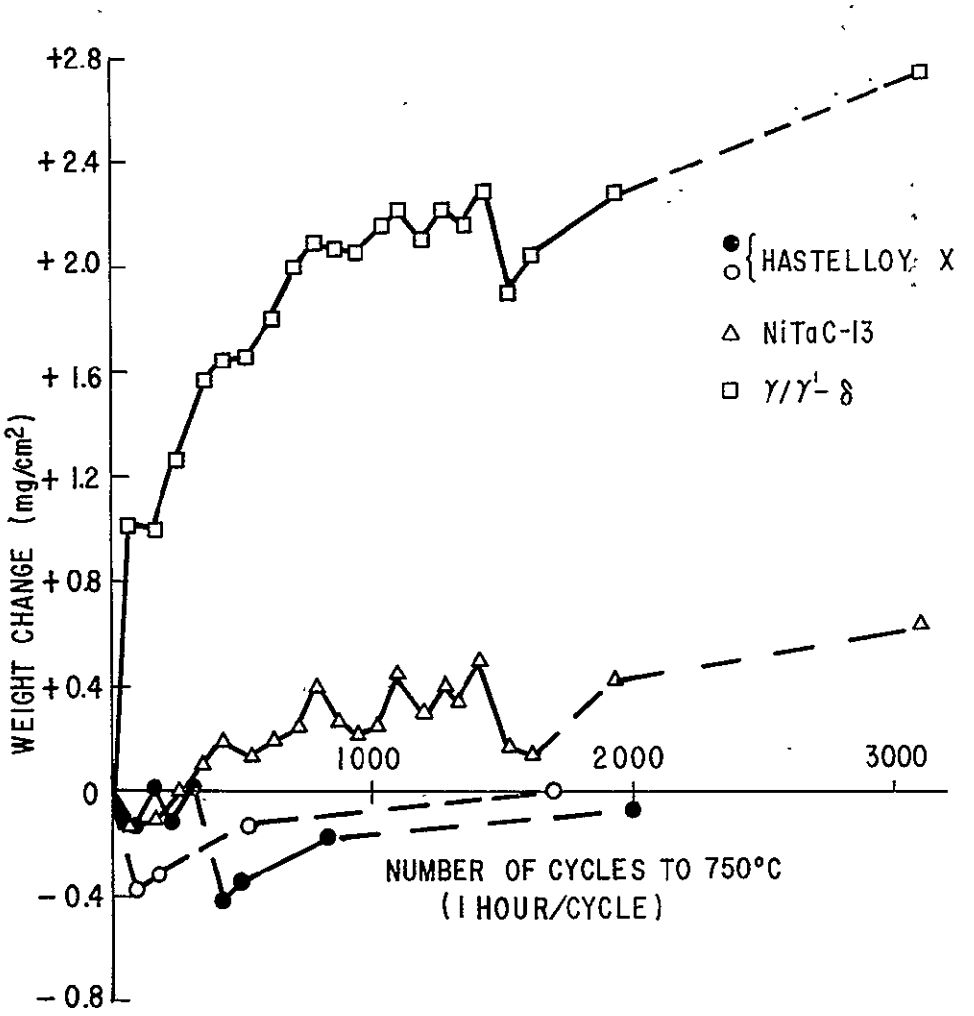

Figure 22. Weight change as a function of number of 1-hour cyclic oxidation exposures to 750°C for NiTaC-13, γ/γ'-δ, and Hastelloy-X.

Previous work on cyclic oxidation of coated rupture bars of NiTaC-13 showed that the roots, shoulders, and ends of the rupture bars exhibited early coating failure (ref. 6). For E.B. coatings, this is believed to be caused by the very thin coating on ends and roots that results from line-of-sight limitations of the process. Once the thin coating is penetrated, oxidation occurring at the coating substrate interface can limit the usefulness of test bars for subsequent stress rupture testing. For this reason, it was decided to coat the rupture bars with a flame-sprayed powder while the gauge sections of the bars were masked with Ta foil. Two spray powders were considered: Ni-20Cr, and Ni-10Cr-5Al. Both coatings were aluminized to accomplish bonding and densification of the powder sprayed coatings. After 486 hours of cyclic oxidation, the aluminized Ni-10Cr-5Al+Al coating was

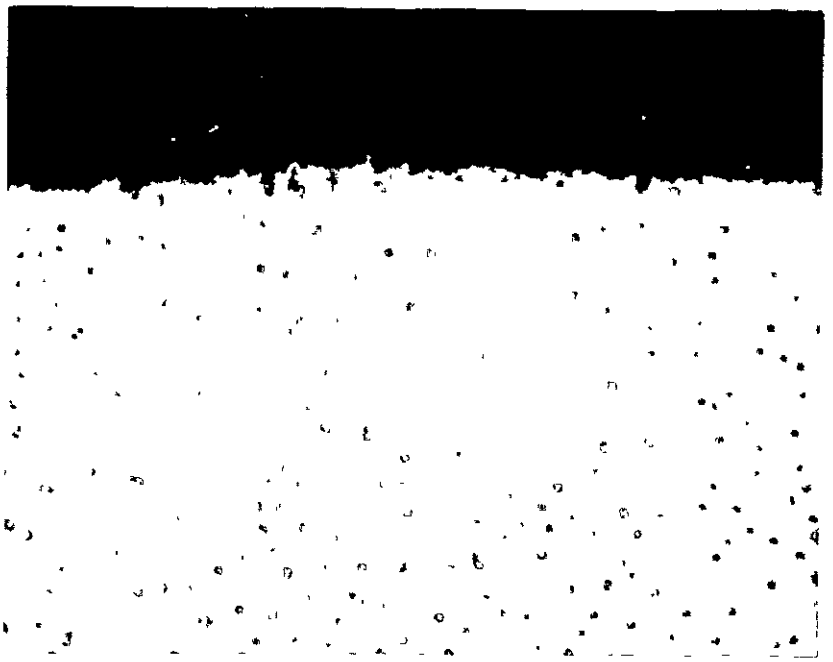

(a) Transverse

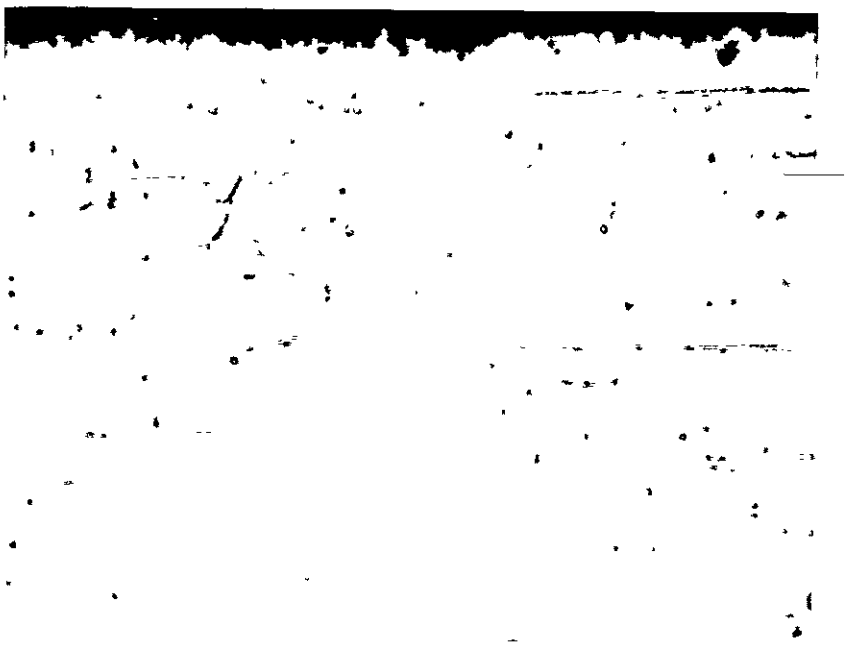

Longitudinal

Figure 23. Transverse and longitudinal sections through (a) NiTaC-13 subjected to 3102 hours of cyclic oxidation to 750°C. 750X.

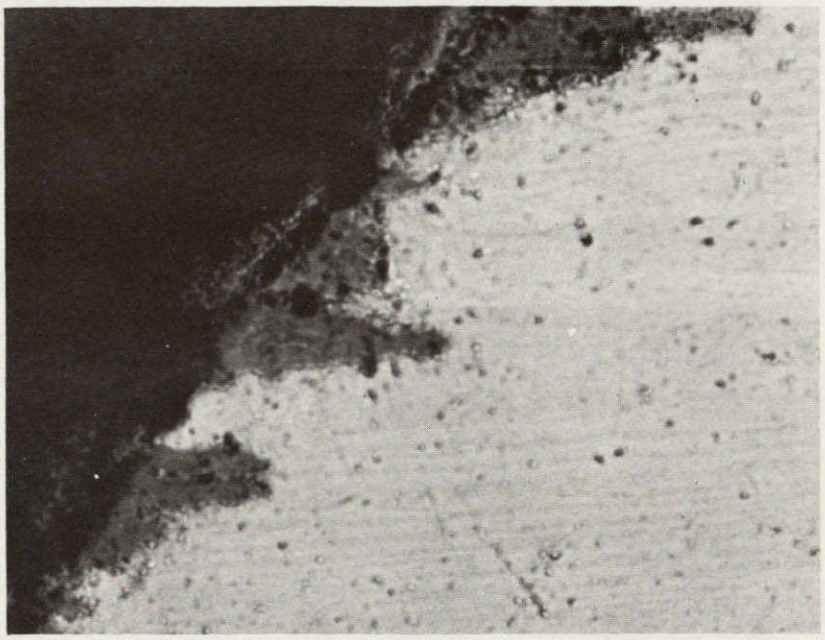

(b) Transverse

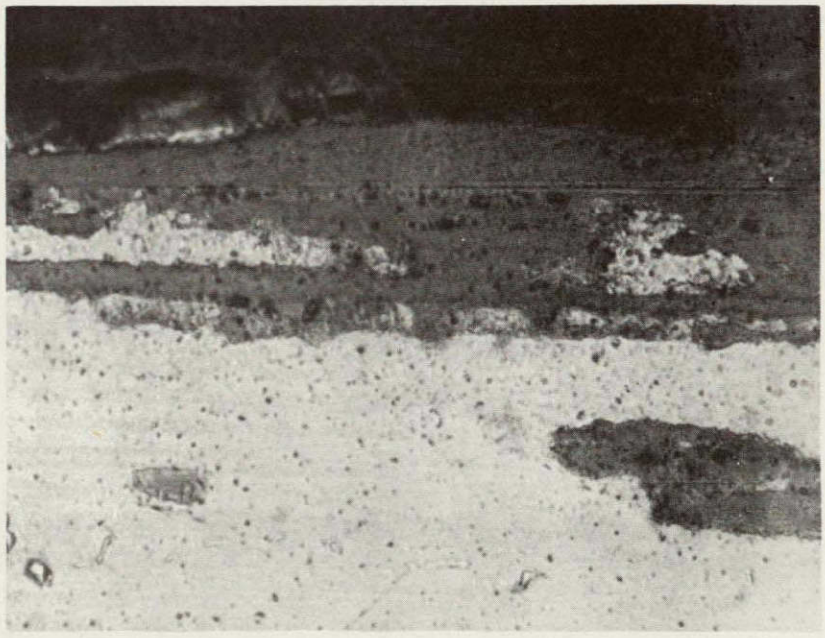

Longitudinal

Figure 23. (Cont'd) Transverse and longitudinal sections through (b) γ/γ'-δ subjected to 3102 hours of cyclic oxidation to 750°C. 750X.

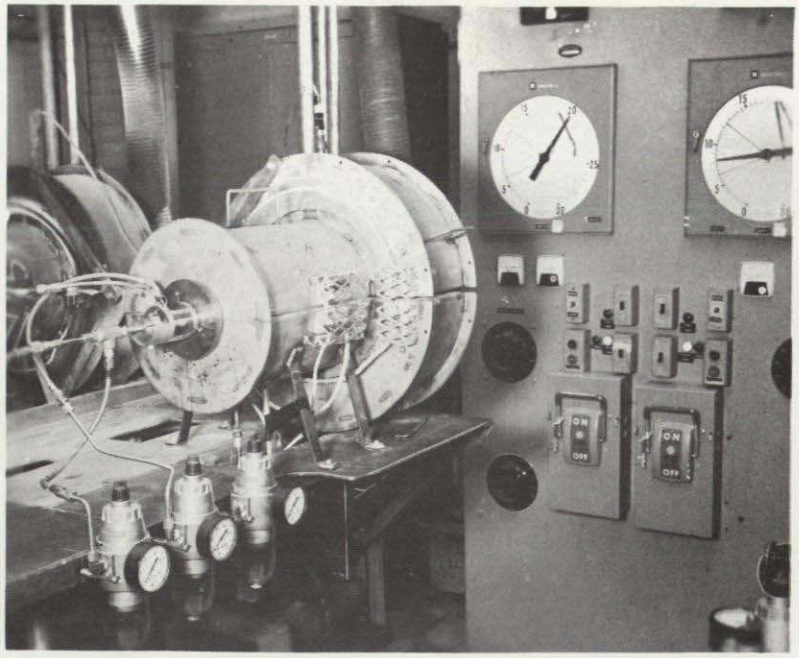

Figure 24. Photograph of one of the burner rigs used at General Electric AEBG, Lynn, Mass. Larger diameter rear of furnace is hinged so it may be pivoted away to remove samples. Temperature in this section of the rig is approximately 1100°C. In cyclic oxidation testing, samples were removed about once an hour, cooled below 93°C, and returned to the furnace. Each day this process was repeated for 8 hours and then the samples were isothermally exposed to 1100°C for 16 hours.

superior in appearance and had less weight loss than the Ni-20Cr+Al. The Ni-10Cr-5Al+Al was therefore selected to coat ends, roots, and shoulders on the rupture bars before the gauge section was E.B. coated. Longitudinal sections through test pins as deposited and after 486 hours of cycling are shown in figure 25.

Coating of the rupture bars was in two steps. First, the powder was sprayed onto the unmasked surfaces, after which the Ta foil was removed. Then the preferred coatings were deposited onto previously masked gauge sections and the bars were pack-aluminized. The coated bars are shown in figure 26.

The 16 coated bars were subjected to the 1100°C burner rig exposure. Four bars with each coating were removed from the burner rig after 150 hours and tested to rupture. These are shown in figure 27.

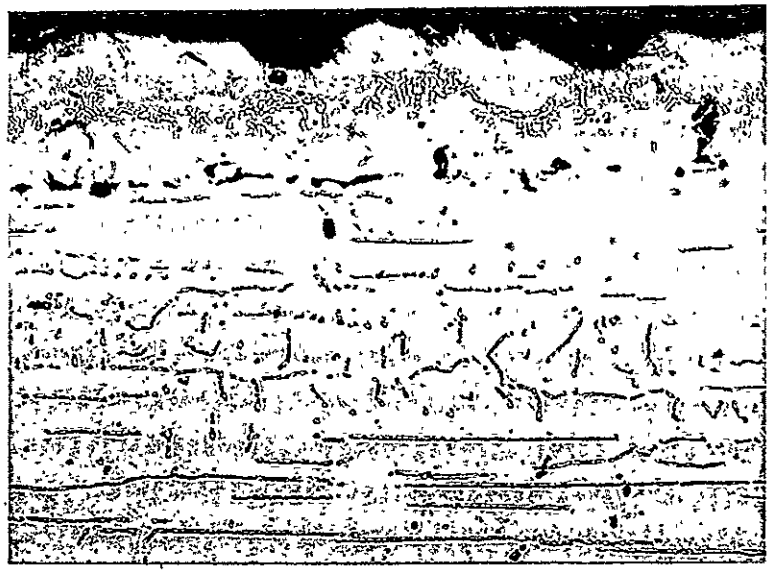

(a)

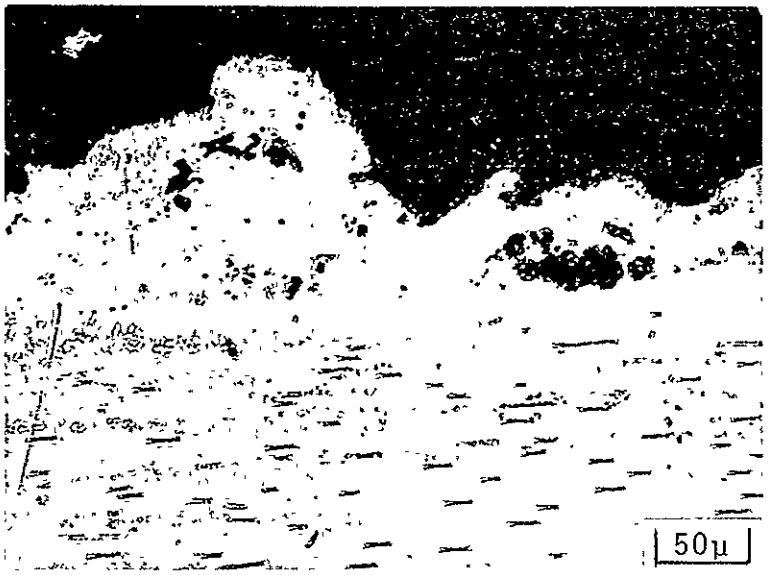

(b)

Figure 25. Spray Ni-10Cr-5Al+aluminize coatings on NiTaC-13 specimens. (Coatings used for end and root protection on test bars during burner rig exposure.) (a) as-deposited, (b) after 486 hours cyclic oxidation (1100° -950° C).

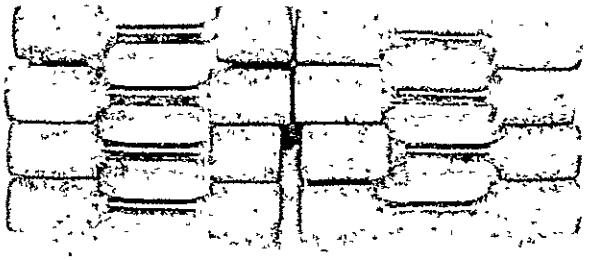

(a)

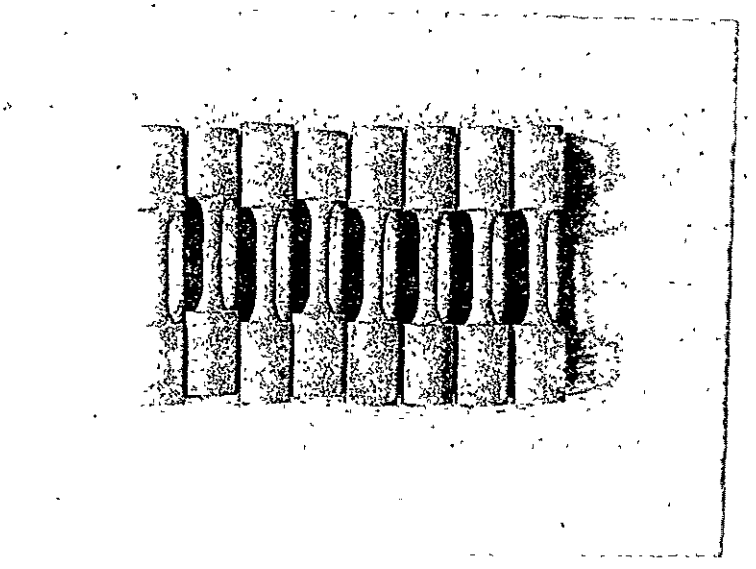

(b)

Figure 26. Coated NiTaC-13 test bars ready for cyclic burner rig exposure. (a) E.B. Ni-20Cr-5Al+aluminize coatings. (b) Spray Ni-20Cr-5Al-0.1Y-0.1C+ aluminize coatings.

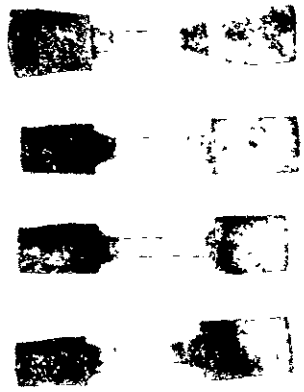

(a)

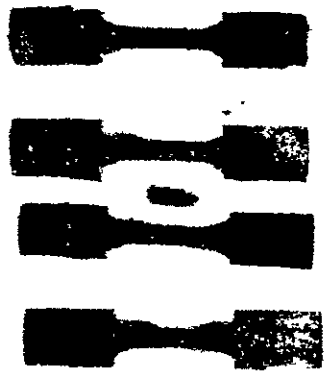

(b)

Figure 27. Coated NiTaC-13 test bars after 150 hours of cyclic burner rig exposure. (a) E.B. Ni-20Cr-5Al+aluminize coatings. (b) Spray Ni-20Cr-5Al-0.1Y-0.1C+aluminize coatings.

Figure 27 shows that the bars were experiencing some distress at the ends and shoulders. This appears as a result of coating cracks which started at the corner formed by the end and shoulder. If a crack formed there, oxidation can proceed along the coating-substrate interface.

The eight test bars scheduled for a 500-hour exposure were removed after 312 hours because of end, shoulder, and root coating failure. The non-gauge surfaces were recoated using E.B. Ni-20Cr-10Al-1Y. Before recoating, the areas were lightly grit-blasted to remove "loose" deposits. The bars were returned for more exposure; seven of the bars were again removed after 48 more hours of exposure. Oxidation attack in the root region was observed. The eighth bar was removed from exposure after 91 hours for a total of 403 hours.

The bars removed after 360 hours of exposure are shown in figure 28.

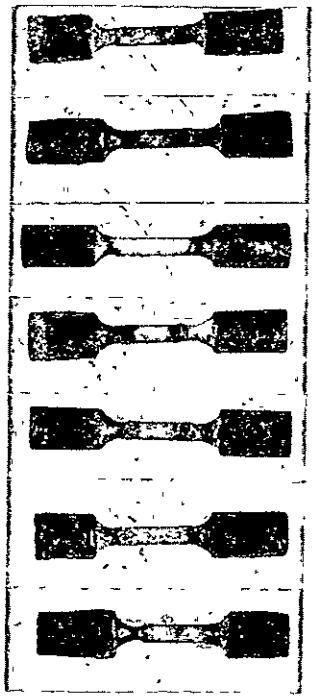

Figure 28. Macrophotographs of coated NiTaC-13 stress rupture bars after 360 hours of cyclic oxidation exposure to 1100° C in a burner rig. The top three bars are coated with Ni-20Cr-5Al-0.1Y-0.1C+Al and the bottom four with Ni-20Cr-5Al+Al. 0.94X.

Considerable oxidation and spallation have occurred with the gauge sections also showing attack originating at the roots and extending along the gauge length. This deep attack of the gauge section was considered in the interpretation of stress rupture results.

The head areas of the exposed bars were remachined for test at 871° and 1100°C in stress rupture. This was necessitated because of the severe oxidation attack in the root regions.

Static Air Furnace Cyclic Exposure

Results of cyclic oxidation in the burner rig indicated that stress rupture testing of the exposed bars might be questionable as a result of the oxidation in the root and shoulder regions. Therefore, it was decided to coat an additional four bars of NiTaC-13 with each of the two preferred coatings. Because of the problems already noted, ends of bars were first E.B. coated with the gauge section masked. The coating used for the ends was Ni-20Cr-5Al. Following end coating, the Ta foil mask was removed and the gauge length was wire spray coated with Ni-20Cr-5Al-0.1C-0.1Y. The bars were then pack-aluminized.

For the E.B. Ni-20Cr-5Al coatings, a new electron beam vacuum melting facility previously unavailable was used. This facility has the capability for the rotation and tilting of the sample during deposition, producing a more uniform depositited coating over the total surface. These samples were coated for a half-cycle, then reversed end for end for the second half-cycle, so that both ends of the samples were coated. These bars were then pack-aluminized.

Because of time limitations, it was decided to cycle these bars in a 1100°C static air furnace. This allowed for 24 hours/day cycling, seven days a week, or 168 hours of cycling each week. The burner rig is not cycled on weekends, so that only 104 hours (maximum) cycling can be accumulated in a week. The equivalence of the burner rig and static air furnace 1100°C cyclic oxidation tests has been demonstrated previously (ref. 6). The dynamic conditions in the burner rig may be more severe than the furnace conditions, but the total effect 6 to 8 cycles/day in the burner rig are less severe than the 24 cycles/day in the automatically cycled furnace test.

The macrographic appearance of the coated stress rupture bars after cyclic oxidation to 1100°C in a static air furnace is shown in figure 29. It can be seen that the E.B. Ni-20Cr-5Al+Al coating has excellent oxidation resistance after 158 and 349 cycles. The tilt capability of the new electron beam facility has avoided the thin-coated areas in the shoulder of the bars. However, substantial oxidation is noted at one end of each bar. In each case, that end contained large carbide particles because bars were cut from the cast ingots with a blocky carbide sort-out zone. The wire spray-coated

Ni-20Cr-5Al-1C-0.1Y+Al bars are shown in figure 29(b). The bars were cycled for 68 to 333 hours. The top sample had fallen from the cycling holder after 68 exposure hours, and rested on the furnace bottom for approximately 5 hours. Considerable interaction between the furnace ceramic and the coating occurred. The other three bars also showed distress at the shoulders and roots, but the E.B. end coating appeared to have withstood cycling better than did the Ni-10Cr-5Al powder spray-coated end (figures 27 and 28). The Ni-20Cr-5Al-0.1C-0.1Y+Al wire spray-coated gauge sections were in excellent condition, as also noted for the burner rig exposures.

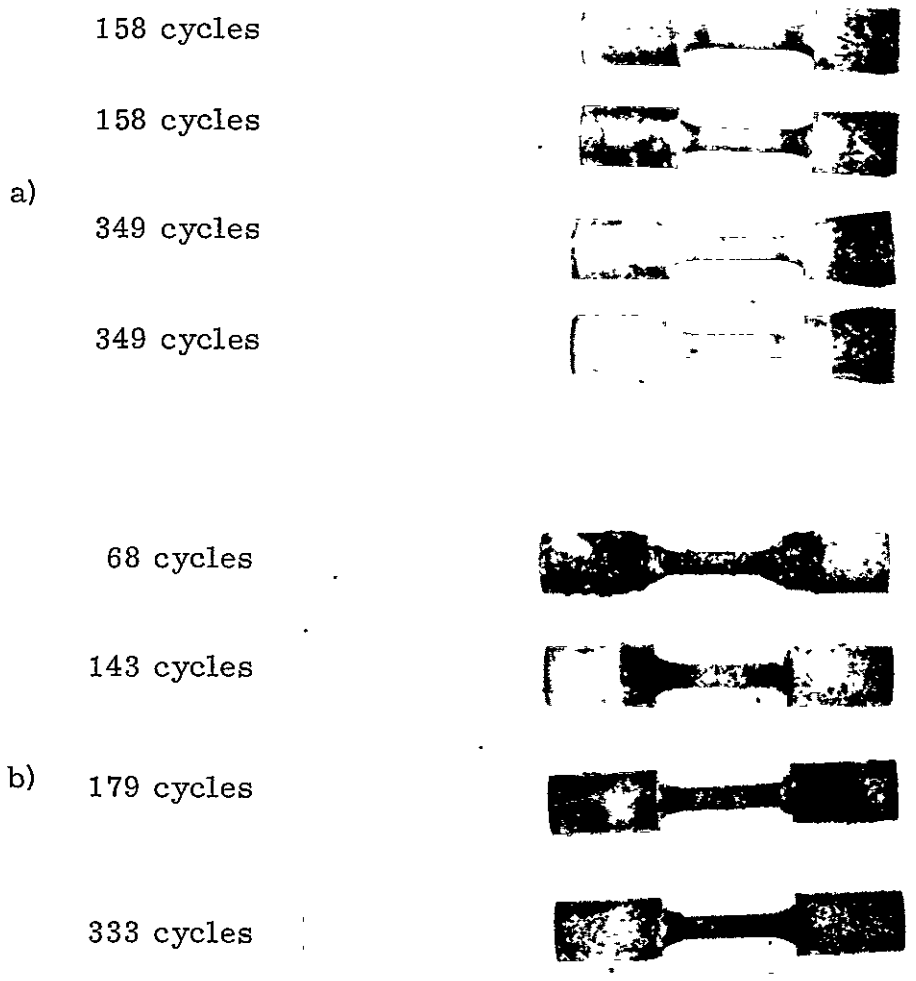

Figure 29. Macrophotographs of coated NiTaC-13 stress rupture bars after cyclic oxidation exposure to 1100°C in a static air furnace. (a) Ni-20Cr-5Al+Al coating, (b) Ni-20Cr-5Al-0.1Y-0.1C+Al coating. 1.1X.

STRESS RUPTURE BEHAVIOR OF CYCLED AND COATED BARS

Review of Previous Results for Coated and Cycled NiTaC-13

An earlier study considered the behavior of NiTaC-13 in a variety of conditions, both coated and uncoated (ref. 6). To put the results of the current study in proper perspective, it is necessary to go into some detail in reviewing the earlier results.

The actual behavior of NiTaC-13 is shown in figure 30(a) in terms of the relation of applied rupture stress to the Larson-Miller parameter P, where P is equal to the absolute temperature times the quantity of Log_{10} of rupture life (in hours) plus a constant of 20. The same relation is shown schematically in figure 30(b). For uncoated, uncycled NiTaC-13, testing in argon results in longer lifetimes than testing in air above some critical temperature where the test environment becomes important. The difference between air and argon rupture lives increases with increasing temperature.

For uncycled NiTaC-13 coated with either E.B. Ni-20Cr-15Al-1Y or with duplex E.B. Ni-35Cr+Al, it was expected that air rupture test would result in lifetimes equivalent to argon tests of uncoated NiTaC-13. Instead, 1093°C rupture lives of coated bars were about equivalent to uncoated air tested bars, while at 871°C, where uncoated NiTaC-13 has essentially the same life in air or argon, the coated bars exhibited about a parameter loss. This is shown schematically in figure 31. The results can be considered as a parameter loss from the argon tested uncoated material over the whole temperature range. It has been shown that the loss in lifetime does not result from the diffusion heat treatment (3 hours, 1160°C, argon) given the coated bars (ref. 6). Possibly the diffusion interaction zone formed between coating and the eutectic substrate may be the cause of the degradation, or the coated surface may be an easier site for stress rupture crack initiation than is the uncoated surface.

When uncoated NiTaC-13 was exposed to 1 hour 1100°C to 200°C temperature cycling, large changes in stress parameter relations were observed (ref. 6). When uncoated bars were cycled in vacuum and tested in argon to prevent any interaction with environment, there was a degradation in behavior caused by cycling. The degradation increased with the number of cycles, as shown schematically in figure 32. Therefore, even with a perfectly protective, noninteracting coating, a degradation in behavior would be expected as a result of cycling. If uncoated NiTaC-13 is cycled in air and tested in air, a much greater degradation is observed, as shown schematically in figure 33. It should be remembered that a 0.254-cm-diameter pin of NiTaC-13 is reduced to 0.23 cm in 50 hours, 0.20 cm in 100 hours, and 0.18 cm in 150 hours of 1100°C cycling oxidation. If degradation in stress rupture resistance were compared based on the original 0.254 cm diameter rather than the diameter after cycling, parametric losses would be still greater.

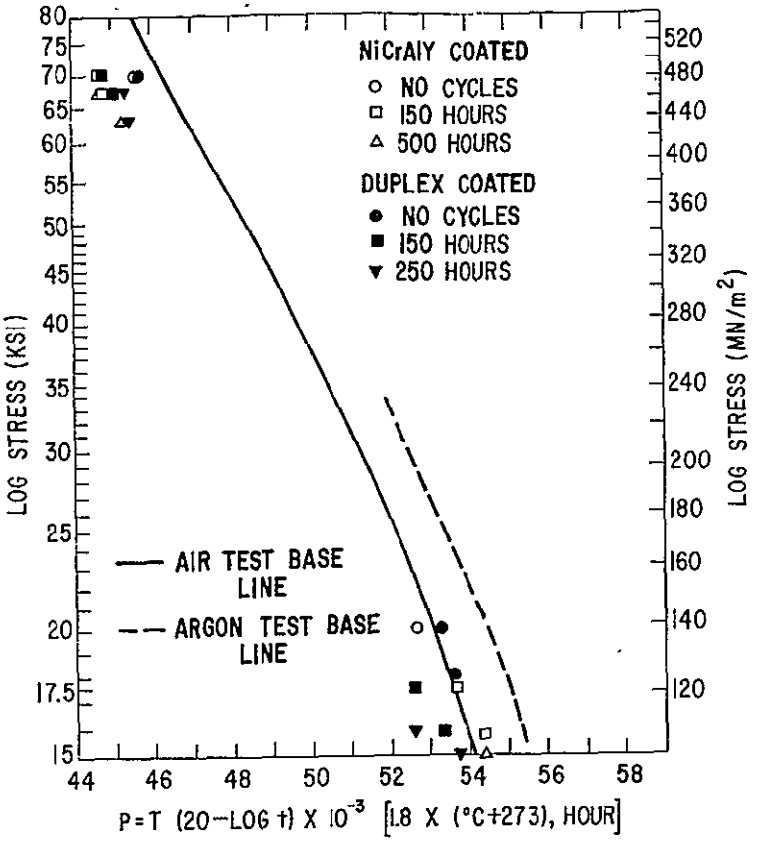

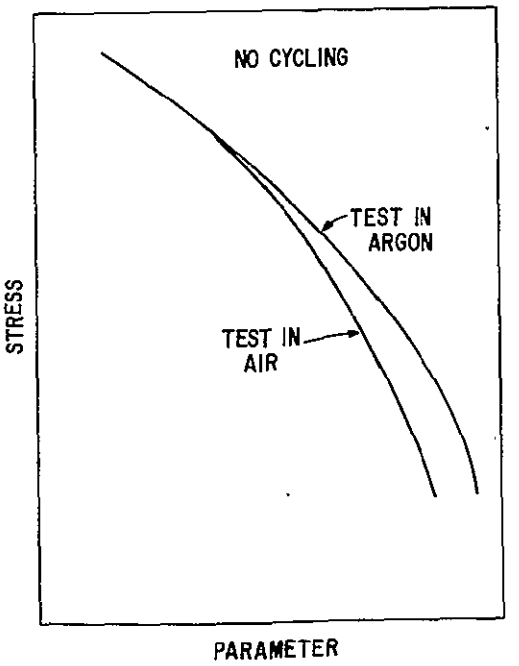

Figure 30. As-directionally solidified base line stress rupture data for NiTaC-13; stress vs Larson-Miller parameter, (a) actual data, (b) schematic.

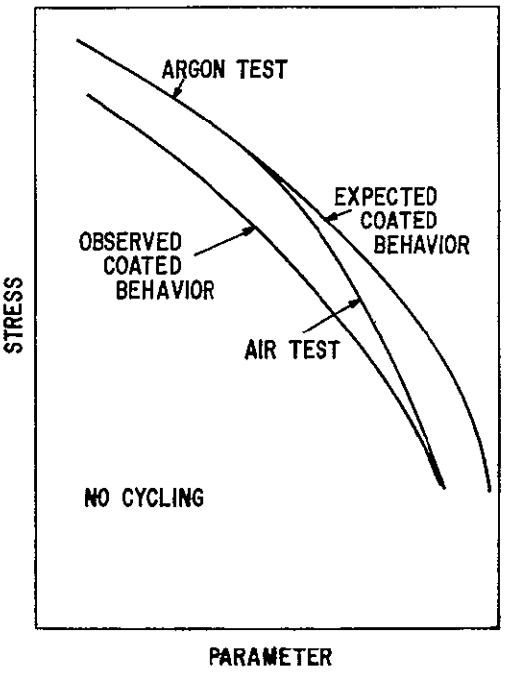

Figure 31. Schematic diagram comparing expected and observed air stress rupture behavior of coated NiTaC-13 to the behavior of uncoated NiTaC-13 tested in air and argon.

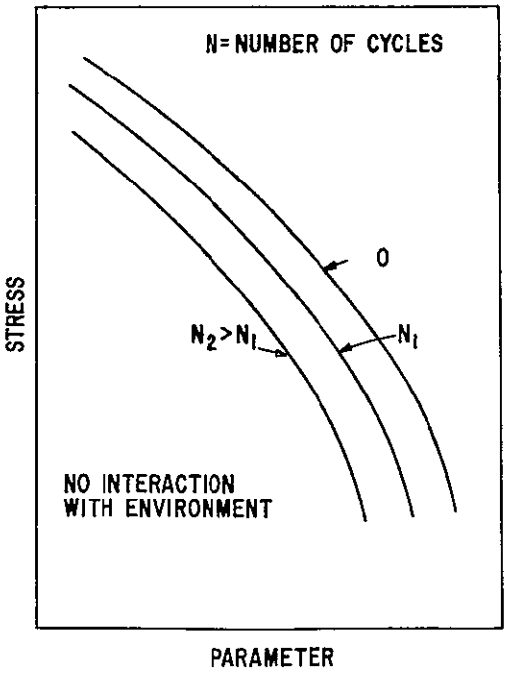

Figure 32. Schematic diagram showing degradation of NiTaC-13 in stress rupture following cyclic exposure to 1100°C in vacuum.

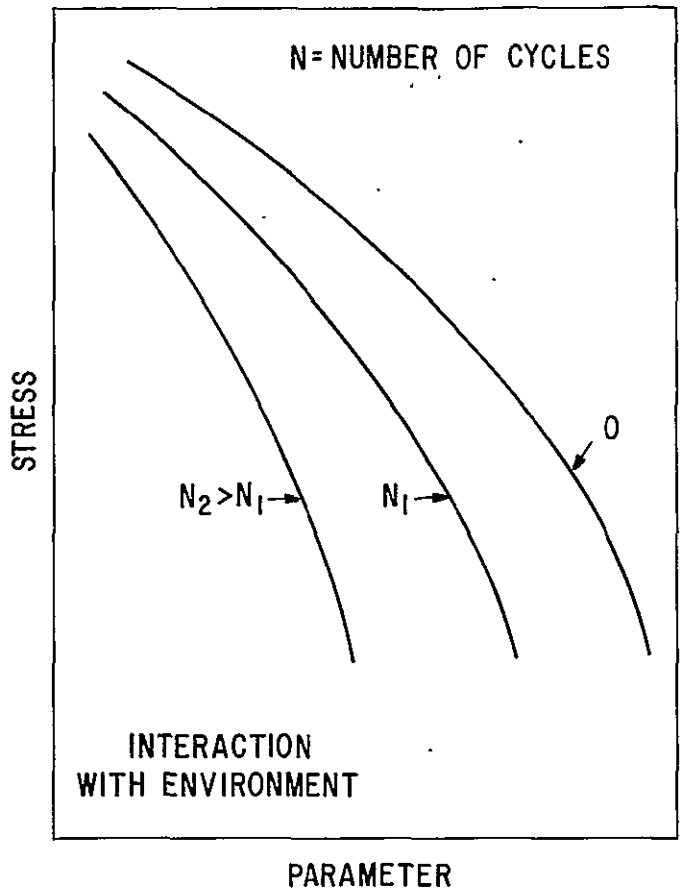

Figure 33. Schematic diagram showing severe degradation of NiTaC-13 in stress rupture following cyclic exposure to 1100°C in air.

The interrelationship between environment and cycling behavior is summarized schematically in figure 34. After a constant number of cycles, three conditions are compared for uncoated NiTaC-13: argon tested with no environmental interaction during cycling (i.e., as if coated with a perfect coating), air tested with no environmental interaction during cycling (i.e., as if coated with a perfect coating during cycling, but with the coating removed before air testing), and air tested with interaction during cycling (i.e., an uncoated bar). The degradation caused by environmental interaction relative to the behavior of the perfect coating material is as expected.(ref. 6).

Results of coated and cycled material are compared in figure 35 to the same three conditions shown in figure 34 (ref. 6). Stress rupture behavior of NiCrAlY coated samples was essentially equal to that of a "perfect coating" test at 1093°C, although somewhat below that behavior at 871°C. The duplex-coated samples showed behavior more like that of the case of perfect coating during cycling with coating removed prior to test. In fact, microstructures of the duplex-coated, cycled bars after rupture testing showed substantial delamination of the coating along a nearly continuous, thick α-Cr layer that

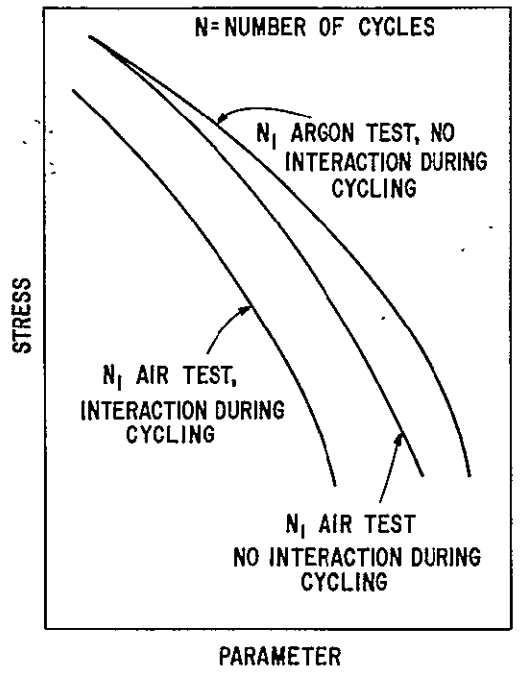

Figure 34. Schematic diagram comparing stress rupture resistance of NiTaC-13 after cycling in vacuum and testing in argon or air, and after cycling in air and testing in air.

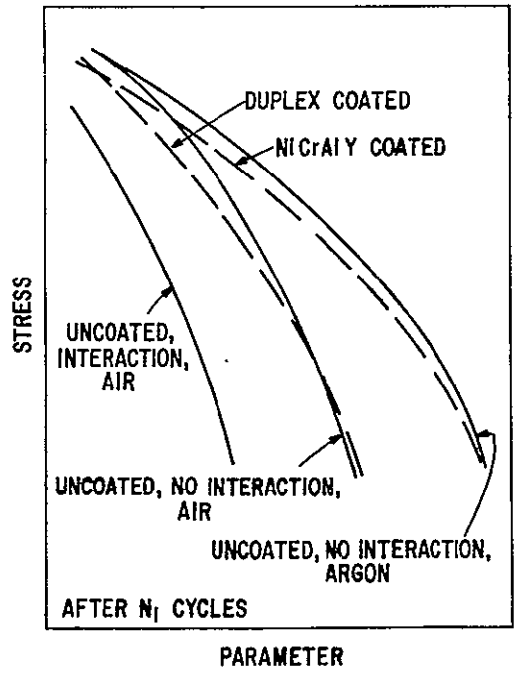

Figure 35. Schematic diagram comparing stress rupture resistance of cycled and coated NiTaC-13 and uncoated NiTaC-13 cycled as in figure 34.

formed during interdiffusion (ref. 6). The α-Cr layer formed in the NiCrAlY coated material was globular α-Cr in a γ or β-NiAl matrix. The NiCrAlY coating showed no delamination. For both coatings, rupture behavior was far superior to the behavior of uncoated, cycled NiTaC-13 tested in air.

Mechanical Properties of Coated and Cycled Rupture Bars

As was shown in figures 27 through 29, substantial coating loss in the heads of samples occurred during cycling. The gauge sections coated with the preferred Ni-20Cr-5Al+Al or Ni-20Cr-5Al-0.1C-0.1Y were well protected, but where the end coatings overlapped the gauge coating, there was oxidation damage. Five of the burner rig cycled samples and one of the static air furnace cycled samples lost so much cross section in the heads that they pulled through the loading grips during rupture testing and were therefore unloaded prior to failure. The rupture lives in air at 871°C/434.4 MN/m^2 and at 1100°C/103.4 MN/m^2 are recorded in Table II as a function of number of oxidation cycles to 1100°C for NiTaC-13 with the two preferred coatings, cycled either in the 0.05 Mach burner rig or the static air furnace. Where duplicate rupture tests to failure were run, substantial differences in life are noted. For example, the burner rig cycled (148 hours) Ni-20Cr-5Al+Al coated bars showed lifetimes of 106 to 173 hours at 434.4 MN/m^2, and 158 to 194 hours at 103.4 MN/m^2. The large differences are probably a result of the quality of the test bars after cycling rather than due to the inherent behavior of the preferred coatings.

TABLE II. - AIR TEST RUPTURE LIVES OF CYCLICALLY EXPOSED COATED NiTaC-13

[1100°C to 93°]

Environment	Coating	Cycles (# hr)	871°C/434.4MN/m^2 Rupture Life (hr)	1100°C/103.4MN/m^2 Rupture Life (hr)
Burner Rig (0.05 mach)	Ni-20Cr-5Al+Al	148	106.2	193.8
		148	172.9	157.7
		360	59.7	--
		360	2.1+(NF)	24.5
		403	--	89.4+(NF)
	Ni-20Cr-5Al-0.1C-0.1Y+Al	148	888.2+(NF)	90.4
		148	73.4	49.1
		360	47.2	50.4
		360	37.5+(NF)	10.3+(NF)
Static Air Furnace	Ni-20Cr-5Al+Al	158	237.9	145.5
		349	137.4	63.5
	Ni-20Cr-5Al-0.1C-0.1Y+Al	94	68.0+(NF)	--
		143	--	110.6
		179	156.8	--
		333	--	106.0

NF - No failure; sample pulled through loading grips.

Comparison of the stress rupture behavior of coated NiTaC-13 for coatings of the present program relative to coatings in the earlier program (ref. 6) is difficult. Numbers of cycles, test temperatures, and test stresses are different between the two studies. However, in figure 36 a bar graph is drawn in an attempt to make a comparison from the available data. For the coatings tested in the earlier program, lifetimes are extrapolated from available data whenever different test conditions were used (ref 6). The four coatings are compared in terms of stress rupture lives at 870°C/434.4 MN/m^2 and at 1100°C/103.4 MN/m^2. Each coating is represented by two bars for each test condition, the top bar being the maximum rupture life after short-time cycling (150 hours) and the bottom bar being the maximum rupture life after long-time cycling (2350 hours).

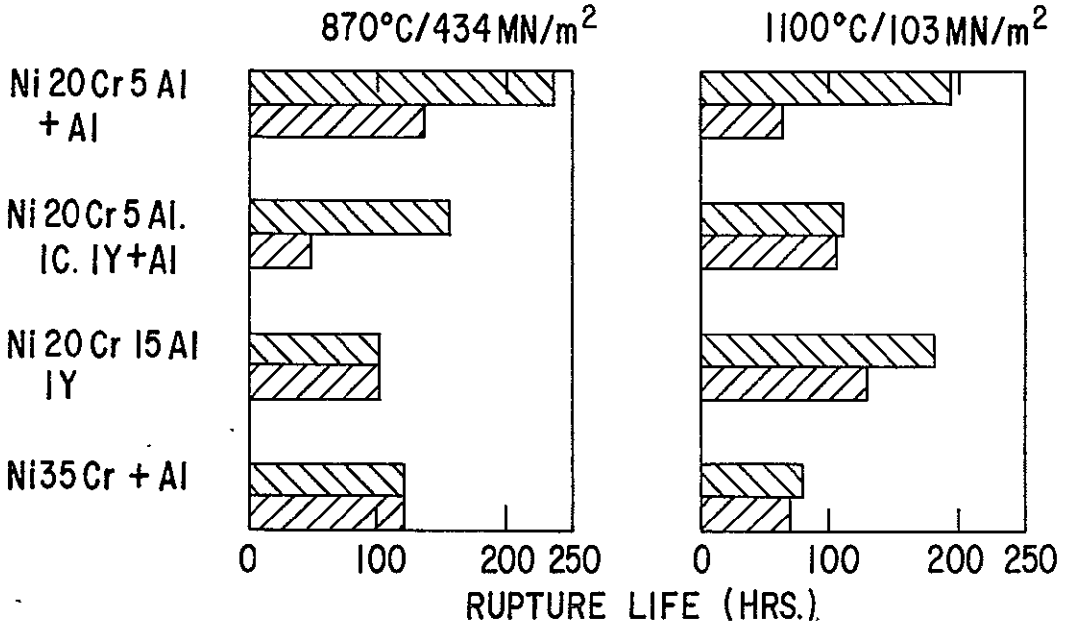

Figure 36. Comparison of stress rupture behavior of NiTaC-13 coated with different coatings after 1100°C cyclic oxidation for 150 hours (top) and ~350 hours (bottom).

Both preferred coatings of the present study appear to be superior to the Ni-35Cr+Al coating at both test conditions. This is especially true when considering that the long time cycle for Ni-35Cr+Al was only 250 hours and the others approximately 350 hours. On the average, both preferred coatings of the present study appear to be slightly inferior (at approximately 350-hour exposures) to the Ni-20Cr-15Al-1Y coating, while the opposite is true at the 150-hour exposure.

These conclusions must be tempered by the difficulties encountered in cyclic oxidation and rupture testing because of failure of the end coatings. As will be shown shortly for the burner rig cycled bars, failures occurred in nearly every case at a point near the root where end coatings had failed.

Lifetimes of bars completely coated with the preferred coatings would be expected to be greater. This is borne out in a comparison of S-R lives of bars coated in the tilting unit (cycled in static air furnace) and those coated prior to the acquisition of the tilting capability (cycled in burner rig) as presented earlier in Table II.

Another point should be made regarding the properties obtained for NiTaC-13 coated with the preferred coatings of the present study. The preferred coatings were chosen on the basis of their prevention of carbide fiber denudation. However, NiTaC-13 has a matrix nearly as strong as the composite and the alloy may not be strongly dependent on the presence of the carbide fibers for reinforcement. For the attainment of the high temperature goals now under study for Ni-base TaC eutectics, carbide reinforcement at high temperatures may become the dominant factor. If this is so, then a coating such as Ni-20Cr-15Al-1Y will be inadequate because of fiber loss. The coatings of the present study will be much more desirable for such eutectics because of the avoidance of fiber denudation.

Macro- and Microscopic Appearance of Coated and Cycled NiTaC-13 After Rupture Testing

The macroscopic appearance of the burner rig cycled samples after rupture testing is shown in figure 37. No difference can be noted between bars coated with Ni-20Cr-5Al+Al and with Ni-20Cr-5Al-0.1C-0.1Y+Al. All show substantial root attack as already discussed, and most show failure near the root where the end coatings have failed.

Microstructures of the carbon containing coating, Ni-20Cr-5Al-0.1C-0.1Y+Al, are shown in figures 38 and 39, for low-temperature testing, short time and long time cycling, respectively. Structures are similar to the cycled pin samples discussed earlier. Failures in the low-temperature tested bars show evidence of crack propagation along sigma phase plate boundaries with the surrounding matrix, much as was described in a previous study (ref. 6). High-temperature tested bars show considerable necking and no evidence of the sigma phase influencing the fracture path. Of course, carbide fibers are observed out to the coating-substrate interface. This is as expected, since pins cycled for 2000 hours showed fibers retained to the coating-substrate interface. A decrease in Al content of the coating for increasing cycle time is indicated by the decrease in volume fraction of β-NiAl in the coating. The loss of Al occurs by interdiffusion with the substrate and by formation and eventual spallation of Al_2O_3 at the coating surface.

A similar series of micrographs of the fracture is shown in figures 40 and 41 for bars coated with Ni-20Cr-5Al+Al. Again, microstructures are as expected from pins cycled much longer times. Excellent bonding of coating and substrate was noted in all samples, with no indication of delamination of the preferred coatings. Little fiber loss is noted after 360 hours of

a)

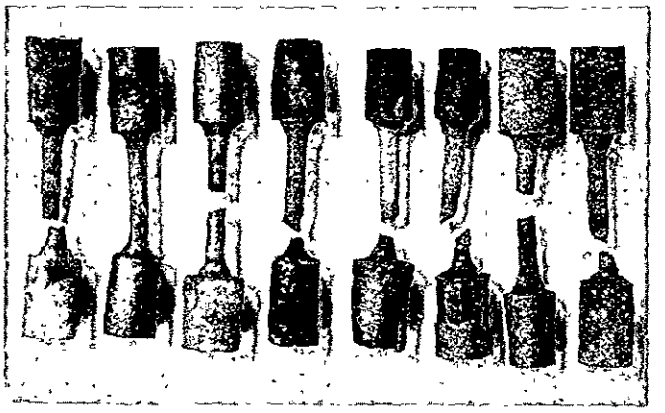

b)

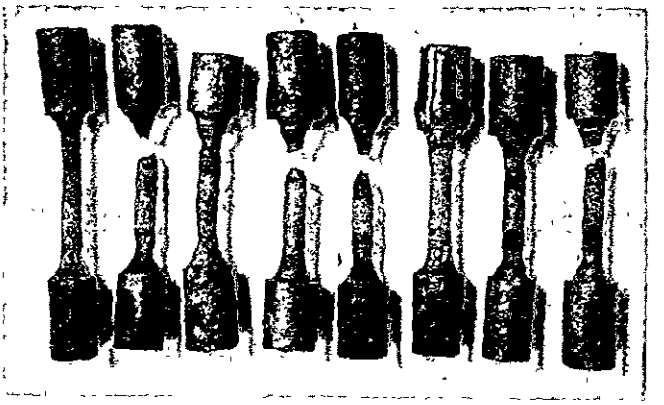

Figure 37. Macroscopic appearance of 1100°C burner rig cycled bars of coated NiTaC-13 rupture tested after (a) 148 hours and (b) 360 hours of exposure.

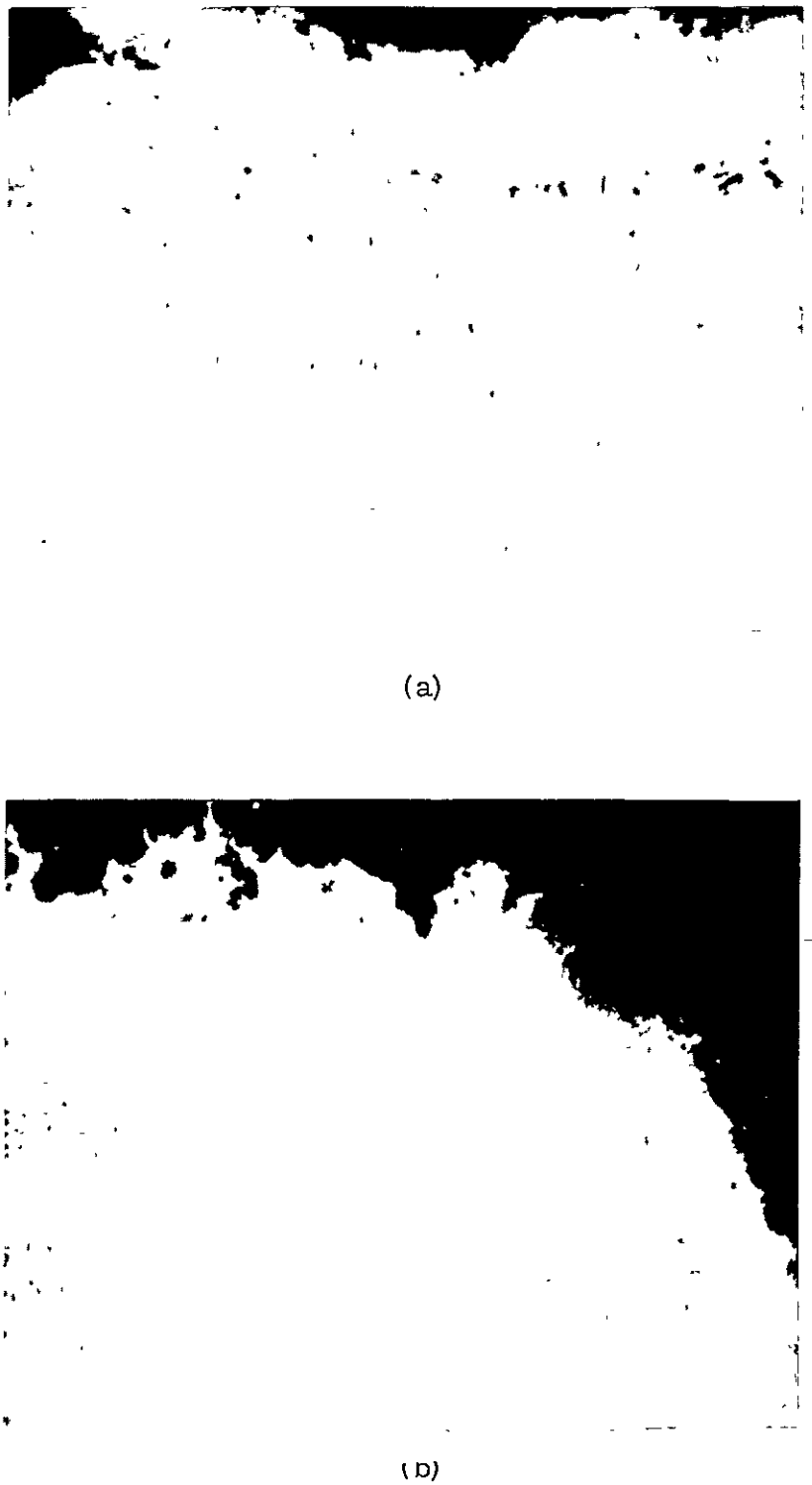

Figure 38. Longitudinal sections through NiTaC-13 bars coated with Ni-20Cr-5Al-0.1Y-0.1C+Al rupture tested at 871°C, 434 MN/m^2 in air after 1100°C cyclic oxidation for (a) 148 hours and (b) 360 hours. 500X

(a)

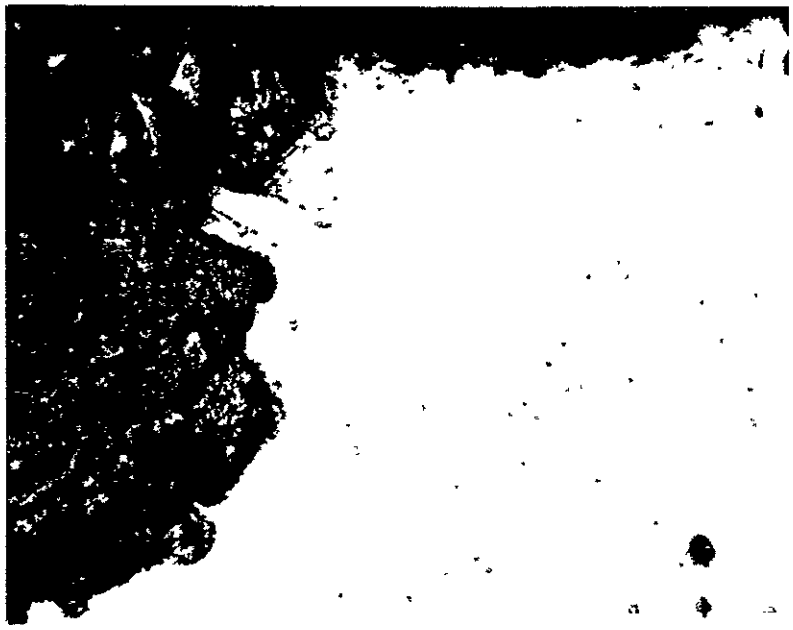

(b)

Figure 39. Longitudinal sections through NiTaC-13 bars coated with Ni-20Cr-5Al-0.1Y-0.1C+Al rupture tested at 1100°C, 103 MN/m^2 in air after 1100°C cyclic oxidation for (a) 148 hours and (b) 360 hours. 500X

(a)

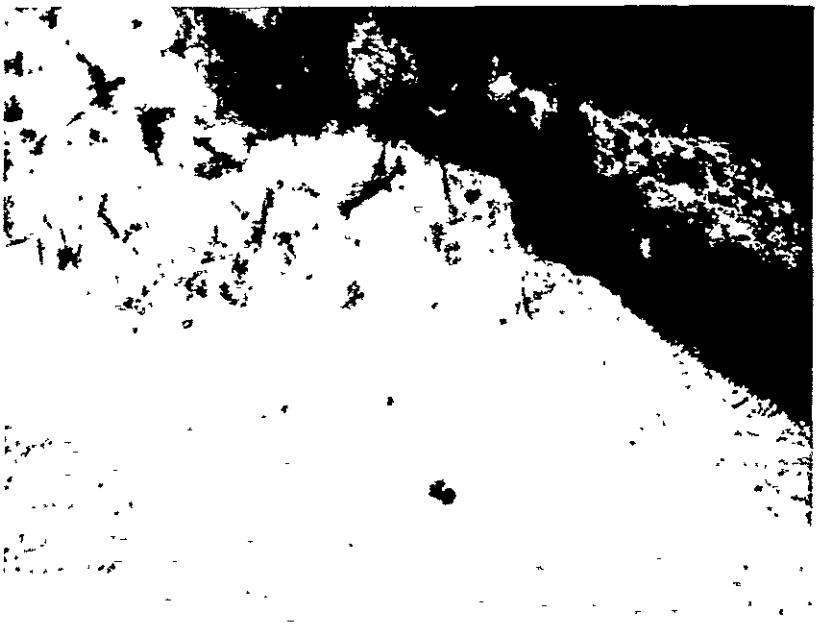

(b)

Figure 40. Longitudinal sections through NiTaC-13 bars coated with Ni-20Cr-5Al+Al rupture tested at 871°C, 434 MN/m^2 in air after 1100°C cyclic oxidation for (a) 148 hours and (b) 360 hours. 500X

(a)

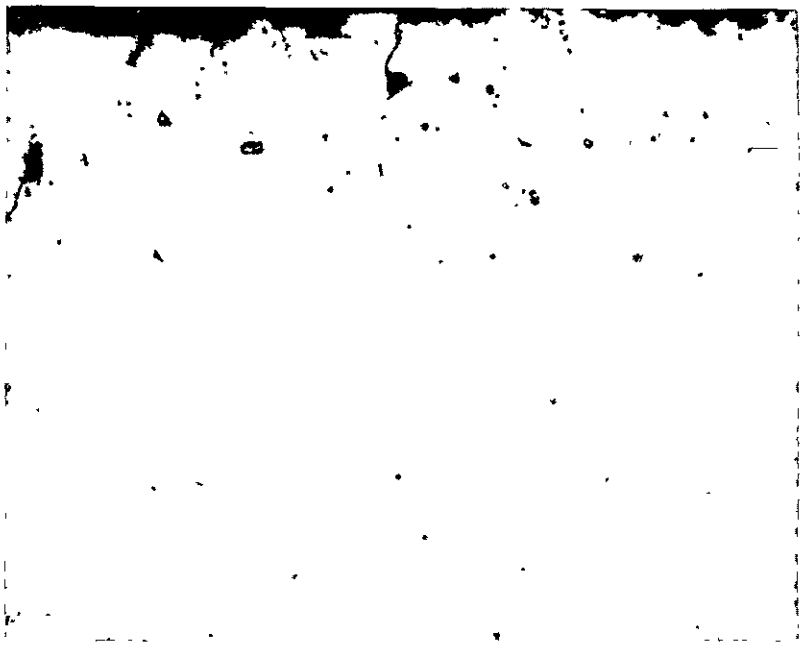

(b)

Figure 41. Longitudinal sections through NiTaC-13 bars coated with Ni-20Cr-5Al+Al rupture tested at 1100°C, 103 MN/m^2 in air after 1100°C cyclic oxidation for (a) 148 hours and (b) 360 hours. 500X

1100°C cycling. Eventually, this carbon-free coating would show substantial denudation, but at a much slower rate than for similar coatings containing yttrium, as was shown earlier in Task I for pin samples.

Figure 42 shows microstructures for the powder-spray Ni-10Cr-5Al+Al coating used on test bar heads. Delamination of the coating from the substrate can be seen, and oxidation of both coating and substrate. Also shown is a micrograph of the region of overlap of the end coating and the carbon containing coating along the gauge of the test bar. The lower Cr content of the end coating is obvious from the lack of formation of α-Cr particles at the coating-substrate interface. After 360 hours of cycling some fiber loss is apparent at the end coating-substrate interface, but not substantial amounts. As was the case for Ni-20Cr-5Al+Al and Ni-35Cr+Al coatings, the Ni-10Cr-5Al+Al end coating shows delayed fiber denudation when compared to yttrium-containing, carbon-free coatings.

TEST OF COATING DUCTILITY

In addition to rupture testing and microstructural analysis of rupture bars, Task II of the present study included a room-temperature coating ductility test of one of the preferred coatings. The Ni-20Cr-5Al+Al coating was chosen for testing. The ductility test used is based on a technique developed by M. F. Henry (refs. 15 and 16) to determine the strain at first fracture of TaC fibers in a Ni-Cr matrix. In that study, rectangular cross-section bars were metallurgically polished on one surface parallel to the growth direction. The bars were then deformed in a three-point bending fixture, with the bars so positioned that the fibers in the polished surface were in tension. Strain was increased incrementally until fibers failed. Plastic replicas of the polished surface were made at each increment of strain so that the fracture strain could be determined accurately. In this way, the sample need never be unloaded during test for examination.

The technique was successfully used for the coating in this study by M. F. Henry, who performed the tests and made the plastic replicas. A schematic of the test is shown in figure 43. The strain at midspan is given as:

$$\epsilon = \frac{6\,h\,\delta}{L^2} ,$$

where h is the sample thickness; L is the distance between the outer loading points; and δ is the midspan deflection. The deflection is obtained by rotating the threaded midspan loading point in the fixture, and is given by:

$$\delta = \frac{0.106\ \text{cm}}{360^\circ}\ \theta,$$

where θ is the angle of rotation of the loading point. For a 0.15 cm thick by 3.18-cm-long span, strain ϵ is related to θ by:

$$\epsilon = 2.67 \cdot 10^{-5}\ \theta$$

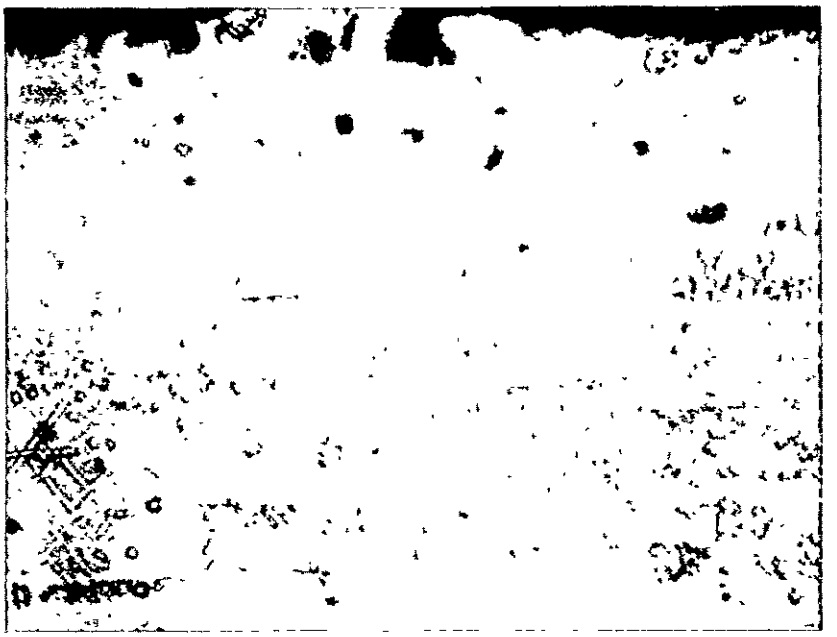

(a)

(b)

Figure 42. Longitudinal section through NiTaC-13: (a) at overlap between Ni-20Cr-5Al-0.1Y-0.1C+Al gauge coating and Ni-10Cr-5Al+Al root coating, 750X; and (b) at root showing Ni-10Cr-5Al+Al delamination. 250X

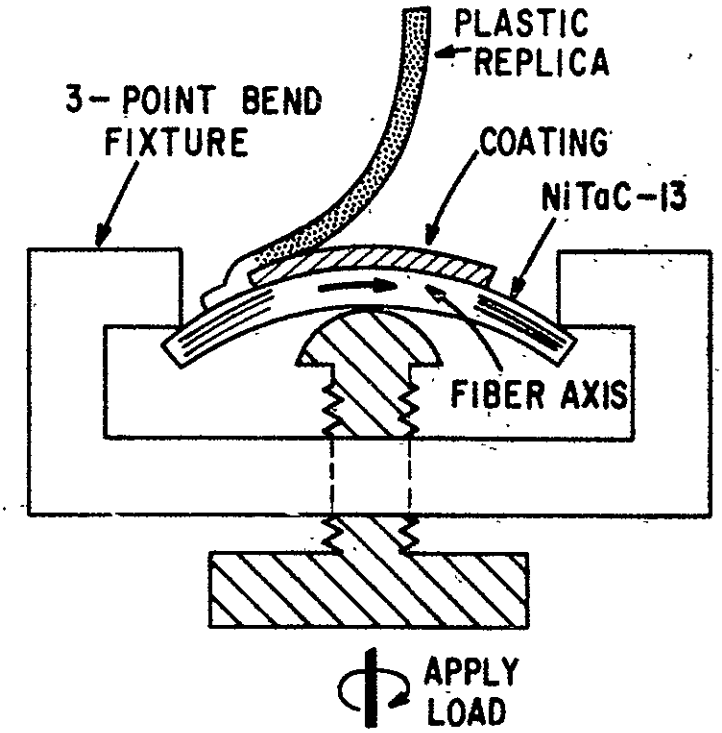

Figure 43. Schematic diagram of a three-point bend fixture used to examine coating ductility.

Figure 44 shows a NiTaC-13 test bar coated with Ni-20Cr-5Al+Al. The Al overlayer was deposited by electron beam vaporization followed by heat treatment so as to selectively aluminize the region of the test bar coated with Ni-20Cr-5Al. Selective aluminization by the pack process would have required masking. The bright region along the top half of the bar is the coating. The remainder of the bar was masked to prevent coating of a line of microhardness indentations. The indentations were made along the bar and across the center of the bar in the uncoated region to act as fiducial marks so that the same region of the replica of the coated surface could be found after each increment of strain. Figure 45 shows a micrograph taken with the scanning electron microscope (SEM) of the fiducials at the midspan.

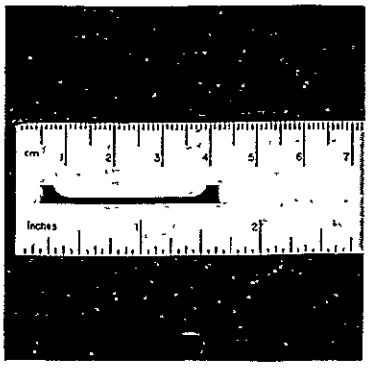

Figure 44. Macrophotograph of coating ductility bar with Ni-20Cr-5Al+Al.

Figure 45. SEM micrograph of replica of fiducial marks used to locate replica center. 400X

Figures 46 and 47 compare SEM photomicrographs of the actual coating surface and replicas of that surface, respectively. The globular nature of the aluminized coating in figure 46. is reflected as dimples in the replicas in figure 47. Cracks in the coating in figure 46 become plastic tongues extending out of the surface in figure 47. The increasing depth of cracking with increasing strain is indicated by the longer tongue in the higher strain replica.

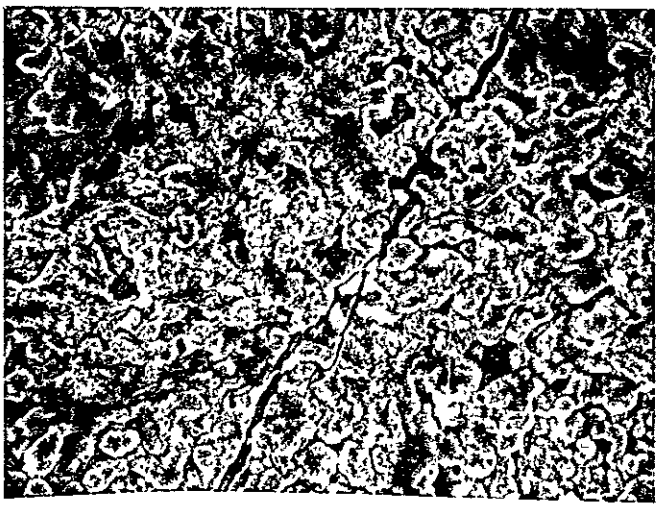

Figure 46. SEM micrograph of crack running through the coating on a three-point bend bar after coating ductility test. 800X

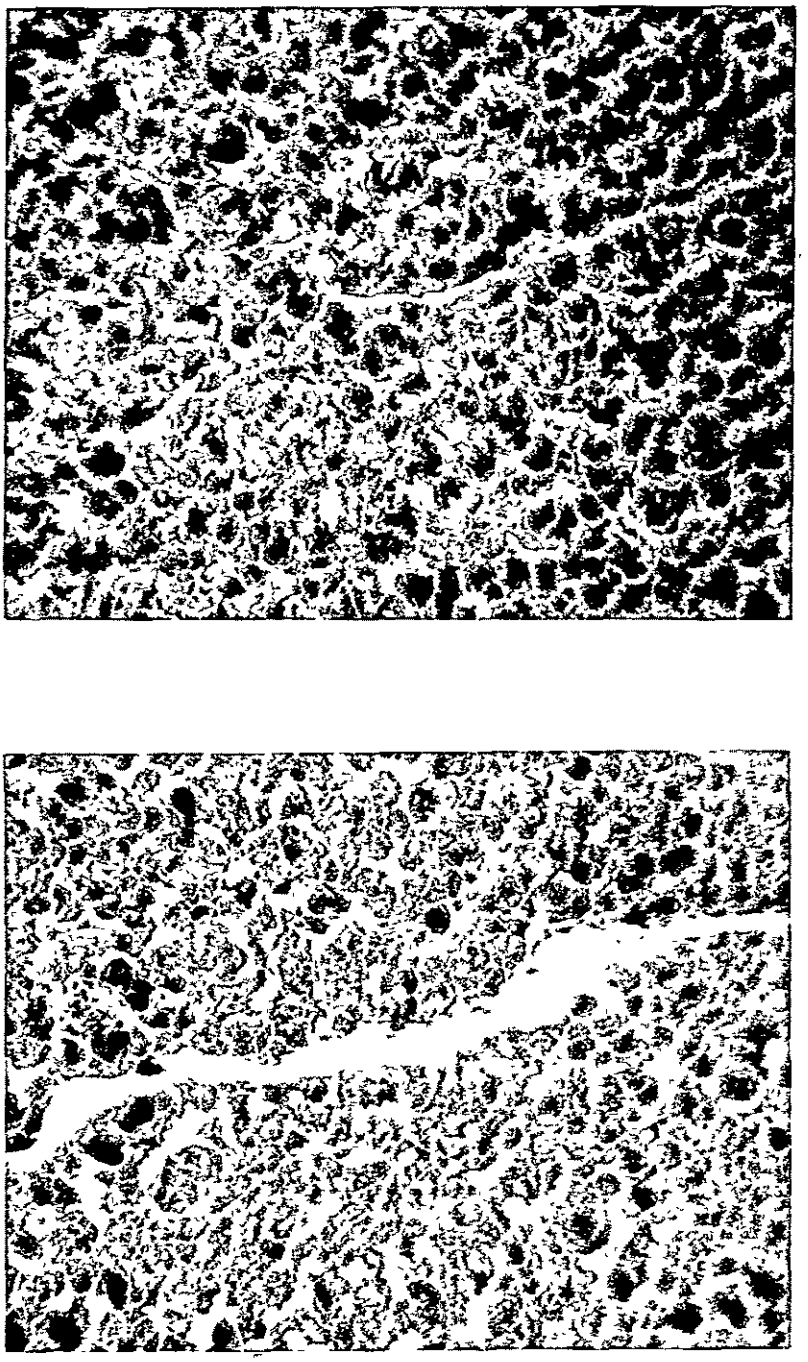

Figure 47. SEM micrographs of replicas of cracks running through the coating on a three-point bend bar after 0.8 (top) and 1.3% strain (bottom). 1000X

A replica of the as-coated bar is shown near the midspan of the specimen in figure 48. The fiducials can be seen at the far right and bottom right of the figure. The coating extends from the center to the left of the micrograph. No cracks could be found in the as-coated replica.

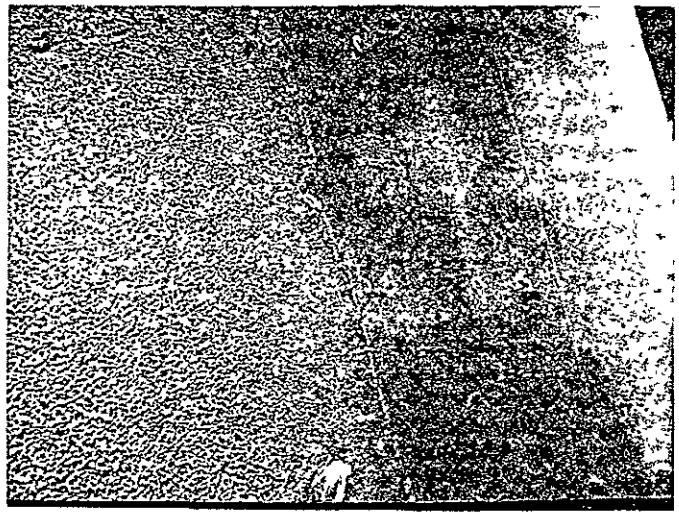

Figure 48. SEM micrograph of replica of as-coated bar. 100X

A replica of the same region as shown in figure 48 is shown in figure 49. after 1.3% strain. Midspan is again in the lower corner of the micrograph. A large number of cracks can be seen in the coating, and the cracks are quite uniformly spaced. The spacing at midspan is about 0.2 mm. Higher magnification photomicrographs of the same region are shown in figure 50 for replicas taken at 1.3%, 0.8%, 0.6%, and 0.5% strain. Crack spacing

Figure 49. SEM micrograph of replica of coated bar strained 1.3%. 40X

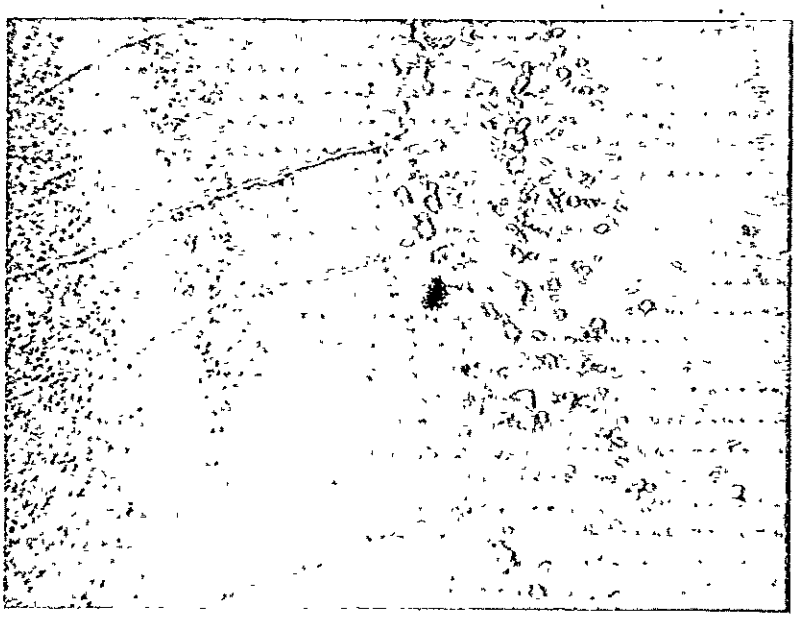

(a)

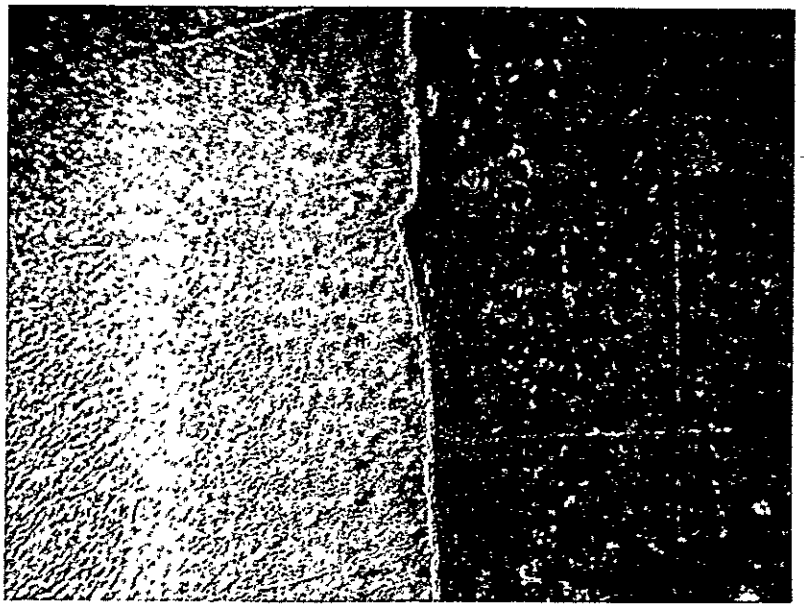

(b)

Figure 50. SEM micrographs of replicas of coated bar strained: (a) 1.3%, (b) 0.8%. 100X

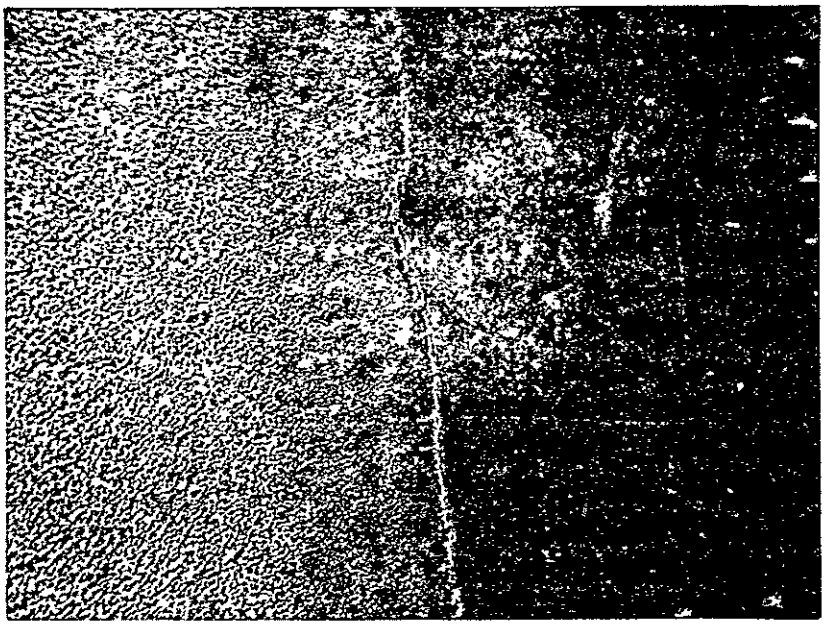

(c)

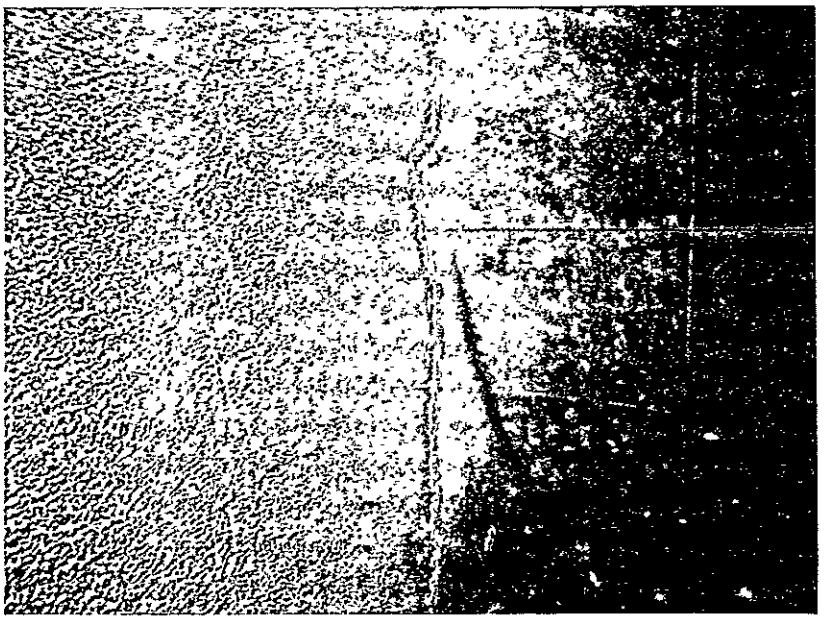

(d)

Figure 50. (Cont'd) SEM micrographs of replicas of coated bar strained: (c) 0.6%, and (d) 0.5%. 100X

decreases rapidly with increasing strain, and few cracks are seen in the 0.6% strain replica. A thorough search at 1000X showed no cracks in the 0.5% strain replica. At the extreme top of the 0.6% strain replica, a crack is barely visible. This crack is shown more clearly in figure 51. The photomicrograph was taken with the crack centered in the field of view. The crack was not apparent at 50X.

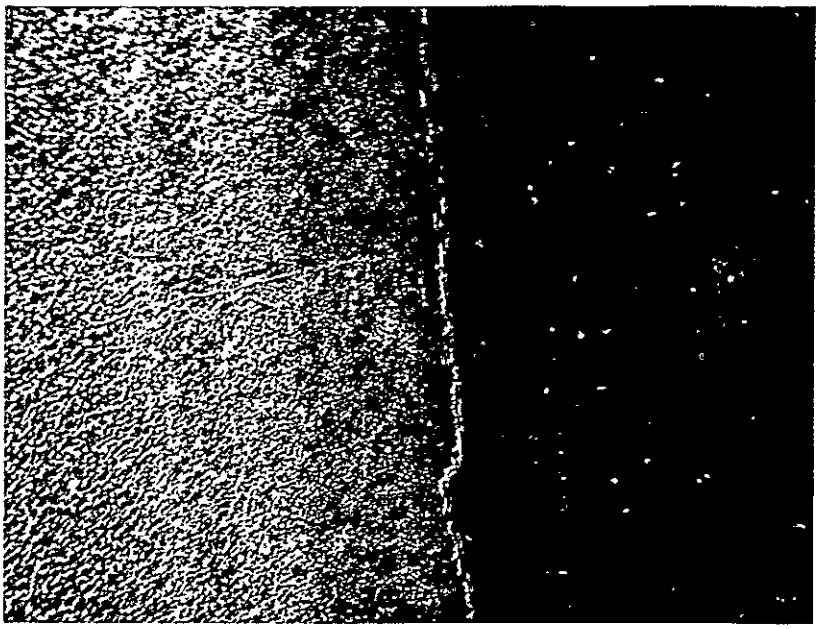

Figure 51. SEM micrograph of replica of coated bar strained 0.6%. 100X

Metallography through the coating-substrate interface has been performed as is shown in figure 52. It can be seen that crack propagation is limited to the coating and does not extend into the substrate alloy.

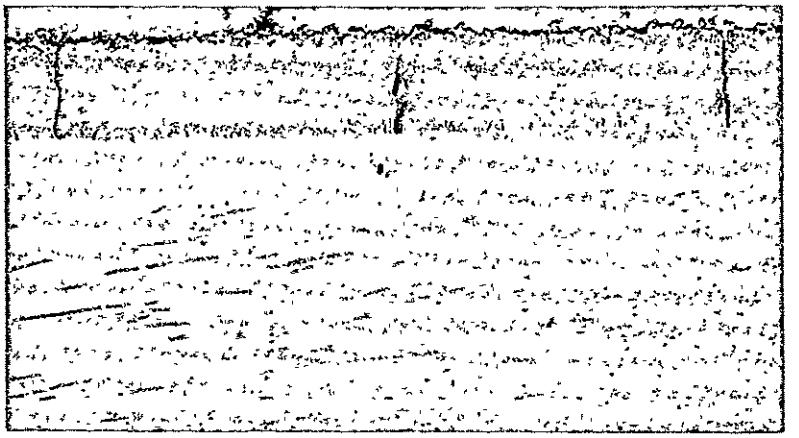

Figure 52. Micrograph of transverse section through tested coating ductility bar coated with Ni-20Cr-5Al+Al. Cracks limited to coating. 250X

The tensile ductility replication technique is a very useful method for determining room-temperature coating crack initiation at very low strains. A magnification of 100X for crack observation is apparently necessary to see the very beginnings of crack initiation. The method can be extended easily to coating crack initiation studies at temperature, provided precautions are taken to ensure that cracks are not initiated during the cooling cycle for replication. The method can also be coupled to acoustic or ultrasonic methods for verification of crack initiation.

SUMMARY OF RESULTS

Environmentally stable coatings for a high-strength, directionally solidified eutectic alloy designated NiTaC-13 were developed in this program. In Task I, three-base system coatings were evaluated by depositing onto pins of aligned NiTaC-13. The coatings applied were:

1. Ni-20Cr-10Al-1Y
   - (a) E.B. deposited.
   - (b) E.B. deposited and subsequent shot peen.
   - (c) Sputtered Pt layer and subsequent E.B. deposit.
   - (d) E.B. deposited and subsequent pack aluminize.
2. Ni-20Cr-10Al-0.1C
   - (a) Mixed powder spray.

3. Ni-20Cr-5Al

   (a) E.B. deposited.
   (b) E.B. deposited and aluminize.

4. Ni-20Cr-5Al-1Y

   (a) E.B. deposited.
   (b) E.B. deposited and aluminize.

5. Ni-20Cr-5Al-0.1C-0.1Y

   (a) Spray coated.
   (b) Spray coated and aluminize.
   (c) Spray coated, no substrate preheat.
   (d) Spray coated, no substrate preheat and aluminize.

6. Co-30Cr-5Al-1Y

   (a) E.B. deposited.
   (b) E.B. deposited and aluminize.
   (c) E.B. Ni and E.B. deposited and aluminize.
   (d) E.B. Ni and E.B. deposit.

The pins were exposed in air in a 1-hour cycle to 1100°C. The coatings were evaluated with respect to oxidation resistance and minimizing coating-substrate interaction.

In all cases, Ni based coatings with and without an aluminized overlay, were superior to cobalt base in oxidation. Ni based carbon bearing coatings minimized fiber denudation while the other coatings did not.

In Task II, two preferred coatings were evaluated: Ni-20Cr-5Al-0.1C-0.1Y spray coated and aluminized, and Ni-20Cr-5Al E.B. and aluminize. These coatings were given detailed evaluation as follows:

(a) Room-temperature ductility measured by bend tests,
(b) Stress-rupture tests at 871°C and 1100°C after cyclic burner rig exposure at 1100°C,
(c) Metallurgical analyses.

Both coatings provided for stress rupture lives far in the excess of lives for uncoated, cycled NiTaC-13. Lives were superior to those for bars coated with Ni-35Cr+Al, and nearly equivalent to those for bars coated with Ni-20Cr-15Al-1Y, reported in an earlier study.

Coating cracking in room-temperature bend tests for Ni-20Cr-5Al+Al occurs at 0.5% to 0.6% strain; however, no crack propagation into the substrate was observed.

The microstructure of burner rig exposed and rupture tested samples were consistent with those of burner rig exposed pins--a coating substrate interaction zone with sigma phase present, and for the non-carbon bearing coatings, a region of fiber loss.

CONCLUSIONS

1. Duplex aluminized NiCrAl-type coatings--based on NASCOAT 70--provide excellent environmental protection for NiTaC-13 (γ/γ'-TaC) type eutectic alloys. Ni-20Cr-5Al+Al, Ni-20Cr-5Al-1Y+Al and Ni-20Cr-10Al-1Y+Al coatings had 3000-hour lifetimes in the 1100° to 90°C cyclic furnace test.

2. The addition of carbon to the coating chemistry substantially eliminates the problem of fiber denudation in TaC-type eutectic alloys. A Ni-20Cr-5Al-0.1C-0.1Y+Al coating showed essentially no denudation after 2000 hours on the 1100° to 90°C cyclic oxidation test.

3. Stress rupture tests, following cyclic exposure for up to 403 hours to 1100°C were conducted at 871°C (434.4MN/m^2) and 1100°C (103.4MN/m^2). NiTaC-13 coated with Ni-20Cr-5Al+Al was marginally superior to NiTaC-13 coated with Ni-20Cr-5Al-0.1Y-0.1C+Al. Both coatings provided for stress rupture lives far in excess of lives for uncoated, cycled NiTaC-13. Lives were superior to those for bars coated with Ni-35Cr+Al, and nearly equivalent to those for bars coated with Ni-20Cr-15Al-1Y, reported in an earlier study.

4. Coating cracking in a bend test at room temperature for Ni-20Cr-5Al+Al occurs at 0.5% to 0.6% tensile strain; however, no crack propagation into the substrate was observed.

RECOMMENDATIONS

This study has demonstrated that duplex aluminized NiCrAl-type coatings containing carbon offer excellent environmental protection for γ/γ'-TaC-type eutectic alloys. In particular, a coating of the type NiCrAlYC+Al should be further developed. It is recommended that a follow-on program should consist of the following tasks:

1. NiCrAlYC compositions and processes refinement.

2. Detailed mechanical properties evaluations with emphasis on thin section testing.

3. High Mach number burner rig testing of preferred coatings.

4. Initiation of 2100°F oxidation testing of selected coatings.

REFERENCES

1. Benz, M.G., E.R. Buchanan, L.V. Hampton, M.F. Henry, M.R. Jackson, L.A. Johnson, J.R. Rairden, T.F. Sawyer, and J.L. Walter, "Exploratory Development for Synthesis and Evaluation of Directionally Solidified Composites for High Temperature Application," AFML TR-73-213, Dec. 1973.

2. Smashey, R.W., U.S. Patent 3,904,402 (Sept. 1975).

3. Walter, J.L. and H.E. Cline, "Morphologies of Refractory Carbides Obtained by Directional Solidification in the Eutectic Systems Ni-TaC, Co-TaC, and Fe-TaC," Proc. Conference on In Situ Composites, September 5-8, 1972, in Lakeville, CT, National Academy of Sciences, Vol.1, p. 61 (1973).

4. Henry, M.F. and E.F. Koch, "Determination of Crystallographic Relationships in the Fibrous Eutectic Ni(Cr)TaC," Praktische Metallog. 10, 439 (1974).

5. Giggins, C.S. and F.S. Petit, "Oxidation of Ni-Cr-Al Alloys between 1000° and 1200°C," J. Electrochem. Soc. 118, 1782 (1971).

6. Jackson, M.R., J.R. Rairden, and L.V. Hampton, "Coatings for Directional Eutectics," NASA CR-134665 (Jan. 1974).

7. Gedwill, M.A. and S.J. Grisaffe, "Oxidation Resistant Claddings for Superalloys," Metals Eng. Quart. (May 1972).

8. Gedwill, M.A. and S.J. Grisaffe, "Aluminized Alloy Boosts Turbine Blade Life," Met. Progr. 66 (Aug. 1974).

9. Gedwill, M.A. and S.J. Grisaffe, NASA-Lewis Research Center, U.S. Patents 3,849,865 (Nov. 1974) and 3,869,799 (March 1975).

10. Grisaffe, S.J. and E. Klechka, NASA-Lewis Research Center, U.S. Patent 3,762,884 (Oct. 1974).

11. Walker, J.L. and J.R. Ross, General Electric Co., U.S. Patent 3,873,347 (March 1975).

12. Rairden, J.R., General Electric Co., U.S. Patent 3,874,901 (April 1975).

13. Felten, E.J., T.E. Strangman, and N.W. Ulion, "Coatings for Directional Eutectics," NASA CR-134735 (Oct. 1974).

14. Bergman, P.A., General Electric AEBG, Lynn, Mass., private communication.

15. Henry, M.F., "Fracture in a Directionally Solidified Ni(Cr)TaC Fibrous Eutectic Under Monotonic and Cyclic Loading," PhD Thesis, Rensselaer Polytechnic Institute, Troy, N.Y. (1974).

16. Henry, M.F., "A Technique for Monitoring Time Dependent Surface Damage," General Electric Company TIS Report.

17. Strangman, T.E., "Refinement of Promising Coating Compositions for Directionally Cast Eutectics," NAS3-18920.

GENERAL ELECTRIC

DISTRIBUTION LIST FOR NASA CR-135050

CONTRACT NAS3-17815

(The number in parentheses shows how many copies if more than one are to be sent to an address.)

Mr. G.C. Deutsch/RW
NASA Headquarters
600 Independence Avenue
Washington, D.C. 20546

National Technical (2)
Information Service
Springfield, VA 22151

Contracts Section B
MS 500-313
NASA Lewis Research Ctr
21000 Brookpark Road
Cleveland, OH 44135

Report Control Office
MS 5-5
NASA Lewis Research Ctr
21000 Brookpark Road
Cleveland, OH 44135

Mr. G.M. Ault
MS 3-13
NASA Lewis Research Ctr
21000 Brookpark Road
Cleveland, OH 44135

Mr. R.W. Hall
MS 49-1
NASA Lewis Research Ctr
21000 Brookpark Road
Cleveland, OH 44135

Mr. S.J. Grisaffe
MS 49-3
NASA Lewis Research Ctr
21000 Brookpark Road
Cleveland, OH 44135

Mr. J. Gangler/RWM
NASA Headquarters
600 Independence Avenue
Washington, D.C. 20546

Acqusition Branch (10)
Scientific and Technical
Information Facility
Box 33
College Park, MD 20740

Library (2)
MS 60-3
NASA Lewis Research Ctr
21000 Brookpark Road
Cleveland, OH 44135

Technology Utilization
MS 3-19
NASA Lewis Research Ctr
21000 Brookpark Road
Cleveland, OH 44135

Mr. J.P. Merutka (13)
MS 49-3
NASA Lewis Research Ctr
21000 Brookpark Road
Cleveland, OH 44135

Mr. J.C. Freche
MS 49-1
NASA Lewis Reseach Ctr
21000 Brookpark Road
Cleveland, OH 44135

Mr. N.T. Saunders
MS 105-1
NASA Lewis Research Ctr
21000 Brookpark Road
Cleveland, OH 44135

Dr. H.B. Probst
MS 49-3
NASA Lewis Research Ctr.
21000 Brookpark Road
Cleveland, OH 44135

Dr. B. Lad
MS 106-1
NASA Lewis Research Ctr.
21000 Brookpark Road
Cleveland, OH 44135

Dr. D. Poferl
MS 6-2
NASA Lewis Research Ctr.
21000 Brookpark Road
Cleveland, OH 44135

Lt. Col. G.S. Weden
AAM RDL MS 77/5
NASA Lewis Research Ctr.
21000 Brookpark Road
Cleveland, OH 44135

Mr. B. Stein
MS 188-B
NASA
Langley Research Ctr.
Langley Field, VA 23365

Library
NASA
Goddard Space Flight Ctr.
Greenbelt, MD 20771

Library/Acquisitions
Jet Propulsion Lab.
4800 Oak Grove Drive
Pasadena, CA 91103

Technical Library, Code JM6
NASA
Manned Space Craft Ctr.
Houston, TX 77058

Mr. J. Esgar
MS 60-4
NASA Lewis Research Ctr.
21000 Brookpark Road
Cleveland, OH 44135

Ms Helen Dore
MS 49-1
NASA Lewis Research Ctr.
21000 Brookpark Road
Cleveland, OH 44135

Mr. J. Ziemianski
MS 6-2
NASA Lewis Research Ctr.
21000 Brookpark Road
Cleveland, OH 44135

Dr. J. Buckley
MS 219
NASA
Langley Research Ctr.
Langley Field, VA 23665

Mr. Howard Larson
Thermal Protection Br.
NASA-AMES Research Ctr.
Moffett Field, CA 94035

Library, ATTN: J. Jenkins
NASA Flight Research Ctr.
P.O. Box 273
Edwards, CA 93523

Library
MS 185
NASA
Langley Research Ctr.
Langley Field, VA 23365

Library
NASA
Marshall Space Flight Center
Huntsville, AL 35812

Mr. S. Dapfunas
Fossil Energy Branch
ERDA
20 Massachusetts Ave.
Washington, D.C. 20545

Mr. P. Goodwin AIR-5203
Naval Air Systems Command
Navy Department
Washington, D.C. 20360

Mr. A.L. Baldi
Alloy Surfaces Co., Inc.
100 S. Justison St.
Wilmington, DE 19899

Dr. I.G. Wright
Battelle Memorial Labs.
505 King Avenue
Columbus, OH 43201

Library
University of Dayton
Research Institute
300 College Park Ave.
Dayton, OH 45409

Mr. D. Hanink
Engineering Operations
Detroit Diesel Allison
General Motors Corp.
Indianapolis, IN 46206

Directorate, AMRDL
(SAVDL-EU-TAP)
ATTN: J. Lane
Ft. Eustis, VA 23604

Reports Acquisition
Aerospace Corporation
P.O. Box 92957
Los Angeles, CA 90009

Mr. W.H. Freeman
Technical Center
Howmet Corporation
699 Benston Road
Whitehall, MI 49461

Mr. Tom Roseberry
Matl. Coat. and Tech. Sec.
Battelle Memorial Inst.
505 King Street
Columbus, OH 43201

Mr. M. Negrin
Chromalloy Corp.
169 Western Highway
West Nyack, NY 10994

Mr. G.W. Perbix
Eutectic Corporation
40-40 100 72th
Flushing, NY 11358

Mr. D. Clingman
General Motors Corp.
Detroit Diesel Allison
P.O. Box 894-W5
Indianapolis, IN 46206

Mr. C.J. Spengler
Met. Engr., Mat. and Met.
Westinghouse Elec. Corp.
R&D Center
Pittsburgh, PA 15235

Mr. A.R. Stetson
Solar Division
Int. Harvester Corp.
P.O. Box 80966
San Diego, CA 92112

Mr. R. Perkins
Lockheed Palo Alto R. Lab.
Dept., 52-31, B204
3251 Hanover Street
Palo Alto, CA 94304

Dr. R.A. Graff
City College of New York
Dept. Chem. Engr.
New York, NY 10031

Dr. J. Gadd
TRW Inc.
23555 Euclid Ave.
Cleveland, OH 44117

Mr. Nick Ulion
Pratt & Whitney Aircraft
United Tech. Corp.
400 Main Street
East Hartford, CT 06108

Dr. J. Wert
Matls. Engr. Dept.
Box 1621 Station B
Vanderbilt University
Nashville, TN 37235

AFML/DO
Library
Wright Patterson AFB
OH 45433

Dr. J. Wurst
U. of Dayton Res. Inst.
Dayton, OH 45409

Mr. Charles Packer
Lockheed Palo Alto R. Lab.
Dept., 52-31, B204
3241 Hanover Street
Palo Alto, CA 94304

Mr. J.W. Glatz, Mat. Engr.
Explor. Dev. Branch
NAPTC R&D Div.
Naval Air Prop. Test Ctr.
Trenton, NJ 08628

Mr. S.V. Arnold AMXMR-K
Army Materials and
Mechanics Research Ctr.
Watertown, MA 02172

Library
AVCO Systems Division
201 Lowell Street
Lowell, MA 01851

Library
Cabot Corporation
Stellite Division
P.O. Box 746
Kokomo, IN 46901

Library MSFD
McDonnel-Douglas Corp.
3000 Ocean Park Blvd.
Santa Monica, CA 90406

Library
Pratt & Whitney Aircraft
United Tech. Corp. 6
West Palm Beach, FL 33402

E.R. Barrett-T/M3417
Materials Technology
TRW Equipment Group
23555 Euclid Avenue
Cleveland, OH 44117

Technical Reports Library
Oak Ridge National Lab.
Oak Ridge, TN 37830

MCIC
Battelle Memorial Inst.
505 King Avenue
Columbus, OH 43201

Mr. C.L. Lundin
Denver Research Institute
University Park
Denver, CO 80210

UAC Library
United Tech. Corp.
400 Main Street
East Hartford, CT 06108

Mr. R. Hecht
Pratt & Whitney Aircraft
United Tech. Corp.
Florida R&D Center
West Palm Beach, FL 33402

Mr. N. Geyer
AFML/LLM
Wright Patterson AFB
OH 45433

Mr. I. Machlin
Code AIR-52031B
Department of the Navy
Naval Air Sys. Command
Washington, D.C. 20361

Mr. J.M. Davidson
Columbia University
H. Krumb School of Mines
Seeley W. Mudd Building
New York, NY 10027

Commanding Officer
Army Mat. and Mech. Res. Ctr.
ATTN: F. Quigley (AMXMR-ER)
Watertown, MA 02192

Mr. W.J. Meyer
SAALC/MMEP5
Kelly AFB, TX 79241

Mr. B. Goldblatt
AVCO Lycoming Div.
550 S. Main Street
Stratford, CT 06497

Mr. R.F. Kirby, Supv.
Materials Engr., Dept. 93-3
Airesearch Company
402 East 36th Street
Phoenix, AZ 85034

Dr. G.W. Goward
Pratt & Whitney Aircraft
United Tech. Corp. 21
400 Main Street
East Hartford, CT 06108

Mr. P.C. Johnson
Mgr., Engineering Services
American Airlines
Main. and Engr. Center
Tulsa, OK 74151

Library
Bendix Corporation
Research Laboratories Div.
Southfield, MI 48075

Commanding Officer
Army Mat. and Mech. Res. Ctr.
ATTN: M. Levy AMXMR-RM2
Watertown, MA 02192

Mr. O.O. SRP
AFM/LLS
Wright-Patterson AFB
OH 45433

Mr. W.D. Long
Kaman Sciences Corp.
Garden of the Gods Road
Colorado Springs, CO 80907

Mr. G.J. Wile
Polymet Corporation
10597 Chester Road
Cincinnati, OH 45215

Mr. R. Grekila
Westinghouse Electric
Research Labs
Beulah Rd., Churchill Bldg.
Pittsburgh, PA 15235

Mr. H.C. Nelson
Mgr-Power Plan Engr.
Braniff International
P.O. Box 35001, MS 300 E
Dallas, TX 75235

Dr. J.J. Fischer, Res. Met.
INCO, Inc.
P.D. Merica Res. Lab.
Sterling Forest
Suffern, NY 10901

Mr. C.J. May
Delta Airlines, Inc.
ATTN: Engr. Records
Atlanta Airport
Atlanta, GA 30320

Mr. W.N. Linger
Director of Engr.
National Airlines, Inc.
P.O. Box 2055, APRT, Mail
Miami, FL 33159

Mr. A. Maclarty
Dir. Power Plant
Pan Amer. World Airways
Jet Center
Jamaica, NY 11430

Mr. H.N. Taylor
Dir. of Propulsion Engr.
United Airlines
International Airport
San Francisco, CA 94128

Mr. H.E. March
Stellite Division
Cabot Corporation
1020 W. Park Ave.
Kokomo, IN 46901

Mr. N.B. Elsner
Mgr., Adv. Mat'ls Br.
General Atomic Co.
P.O. Box 81608
San Diego, CA 92138

Dr. R.C. Tucker, Jr.
Linde Div., Coat. Ser. Dept.
Union Carbide Corp.
1500 Polco Street
Indianapolis, IN 46224

Mr. J.R. Kightlinger
Mgr., Power Plant Engr.
Continental Airlines
International Airport
Los Angeles, CA 90009

Mr. M. Dow
Dir., Power Plant Engr.
Eastern Airlines, Inc.
International Airport
Miami, FL 33148

Mr. R.L. Rhodes
Director of Engineering
Northwest Airlines, Inc.
International Airport
St. Paul, MN 55111

Mr. C.A. Fisher
Dir., Power Plant Engr.
Trans World Airlines
P.O. Box 20126-R2-452 MCI
Kansas City, MO 64195

Mr. W.N. Holtz
Mgr., Power Plant Engr.
Western Airlines, Inc.
International Airport
Los Angeles, CA 90009

Mr. G.R. Sippel
Supv. Appl. Matl. Research
Allison
Detroit Diesel Div. GMC
Indianapolis, IN 46206

Prof. R.A. Rapp
Dept. of Metall. Engr.
Ohio State University
Columbus, OH 43210

Energy, Mines & Resources
Canada Sci. & Tech.
Canada Ctr.
555 Booth Street
Ottawa, Canada K1A0G1

Mr. Y. Telang
Matls. Mgr., Prod. Plan. & Res.
Ford Motor Company
P.O. Box 2053
Dearborn, MI 48121

Mr. H. Johnson
AFML-LTM
Wright-Patterson AFB
OH 45433

Mr. R. Stueber
Cromalloy R&T
Orangeburg, NY 10962

Dr. E. Gregory
Corporation R and D
Airco
Murray Hill, NJ 07974

Mrs. Betty Hollis
Lirarian
Cabot Corporation
1020 West Park Ave.
Kokcmo, IN 46901

Mr. L. Hjelm
AFML-LL
Wright-Patterson AFB
OH 45433

Mr. J.W. Beery
4950 Testw-Tzhm
Wright-Patterson AFB
OH 45433

Prof. L. Seigle
Engineering College
State Univ. of New York
Stonybrook, LI NY 11790

Dr. B. Swaroop
Corporate R&D Center
Kelsey-Hayes Co.
2500 Green
Ann Arbon, MI 48105

Mr. R.J. Janowiecki
Dayton Laboratory
Monsanto Research Corp.
1515 Nicholas Road
Dayton, OH 45407

Mr. J. Fairbanks, Code 6146
Naval Ship Engr. Ctr.
Prince George Center
Hyattsville, MD 20782

Dr. R.J. Diefendorf
School of Engineering
Materials Division
Renesselaer Polytech. Inst.
Troy, NY 12181

Mr. R. Penty
Fiber Materials Inc.
Biddeford Ind. Park
Biddeford, ME 04005

Mr. R.T. Begley, Mgr.
Metallurgical and Metals
Westinghouse Res. Labs.
Beulah Road
Pittsburgh, PA 15235

Mr. R.C. Braden
Mech. Prop. Data Ctr.
Belfour Stulen Inc.
Traverse City, MI 49684

Dr. P.S. Chopra
Exper. Breeder Reactor
Argonne National Lab.
9700 S. Cass Ave.
Argonne, IL 60439

Mr. A.R. Ciuffreda
Exxon Research & Eng. Co.
P.O. Box 101
Florham Park, NJ 07932

Mr. E.R. Craig M.S. S-29
General Electric Co.
310 Guigne Drive
Sunnyvale, CA 94086

R.W. Heckel
Dept. of Met. & Matl's
Carnegie-Mellon Univ.
Scaife Hall
Pittsburgh, PA 15213

Dr. D.J. Duquette
RPI-Materials Div.
Troy, NY 12181

Mr. A.R. Bobrowsky
Materials Research Labs.
University Park, PA 16802

Mr. D.F. Bryan, K16-15
The Boeing Co.
3801 S. Oliver
Wichita, KS 67210

Mr. C.E. Cheng
Materials Science Div.
Argonne National Lab.
9700 S. Cass Ave.
Argonne, IL 60439

Mr. J.G.Y. Chow
Brookhaven Nat'l Lab.
Bldg. 703
Upton, NY 11973

Dr. C.E. Feltner, Mgr.
Metallurgical Department
Ford Motor Company
P.O. Box 2053
Dearborn, MI 48121

Mr. A. Fox
Bell Lab. Room 20127
Mountain Ave.
Murray Hill, NJ 07974

Dr. J.A. Friedericy 93031
Airesearch Mfg. Co.
2525 W. 190th St.
Torrence, CA 90509

Dr. S. Ghosh (418-19-30)
Chrysler Corp.-9410
P.O. Box 1118
Detroit, MI 48231

Mr. W.L. Greenstreet
Oak Ridge Nat. Lab.
P.O.Box Y
Oak Ridge, TN 37830

Dr. M.S. Seltzer
Metal Science Section
Battelle Labs.
505 King Street
Columbus, OH 43201

Mr. H.F. Hardrath 188-M
NASA, Langley Res. Ctr.
Hampton, VA 23665

Mr. H.A. Hauser Mer EBZD
Pratt & Whitney Aircraft
East Hartford, CT 06108

Mr. R.F. Hodson
Strut. Mech., Plant 35
Grumman Aerospace Co.
Bethpage, Long Island, NY 11714

Mr. G.J. Dooley III
Director, Met. & Proc. R&D
Oregon Metal Corp.
530 W. 34th Street
P.O. Box 80
Albany, OR 97321

Mr. H.O. Fuchs
Mech. Eng. Dept.
Stanford Univ.
Stanford, CA 94305

Mr. M. Gold
Fossil Power Gen. Div.
Babcock and Wilcox Co.
20 S. Van Buren Ave.
Barberton, OH 44203

Mr. P.S. Giupton
Monsanto Co.
P.O. Box 1311
Texas City, TX 77590

Mr. J.R. Hancock
Midwest Research Inst.
425 Volker Blvd.
Kansas City, MO 64110

Mr. D.W. Harris (EAV)
Naval Weapons Lab.
Dahgren, VA 22448

Mr. F.P. Nitz
Rocketdyne AC37
6633 Canoga Ave.
Canoga Park, CA 91304

Dr. M.A.H. Howes
Metals Division
ITT Research Inst.
10 W. 35th Street
Chicago, IL 60616

Mr. W.S. Hyler
Battelle Labs.
505 King Ave.
Columbus, OH 43201

Prof. A.L. Kaye
Purdue Univ.
Calumet Campus
2233 171st Street
Hammond, IN 46323

Mr. K.R. Lehr
Rollway
Box 1397
Syracuse, NY 13201

Prof. A.J. McEvily
Metallurgy Dept. U-136
University of Conn.
Storrs, CT 06268

Mr. J. Mogul
Dir., Matl's Engr.
Curtiss-Wright Corp.
1 Passaic St.
Wood Ridge, NJ 07075

Mr. M.T. Jakub
General Atomic
Box 81608
San Diego, CA 92138

Mr. O. Jonas
1113 Faun Road
Wilmington, DE 19803

Mr. J. LeCoff
Catalytic Inc.
Center Square West
15500 Market St.
Philadelphia, PA 19102

Mr. W. Leeming
Sundstrand Aviation
4747 Harrison
Rockford, IL 61101

Dr. M.M. Lemcoe
Battelle Labs.
505 King Ave.
Columbus, OH 43201

Mr. R. Mrdjenovich
Prin. Devel. Engr.
Ford Motor Co.
Box 2053
Dearborn, MI 48121

Mr. E.H. Schmidt
Airesearch Ind. Div.
P.O. Box 92992
Los Angeles, CA 90009

Mr. R.J. Sarraf
Atomics International
8900 DeSoto Ave.
Canoga Park, CA 91304

Mr. P.J. Valdez
2200 Pacific Hgwy.
San Diego, CA 92138

Mr. R.R. Whymark
Interand Corp.
450 E. Ohio St.
Chicago, IL 60611

Dr. Fritz Sautter
Bldg. 120
Watervliet Arsenal
Watervliet, NY 12189

Dr. M. Gell
Mats. Eng. & Res. Lab.
Pratt & Whitney Aircraft
East Hartford, CT 06111

Mr. H.T. Corten
321 Talbot Lab.
Univ. of Illinois
Urbana, IL 61801

Mr. E. Straub, Jr.
Fairchild Republic Co.
Hagerstown, MD 21740

Mr. H.E. Watson
Code 6394
Naval Research Lab.
Washington, D.C. 20375

Mr. Donald W. McGrath
Dept. 93-18, Space Lab.
Airesearch Mfg. Co.
2525 W. 190th Street
Torrence, CA 90509

Mr. R.G. Moen
Turbine Eng.-R
4608 N. Marborough
Milwaukee, WI 53211

Mr. D.E. Levster
Babcock and Wilcox Co.
Box 1260
Lynchburgh, VA 20505

Mr. W.F. Emmons
6621 Silverthorne Circle
Sacramento, CA 95842

Mr. F.M. Anthony (B-81)
Bell Aerospace Co.
P.O Box One
Buffalo, NY 14240

Dr. John H. Gerstle
The Boeing Co.
P.O. Box 3707
Seattle, WA 98124

Mr. Donald McGrath
Materials Engineering
Airesearch Mfg. Co.
2525 West 190th Street
Torrence, CA 90509

Mr. B. Schulz
AFML/LC
Wright-Patterson AFB
OH 45433

Mr. R.E. Engdahl, Pres.
Deposits & Composites Inc.
1821 Michael Faraday Dr.
Reston, VA 22090

Capt. R.M. Dunco
AFML/LLM
Wright-Patterson AFB
OH 45433

Mr. J. Williamson
AFML/LTM
Wright-Patterson AFB
OH 45433

Mr. Lester B. Engel, Jr.
Chief Metallurgist
Turbodyne Corporation
711 Anderson Ave. N
St. Cloud, MN 56301

Mr. J.W. Chang
MASE
Tinker AFB
OK 73145

Capt. D.W. Zabrierek
AFAPL/TBP
Wright-Patterson AFB
OH 45433

Mr. J.W. Beery
Chief, Engineering
4950 Test W/TZHM
Wright-Patterson AFB
OH 45433

Mr. J. Newhart (PE62)
NAPTC
Trenton, NJ 08628

Mr. J.J. Crosby
AFML/LLM
Wright-Patterson AFB
OH 45433

Mr. Don Boone
Airco Temescal
2850 Seventh Street
Berkeley, CA 94710

Mr. Robert Beck
Mat. Dev. & Manuf. Engr.
Teledyne CAE
P.O. Box 6971
Toledo, OH 43612